

STUDIES ON CONTROL OF INTEGRATED PLANTS

by
Erik Alten Wolff

A Thesis Submitted for the Degree of Dr. Ing.

University of Trondheim

The Norwegian Institute of Technology

Submitted July 1994

ABSTRACT

Chemical process plants often apply integration, or coupling between units, to enhance energy and raw material efficiency. This integration between units introduces interaction and may make the plant difficult to operate. This thesis studies how the control properties of plants are affected by integration. Integration topics that are considered are mass recycle, information integration between control levels and heat integration.

This work presents procedures and new analysis tools that give a better evaluation of a plants inherent control properties. The gains from such an enhanced analysis are demonstrated through examples.

Mass recycle in chemical reaction systems is investigated with respect to control quality. The multivariable effects of introducing recycle are described and analyzed with respect to interaction and disturbance rejection. Several purge actuator configurations are studied and it is shown how their fundamental difference in propagating secondary effects is important. The effect on the results of varying model detail is also studied.

The integration of information between control levels is investigated with respect to interaction. Applied to cascade control in distillation the results show how controller tuning can be tailored to achieve one way interaction only. This work shows how a secondary control loop may alter the preferred choice of quality control configuration.

An integrated distillation design for separating ternary mixtures is given a comprehensive dynamic analysis for the first time. It is shown that utilization of all the available degrees of freedom for control is difficult. "Holes" in the operating range where fulfilling the specifications is impossible are described. Control solutions are presented and the design is compared to conventional ternary distillation schemes.

Finally, integration specific features that limit a plants control properties are studied. Guidelines for design of operable plants are proposed to counter such limitations.

ACKNOWLEDGEMENTS

This thesis is the product of 4 years of work here at NTH, which has been an inspiring institution to stay at.

The biggest thanks go to my supervisor, Sigurd Skogestad, for showing me the right directions and pushing me forward. His insights in process control and research discipline have been a model to follow. Thanks also to his group of students, past and present, for providing a great environment and many good discussions. Big thanks to Eva for proofreading and valuable comments.

I am grateful to Professor J.D. Perkins for letting me stay 6 months at Imperial College, which expanded my horizons and gave me many new friends.

Thanks to Lise and Arnfinn Hejes Fond and NTH fond for helping finance visits to international conferences.

Financial support from the Royal Norwegian Council for Scientific and Industrial Research (NTNF) is gratefully acknowledged.

Last, but not least, I thank my wife Liv for her tremendous support.

Contents

1	Introduction	1
1.1	Motivation	1
1.2	Relations to other work	2
1.3	Basic definitions	4
1.4	Thesis overview	4
	References	6
2	A Procedure for Controllability Analysis	7
2.1	Introduction	8
2.2	Control objectives and limitations	9
2.3	Scaling of variables	9
2.4	Tools for controllability analysis	10
2.4.1	Functional and state controllability	11
2.4.2	RHP-zeros	11
2.4.3	Time delays	11
2.4.4	RHP-poles	12
2.4.5	Singular value analysis	12
2.4.6	Condition number	13
2.4.7	Relative gain array (RGA)	14
2.4.8	Disturbance sensitivity	14
2.4.9	Partial disturbance sensitivity	15
2.4.10	Novel “range” based disturbance rejection measures	16
2.4.11	Relative order and phase lag	18
2.4.12	Special measures for decentralized control.	18
2.5	More detailed analysis.	19
2.6	Example: FCC	20
2.7	Evaluation	25
2.8	Conclusion	25
	References	25
	Appendix	27
3	Controllability of Integrated Plants applied to Recycle Systems	29
3.1	Introduction	30
3.2	Analysis tools	31
3.2.1	Measures of interaction	31

3.2.2	Measures of disturbance rejection	32
3.3	Case study	34
3.3.1	Problem description	34
3.3.2	Analytical results	35
3.3.3	Open loop simulations	37
3.3.4	Controllability analysis	40
3.3.5	Closed loop simulations	44
3.4	System dependencies	45
3.4.1	Reaction type	45
3.4.2	Separation system dynamics	45
3.4.3	Recycle loop dynamics	46
3.4.4	Unit time constants	47
3.5	Conclusion	47
	Nomenclature	47
	References	48
	Appendix	49
4	Control Configuration Selection for Distillation Columns Under Temperature Control	51
4.1	Introduction	52
4.2	Distillation control	53
4.3	Closing secondary loops	55
4.3.1	General results.	55
4.3.2	Analysis tools	56
4.3.3	Temperature cascade for distillation column	56
4.4	Distillation example	58
4.4.1	Selection of tray for temperature sensor	58
4.4.2	Controllability analysis	59
4.4.3	Simulations	62
4.4.4	Actuator behavior	63
4.5	(L/D)(V/B) Configuration	65
4.6	Using two cascades	67
4.7	Discussion	69
	References	70
5	Dynamics and Control of Integrated Three-Product (Petlyuk) Distillation Columns	72
5.1	Introduction	73
5.2	Degrees of Freedom	75
5.3	Case Study	76
5.4	Steady state optimal operating point	78
5.4.1	Four compositions specified	78
5.4.2	Three compositions specified	80
5.5	Control of the Petlyuk column	81
5.5.1	Linear Analysis Tools	82

5.5.2	Analysis of three-point control, LVS-configuration	82
5.5.3	Nonlinear simulations with three point control	85
5.5.4	Analysis of four-point control, LVR _L S configuration	86
5.5.5	Problems with Four-point control	87
5.5.6	Four-point control with multiple sidestreams, LVR _S S configuration.	87
5.5.7	Possible operational problems	89
5.5.8	Control comparison with conventional configurations	91
5.6	Design suggestions	91
5.7	Conclusion	92
	References	93
6	A Procedure for Operability Analysis	95
6.1	Introduction	96
6.2	Operability and Control	96
6.2.1	Elements of operability	96
6.2.2	Sequencing the operability tasks	97
6.3	Example	99
6.4	Operability Study	100
6.4.1	Stability	100
6.4.2	Optimization	100
6.4.3	Measurements	100
6.4.4	Scaling	101
6.4.5	Choosing manipulated variables	101
6.4.6	Flexibility	104
6.4.7	Controllability	104
6.5	Simulations	109
6.6	Discussion	110
	References	110
	Appendix	111
7	Operability of Integrated Plants	113
7.1	Introduction	114
7.2	Previous work	115
7.3	Plant-wide control system design	117
7.3.1	“Top-down” selection of controlled and manipulated variables	117
7.3.2	“Bottom-up” design of control systems	118
7.3.3	Implications for integrated plants	119
7.4	Effects of integration	120
7.4.1	Operability limitations	120
7.4.2	Operability tradeoffs	121
7.5	Illustrative cases	122
7.5.1	Example 1: HDA plant	122
7.5.2	Example 2: Distillation column pumparound	126
7.6	Guidelines	127
7.7	Conclusion	128

8	Postscript	131
8.1	Discussion	131
8.2	Conclusions	132
8.3	Directions for future work	133
A	A Note on the Pairing of Large Systems Based on the RGA	135
A.1	Introduction	136
A.2	Method	137
A.3	Examples	138
A.3.1	Example 1: Select one of several pairings.	138
A.3.2	Example 2: Counterexample to conventional pairing rule.	139
A.3.3	Example 3: Convergence properties	139
A.3.4	Example 4: Indefinite pairing subject to uncertainty	140
A.3.5	Example 5: Pairing on negative RGA	141
A.4	Frequency dependent Λ^∞	142
A.5	Susceptibility to pair on negative λ_{ij}	142
A.6	Algorithmic pairing procedure	143
A.7	Discussion	143

List of Figures

1.1	Block diagram of process and possible control system. Solid lines: open loop. Dashed lines: closed loop.	3
2.1	Comparison of disturbance rejection measures given by Eq. 2.13 and Eq. 2.15.	17
2.2	Illustration of how a manipulated input to one unit is a disturbance to another unit.	17
2.3	FCC reactor.	20
2.4	RGA-elements, $ \lambda_{ij}(j\omega) $, for proposed pairings.	21
2.5	Necessary control action for perfect control and plant/disturbance alignment.	22
2.6	CLDG for FCC process. Comparison of two different pairings.	23
2.7	PRGA for output y_1 and y_3	23
2.8	Combined PDG-matrix, G_{PDG} for u_3 in manual and $y_1 - y_3$ uncontrolled	24
3.1	Recycle example with alternative purge control configurations.	34
3.2	Open-loop step responses of disturbances to measurements.	38
3.3	Open-loop step responses of manipulated inputs to measurements.	39
3.4	Inverse response from step in feed flow, $\Delta F = 0.1 \text{ m}^3/\text{s}$. Configuration II.	40
3.5	1,1-RGA-element (for the pairing u_1 to y_1)	41
3.6	Closed loop disturbance gain CLDG for all three configurations. Loops are paired $u_1 - y_1$ and $u_2 - y_2$	41
3.7	CLDG for all three configurations, reversed pairing.	42
3.8	$\max_d \min_u y$ and $\max_d \min_u u$ for recycle problem.	43
3.9	Minimum control error decomposed into effect of separate disturbances. Configuration II.	43
3.10	Effect of P on x_{SI} and k on P , controlled system, configuration I.	44
3.11	1,1-RGA element with dynamics introduced to various units. Ratio control, configuration I.	46
4.1	Block diagram with secondary loop closed.	53
4.2	Typical distillation column using LV-configuration.	54
4.3	Composition control using temperature in secondary loop. CM is for composition measurement.	57
4.4	Steady-state column temperature profile at different operating points. (Bottom is Tray 1.)	59

4.5	Effect on the frequency-dependent RGA, $\lambda_{11}(\tilde{G}(j\omega))$, of varying gain in the secondary loop, $c_x = K_c$	60
4.6	Loop gain for the secondary temperature loop with $K_c = 5.53$	61
4.7	Improved disturbance rejection with temperature cascade.	61
4.8	Improved open loop disturbance rejection with temperature cascade, $K_c = 1.84$. Plot shows response in Δx_B to a 1% disturbance in the feed rate, F	62
4.9	Time simulations with composition loops closed.	63
4.10	Response to a setpoint change in x_D ($\Delta x_D = 0.01$) for various filter time constants τ_f	64
4.11	Response to a 50% step change in feed rate F with and without integral action in the secondary loop.	65
4.12	Closed loop disturbance gain of LV and $(L/D)(V/B)$ configuration with secondary loop installed.	66
4.13	Simulations of LV and $(L/D)(V/B)$ configuration with secondary loop installed.	67
4.14	Comparison of PRGA with one and two secondary loops installed. Diagonal entries (corresponding to λ_{11}) are omitted.	68
4.15	Closed loop disturbance gain for the LV configuration with two secondary loops.	69
4.16	Comparison of simulation results with one and two secondary loops.	70
5.1	Petlyuk column representations.	74
5.2	Degrees of freedom in distillation (indicated by valve position).	76
5.3	Energy use (Boilup rate, V/F) as function of extra DOF.	78
5.4	Boilup V/F as a function of internal stream splits R_L and R_V . Four product compositions specified. (SPEEDUP calculations.)	79
5.5	Boilup V/F as a function of prefractionator compositions. Four compositions specified. (ASPEN calculations.)	80
5.6	Boilup V/F as a function of internal stream splits R_L and R_V . Four product compositions specified. (ASPEN calculations.)	80
5.7	Boilup rate V/F and x_{S1} as a function of R_L when relaxing the constraint $x_{S1} = x_{S3}$	81
5.8	Relative gain array, λ_{ii} for LVS configuration.	84
5.9	Closed loop disturbance gain, δ_{ij} , for LVS configuration.	84
5.10	Necessary control action for perfect control, $(G^{-1}G_d)_i$	85
5.11	Time response to disturbances and setpoint change, LVS configuration.	86
5.12	$x_{S2} = 0.994 \rightarrow 0.992$ setpoint ramp decrease from $t = 2$ to $t = 6$, LVR_L -configuration.	87
5.13	Composition profile in main column section.	88
5.14	Surface plot of solution points for boilup as a function of R_L and R_V	90
6.1	Consequential relations between operability conditions.	98
6.2	HDA plant	99
6.3	Required control action for perfect control (Maximum value).	103

6.4	Relative gain array, λ_{ii} , for the preferred pairing.	106
6.5	HDA plant with decentralized control loops corresponding to preferred pairing	107
6.6	Performance relative gain, γ_{ij} showing interaction from loops 2 and 4 on loop 3.	107
6.7	Closed loop disturbance gain, Δ_{ij}	108
6.8	Simulation results for HDA plant under decentralized control.	109
7.1	Production control schemes	118
7.2	Control system hierarchy	118
7.3	Heat exchanger network with alternative control bypass placements. . .	119
7.4	HDA-process with no heat-integration, flowsheet F_0	123
7.5	Alternative integration schemes for the HDA process	124
7.6	Feed effluent heat exchange around reactor.	124
7.7	Distillation column pumparound	126
7.8	Column pumparound: proposed modifications to enhance operability. .	127
A.1	Frequency dependent Λ^∞ for the HDA process. λ^∞ is listed top down for the recommended control loops.	142

Chapter 1

Introduction

1.1 Motivation

Energy and raw material efficiency have become increasingly important design considerations over the last decades. Industrial competition, as well as environmental concerns, demand that these commodities be used and reused before they exit the plant. This has led to more and longer paths for flows and duties through the plant. The increased requirements on plant efficiency have caused techniques such as pinch technology to become almost mandatory. At the same time the role of inventory has changed. No longer does one want immense buffer tanks and plenty of storage, as this poses risks for safety and gives increased capital and operating expenditure. Newer techniques, such as reactive distillation, aim even further by combining several units into a single entity.

These changes in design have changed process plants from a train of independent units to a group of interconnected units. These interconnections between units put constraints on operation. Consider a steam boiler that is heated by a process effluent. If this effluent stream is reduced or becomes colder, then the boiler will have reduced capacity and the steam consuming process units will be affected. The resulting constraints on plant operation from such interconnections have been acknowledged as potential “troublemakers”, in that the degrees of freedom for control are reduced or restrained. Interconnected, or integrated plants thus have added control requirements as compared to a set of independent units.

The context of integrated plants is often viewed as total production facilities, for example an ethylene plant. Integration is not limited to such a large scale, just consider a car heater. The coupe is heated by removing energy from the primary cooling circuit instead of leaving it to the secondary cooling circuit (radiator). Luckily for us (here in Norway), control is easy, otherwise we might have had overcooled (and inefficient) engines as well as overly hot rides. More often than not, complex links between units make design of the control system (as well as the process itself) difficult.

“A chain is only as strong as its weakest link”, or for the chemical engineer; a process is only as good the underlying design allows. For example, a blending operation might give off-spec product for any impeller speed, while two baffles could set things right. This is meant to illustrate that *structural decisions* limit the available potential for any given design. This is equally true for plant control; *control quality is limited by the underlying control structure*. Example: even the best control algorithms fail with a bad set of actuators. Thus, there is an incentive to find the best possible control structure, which as the limiting case represents an *inherent quality* of the plant. With the introduction of integrated processes this search becomes more difficult.

Evaluating control of single process units has a long tradition within academia, where the combination of case studies and theoretical results have given guidelines and heuristics for applying control. Plants with integrated units, though, have not been treated in comparable detail. There is presently a need to investigate the control properties of integrated plants and to establish an analytical practice beneficial for the control system design. Work in this thesis will present problems with integration and control that range from small to large, integrating energy and mass as well as control information.

1.2 Relations to other work

This section will try to put the thesis in perspective to other schools within process control and related areas. This should give the presented material an ‘identity’ compared to other work and maybe help clarify some of the authors intentions.

This thesis includes studies on diverse chemical installations where the general knowledge is as much in focus as the specific cases. The analysis of dynamic behavior is based upon linear models, although nonlinear models are also used, for example in simulations. The linear methodology is more comprehensive with respect to available tools and is also more generic, allowing a unified treatment of problems. This self-imposed limitation within analysis is not conservative, or as Morari (1992) puts it: “In most cases, a controllability evaluation based on linear models [...] suffices, even when the system is strongly nonlinear and when a linear control system is inadequate”. Focusing on the frequency domain and continuous plants were done for largely the same reasons and also to promote simplicity. The work in this thesis predominantly considers decentralized control, as it is felt that advanced control might obscure or hide the inherent effects of integration.

This thesis is not a reference on linear analysis theory or controller design, although much material on the first point is presented here. Models are used to illustrate principles in this work and are not in general comprehensive (depending on the definition, of course). Modeling detail given in the chapters is also generally low, with references to original sources where applicable.

The process description most commonly used is shown in Fig. 1.1, with the process plant G , the disturbance plant G_d and the controller C . Typically, G and G_d are described by frequency responses (gain matrices). G and G_d link the measurements y , manipulated variables u , disturbances d and references r . When studying the inherent

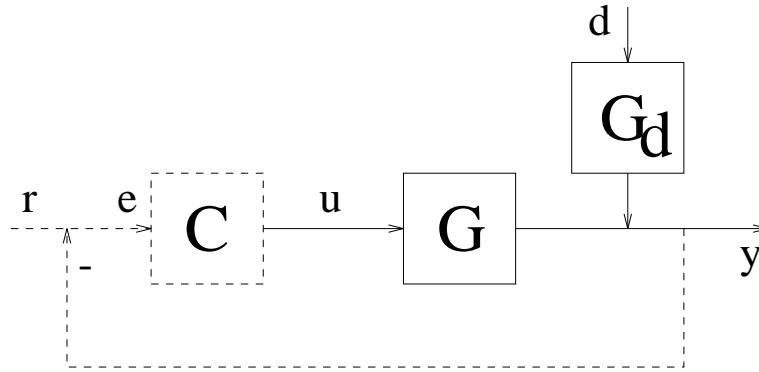


Figure 1.1: Block diagram of process and possible control system. Solid lines: open loop. Dashed lines: closed loop.

properties of the plant (meaning G and G_d), the controller is often omitted. Introducing the controller in Fig. 1.1 (dashed connections) gives what is termed the *controlled* or *closed loop* system, where the controller C tries to make y follow r in spite of d . The performance now also depends on the specific choice of C . Later chapters mainly focus on how u , y , d and r relate to each other, especially when process integration makes the plant large, complex or otherwise special.

Another school in design of processes and control systems employs algorithmic searches over the full space of possible designs and configurations, usually by solving mathematical programming problems. Such formulations usually involve both discrete and continuous variables, often giving rise to a mixed integer nonlinear programming problem (MINLP). Although optimization is used in this thesis where necessary, the algorithmic approach was not found to be beneficial for the issues that are treated here. Rosenbrock (1977), for example, attributes much of the gap between theory and practice to attempting to turn engineering problems into mathematical problems, which could be solved algorithmically. As Rosenbrock put it: "...this is not a satisfactory way of attacking most engineering problems".

The role of integration in process control has been perceived in widely different ways in the control community. This is illustrated nicely by control of heat integrated systems, where Ponton and Liang (1992) hold that "...the principle of deriving a control system for an integrated energy recovery network of this sort from the unintegrated form by replacing valves on utility stream by bypasses appears to be straightforward". Kravanja and Glavič (1989) hold a rather different view, claiming that some of the energy utilization in their example "...can be exploited owing to the proper consideration of the dynamic performances of the total system and by designing a suitable control configuration". The attitude in this thesis is closer to the latter, regarding analysis of dynamic properties as important and generally valuable for attaining good plant performance.

There exist philosophies in the area of plant operation that are related to process control and integration, one example is **JIT** (Just In Time) from manufacturing. By aiming at reducing activities that do not add value to the product, strict guidelines emerge in areas like production planning, inventory control, design, etc.. The interplay

between such considerations and process control are only of secondary importance in this thesis, as part of the long term objectives of control.

1.3 Basic definitions

Controllability The term “controllability” is frequently used in this thesis and deserves a clarification. We follow the definition of Ziegler and Nichols (1943), who defined controllability as “the ability of the process to achieve and maintain the desired equilibrium value”. This description fits the role as a performance measure, we want *good* controllability or a controllable plant. This is opposed to Kalmans state controllability which is rather a numerical definition. This doesn’t mean that controllability can’t be measured numerically, only that it is defined through a wider set of properties.

Control strategy Several tasks are involved in the design of control systems; selection of actuators (inputs), measurements (outputs) and the choice of controller structure (example: decentralized, multivariable). This thesis denotes this collection of tasks “control strategy”. Controller tuning and specific implementation (such as linear quadratic gaussian or μ -optimal) are not assumed part of the control strategy. These tasks are denoted controller design.

Operability This thesis also gives attention to “operability”, which is meant to cover all desirable operational properties of a process. It is here defined as the ability of the plant (together with the control strategy) to achieve acceptable static and dynamic operation. Operability is seen as the result of a full evaluation, not a single number. It is thus rather more vague than controllability, but work presented in chapter 6 should give it meaning and substance.

Integration Integration is a concept for changing reaction, flow and energy patterns, although the appearance of integration may be widely different from case to case. In general it may be viewed as constraints imposed upon the system, which are more that countered by the corresponding economic savings (or other gains).

Integration will often be identified as an addition to the basic construction, i.e. not fundamentally necessary, but of economic importance. Assessing the inherent qualities of this addition may involve comparisons with the unintegrated plant.

1.4 Thesis overview

The thesis is composed of 6 chapters that are written as separate articles. They may be read independently and also include their own bibliography. The chapter sequence has been chosen to reflect a change of scope; starting with a single unit, progress with inter-unit and intra-unit integration before looking at topics in plant-wide control.

Chapter 2 lays the foundation for much of the analysis work in later chapters, describing controllability analysis tools and their application. Fluid catalytic cracking is used as an example to show their use and the benefit of their interplay. This chapter

shows that dynamic analysis preempts much of the insight traditionally sought through simulation.

Chapter 3 examines control structures and dynamics for plants with reaction and recycle. The effect of the purge actuator is examined in detail. This work shows how the interaction and disturbance rejection properties depend on the secondary changes propagating through the recycle loop and thus on the purge actuator structure. The effects of modeling detail are discussed for recycle systems.

Chapter 4 is a study of the effect on controllability of using temperature cascades in distillation composition control. Temperature measurements are typically much faster and more reliable than composition measurements. This fact, and the opportunity to update column temperature setpoints with composition measurements, change the interaction and disturbance rejection properties of the column. Several temperatures may also be utilized for added benefits. Alternative composition control configurations are evaluated and compared with ordinary binary distillation.

Chapter 5 looks at a promising alternative to sequential distillation sequences for separating ternary mixtures with reduced energy and capital cost. The “Petlyuk Column”, as it is often called, consists of a prefractionator that is refluxed with vapor and liquid sidedraws from a “main” column. The concept, often termed “Thermally Coupled Distillation”, has been used widely in cryogenic distillation due to the extreme cost of energy at low temperatures. Today, they are considered viable also for other applications (Finn, 1993). The Petlyuk design is one of the most complex alternatives within this design trend.

Chapter 6 presents a procedure for operability analysis of entire plants. This work proposes sequencing of the analysis tasks (that comprise operability) to consolidate their individual contributions.

Chapter 7 gives a review of plant-wide control and control of integrated plants. Then follows an analysis of the many trade-offs in design and control of integrated plants. Guidelines for control of integrated plants are presented and illustrated through simple cases.

Appendix A attacks the problem of selecting control strategy for large plants through the use of the relative gain array. A procedure is presented that gives a definite and automated pairing from the gain matrix.

Preliminary versions of the chapters in this thesis have been presented at several conferences:

- Chapter 2: 1992 IFAC Workshop “Interactions between Process Design and Process Control” (Proceedings p. 127-132).
- Chapter 3: 1992 AIChE Spring Mtg. (Paper 67a).
- Chapter 4: 1993 European Control Conference (Proceedings p. 637-642).
- Chapter 5: 1993 AIChE Annual Mtg. (Paper 195a).
1994 EFChE Symposium ESCAPE-4 (Proceedings p. 111-118).
- Chapter 6: 1994 EFChE Symposium ESCAPE-4 (Proceedings p. 95-102).
- Chapter 7: IFAC Mtg. PSE-94 (Proceedings p. 63-69).

In addition to work presented in this thesis, the author has also cooperated in other

projects concerning control of heat exchanger networks and controllability analysis:

E.A. Wolff, K.W. Mathisen and S. Skogestad, 1991, "Dynamics and controllability of heat exchanger networks", *EFChE Symposium COPE-91*, Barcelona, Spain, Oct. 91. Published in: Puigjaner and Espuna (Eds.), *Computer-Oriented Process Engineering*, Elsevier, 117-122.

K.W. Mathisen, S. Skogestad, and E.A. Wolff, 1991, "Controllability of heat exchanger networks", Paper 152n, *AIChE Annual Meeting*, Los Angeles, Nov. 1991.

K.W. Mathisen, S. Skogestad and E.A. Wolff, 1992, "Bypass Selection for Control of Heat Exchanger Networks", *Computers and Chem. Engng.*, **16** (Supplement from *European Symposium on Computer Aided Process Engineering (ESCAPE-1)*, Elsinore, Denmark, May 1992), S263-S272.

S. Skogestad and E.A. Wolff, 1992, "Controllability measures for disturbance rejection", *Preprints IFAC workshop on Interactions between process design and process control*, London, Sept. 1992.

The authors contribution in the first area involved creating a modeling framework based on structural network information and some analysis. The second contribution involved calculation and verification work.

References

- [1] Finn, A.J., 1993, "Consider Thermally Coupled Distillation", *Chem. Eng. Progress*, October 1993, 41-45.
- [2] Kravanja, Z. and P. Glavič, 1989, "Heat Integration of Reactors - II. Total Flow-sheet Integration", *Chem. Eng. Sci.*, **44**, 11, 2667-2682.
- [3] Morari, M., 1992, "Effect of Design on the Controllability of Chemical Plants", *Preprints IFAC workshop on Interactions between process design and process control*, London, Sept. 1992.
- [4] Ponton, J.W. and D.M. Liang, 1992, "A Hierarchical Approach to the Design of Process and Control Systems", *Trans IChemE*, **71**, Part A, 181-188.
- [5] Rosenbrock, H.H., 1977, "The Future of Control", *Automatica*, **13**, 389-392.
- [6] Ziegler, J.G. and N.B. Nichols, 1943, "Process Lags in Automatic-Control Circuits", *Trans. of the ASME*, **65**, 433-444.

Chapter 2

A Procedure for Controllability Analysis

Erik A. Wolff*, Sigurd Skogestad[†], Morten Hovd and
Knut W. Mathisen
Chemical Engineering
University of Trondheim - NTH
N-7034 Trondheim, Norway

Presented at
IFAC workshop on Interactions between process design and process control, London,
Sept. 1992.

Abstract

In this paper we give an overview of some of the tools available for linear controllability analysis. We present a procedure which may be described by the following main steps;

For a given model

1. Scale the plant
2. Compute controllability measures
3. Analyze controllability

New controllability measures are presented and we discuss the benefit of applying several controllability measures for enhanced understanding. An FCC reactor is used as an example.

*Present Address: ABB Environmental, Box 6260 Etterstad, N-0603 Oslo, Norway

[†]Address correspondence to this author. Fax: 47-7-594080, E-mail: skoge@kjemi.unit.no.

2.1 Introduction

A common procedure is to design a plant based on steady-state considerations and then add on a control system at a later stage of the project. This may be acceptable if one at the early design stage can assess whether the plant will be easy to control or not.

Consider for example the benchmark example released by Tennessee Eastman (Downs, 1990). This is an integrated plant with reaction, separation and recycle. An analysis of the plant model reveals that it is unstable, has a high degree of interaction and a complicated dynamic behavior. One may proceed and try to design a control system for this plant. However, before embarking on this it would certainly be useful to know how well this process may be controlled with the best possible controller, that is, what is the controllability of the plant.

A plant with few “inherent control limitations” has good “achievable control performance” and is called “controllable” or “dynamic resilient.” Since a plant’s dynamic resilience can not be altered by change of the control algorithm, but only by design modifications, it follows that the term dynamic resilience provides a link between process design and process control.

Unfortunately, in standard state-space control the term “controllability” has the rather limited definition in terms of Kalman’s state controllability; “The system is state controllable if given any two states c_0 and c_1 , there exists a time $t_1 > 0$ and a control u defined on $[0, t_1]$ which takes the state from $x(0) = c_0$ to $x(t_1) = c_1$.” This was the reason why Morari (1983) introduced the term “dynamic resilience.” However, in engineering practice a plant is called “controllable” if it is possible to achieve the specified control objectives (Rosenbrock, 1970). We will use the term “controllability” in this more general sense and use the term “state controllability” where appropriate to avoid confusion.

Rosenbrock (1970) gives a thorough discussion of the issues of state controllability and state observability and also defines the term “functional controllability,” which for SISO systems is equivalent to requiring $g(s) \neq 0$ and for MIMO system $\det(G(s)) \neq 0$. He also introduces the important notion of right half plane (RHP) (transmission) zeros for multivariable systems. Morari (1982) and Stephanopoulos (1982) give good discussions on the issues of control structures and controllability of integrated plants. An initial approach towards quantitative analysis of controllability is given by Morari (1983) who makes use of “perfect control,” that is, the best achievable control performance. Perkins (1989) gives a good survey of the literature up to 1989.

Although linear controllability analysis has been given credit for even very nonlinear applications (for example, Silverstein and Shinnar, 1982), relying on a single measure, especially evaluated at steady state, may yield erroneous conclusions (Skogestad *et al.* 1990). There is a need to clarify the available results from controllability analysis and to advise on their use. This work reviews the available controllability measures and illustrates how their combined use is beneficial in analysis. We also give directions for which measures should be applied and discuss which problems that otherwise may go unattended.

2.2 Control objectives and limitations

To examine the controllability of a plant a mathematical model is needed. It is important to stress that for control considerations it is the *initial part* of the response, corresponding to the closed-loop time constant, that is of main interest. In particular it is important to get a good model of possible RHP-zeros, time delays, and of the interactions in the interesting frequency range. The steady-state behavior is usually of minor interest. One exception is the “sign” of the plant, i.e., $\det G(0)$, which must be known. Otherwise it does not really matter very much what would have happened after several hours if the plant was left uncontrolled. The reason why chemical engineers are often very preoccupied about the steady-state is that this is our natural way of thinking and because steady-state models are often easily available.

In this paper we consider linear transfer function models on the form

$$y(s) = G(s)u(s) + G_d(s)d(s) \quad (2.1)$$

where u is the vector of manipulated inputs, d the vector of (physical) disturbances and y is the vector of outputs (controlled variables). The objective is to keep the error $e = y - r$ small, where r is the vector of reference signals (setpoints). $G(s)$ and $G_d(s)$ are transfer matrices, which need not be square. In many cases we shall only consider a single disturbance at a time and d is a scalar and in this case we write g_d instead of G_d to show explicitly that d is a scalar. The Laplace variable s is usually omitted to simplify notation.

The main objective of the control system is to keep the outputs y close to their setpoints r and to reject disturbances (often called “load changes.”) The ideal controller will accomplish this by inverting the process such that the manipulated input becomes $u = G^{-1}r - G^{-1}G_d d$. In practice, something close to this may be achieved with feedback control. With $u = C(s)(r - y)$, the response of the system is

$$y = Tr + SG_d d \quad (2.2)$$

$$u = G^{-1}Tr - G^{-1}TG_d d \quad (2.3)$$

Here the sensitivity is $S = (I + GC)^{-1}$ and the complementary sensitivity is $T = GC(I + GC)^{-1}$. It follows that at low frequencies where feedback is effective ($\omega < \omega_B$), $S \approx 0$ and $T \approx I$ and the controller corresponds to inversion of the plant. Consequently, ideal control (inversion) requires fast feedback (high bandwidth).

On the other hand, inherent limitations of the system prevent fast control. These limitations may include a close to singular plant such that the necessary input signals become large, non-minimum phase characteristics such as time-delay and RHP-zeros, constraints on the input variables and model uncertainty. These limitations make it desirable to have a low bandwidth. *If these requirements for high and low bandwidth are in conflict then controllability is poor.*

2.3 Scaling of variables

One of the controllability measures, the relative gain array (RGA), has the advantage of being scaling independent, but for other controllability measures it is crucial that

Analysis tool	Feature
State controllability	Feasibility of control
RHP-zeros	Bandwidth limitations
Time delays	Bandwidth limitations
RHP poles	Stability
Singular values	Plant directions
Condition number	Ill conditioned-ness
Relative gain array	Interaction
Disturbance sensitivity	Disturbance/plant alignment
Partial disturbance sensitivity	Size of control system
“Range” based criteria	Measurement, input and disturbance range
Relative order	Control strategy selection
Performance relative gain array	One way loop interaction
Closed loop disturbance gain	Disturbance rejection, bandwidth

Table 2.1: Available controllability analysis tools.

the variables are scaled properly. In general, the variables should be scaled to be within the interval -1 to 1, that is, their desired or expected magnitudes should be normalized to be less than 1 at each frequency. Recommended scalings:

- Inputs (u): Normalize u_j with respect to its allowed range.
- Outputs (y): Normalize e_i with respect to its allowed range.
- Disturbances (d): Normalize d_k with respect to its expected range.

To achieve this we scale the transfer matrices G and G_d . For example, we assume that at each frequency $g_d(j\omega)$ (or the columns in $G_d(j\omega)$) is scaled such that the worst (largest) disturbance corresponds to $|d(j\omega)| = 1$.

Comment: In this paper we scale directly the *transfer matrices* G and G_d and assume that the expected or allowed magnitude of the signals d , u , e and r does not vary with frequency. If their magnitudes vary then we should rather scale the *signals* using frequency-dependent weights. This signal approach is also more general, for example, if the setpoints do not have the same size as the allowed errors (as we implicitly have to assume).

2.4 Tools for controllability analysis

In this section we will briefly discuss a number of methods for evaluating controllability. All measures are controller independent. We first present general measures, while special measures for decentralized control are given towards the end. A brief summary of the analysis tools considered is given in Table 2.1.

2.4.1 Functional and state controllability

Probably the first thing that should be checked is that the plant is functional controllable. Essentially, a plant is not functional controllable if the rank of $G(s)$ is, for all s , less than the number of outputs we want to control. For square plants the requirement is that we should not have $\det G(s) \neq 0$ (Rosenbrock, 1970). The extension of this to the structural case, which is what we actually are interested in, is discussed in detail in Georgiou and Floudas (1989). A typical example when a plant is not functional controllable is when an entire row of $G(s)$ is zero (“there is no downstream path to a particular output”). Another case is, for example, in a heat exchanger network where we have two control inputs (bypasses) that can only affect the two control outputs (temperatures) by transferring heat through the same stream (the downstream paths coincide) (see Georgiou and Floudas, 1989).

For unstable plants it should be checked that the unstable states are state controllable and state observable, but otherwise this issue is not of particular interest, as states that we really care about should be included in the output vector y .

2.4.2 RHP-zeros

A zero is defined as values for s for which $G(s)$ loses rank and for square plants that may be computed as the solutions to $\det G(s) = 0$ (a more careful definition involving the system matrix may be needed in the case the model has internal pole-zero cancellations). A right half plane (RHP) transmission zero of $G(s)$ limits the achievable bandwidth of the plant. This holds regardless of the type of controller used (Holt and Morari, 1985). One way of seeing this is to note that a RHP transmission zero becomes a RHP pole of the plant inverse, and inverting the plant (perfect control) is therefore not possible. Thus, plants with RHP transmission zeros within the desired bandwidth should be avoided. If we use a multivariable controller then RHP-zeros in the elements do not imply any particular problem. However, if decentralized controllers are used, then we generally avoid pairing on elements with “significant” RHP-zeros (RHP-zeros close to the origin), because such a loop may go unstable if left by itself (with the other loops open).

The upper limit on the bandwidth is approximately $\omega_B < z$ where z is the location of the RHP-zero (the exact expression depends on the direction of the RHP-zero). If a RHP transmission zero cannot be avoided, it should preferably be at as high a frequency as possible, and lie in a plant direction (Morari and Zafirou, 1987) such that it affects an output where the performance requirements (as required, e.g., for disturbance rejection) are lax.

The implications of RHP-zeros are not clear for non-square plants.

2.4.3 Time delays

Time delays have essentially the same effect as RHP-zeros with $\omega_B < 1/\theta$ where θ is the time delay. If a plant has time delay, evaluating the control structures (and selection of manipulated variables for the non-square case) can be done by calculating the minimum response time described by Holt and Morari (1985) or the minimum

necessary delay, Perkins and Wong (1985). Both approaches examine the placement of delays in the gain transfer function matrix.

Holt and Morari use the decomposition $G = G_-G_+$, where G_- and G_+ are the invertible and non-invertible part of G respectively, to find lower and upper bounds on the dynamic resilience. This leads to an array of minimum response times for all outputs. One can also use this method to evaluate the cost of using a dynamic decoupler compared to a static one. Decreasing or increasing certain delay elements of the transfer function matrix can in some cases improve the dynamic resilience.

Improving dynamic resilience by increasing delay elements may be possible by allowing competing effects to cancel. This can be illustrated by the following example: a set point change in y_i is accomplished mainly by adjusting u_j . If the delay between $y_{k \neq i}$ and u_j (denoted Θ_{kj}) is smaller than between y_k and all other manipulated inputs, then increasing Θ_{kj} will give y_k less offset by allowing the effect of u_j to be canceled by the other manipulated inputs.

The method of Perkins and Wong finds the minimum necessary delay (MND) to allow independent specification of all outputs. The MND is a scalar measure, making it easier to use in discriminating between possible solutions to the problem.

The methods described are only applied to the delay-part of the transfer function matrix, and as such do not make use of gain information. The lack of a unifying approach reduces the usefulness while the procedures can still be helpful for screening controller structures at an early stage where only delay information is available. A typical example could be a heat exchanger network covering a large plant site.

2.4.4 RHP-poles

Poles of $G(s)$ in the right half plane also put limitations on the control system through stability considerations. The bandwidth of the closed-loop system must be above the frequency of the RHP-pole to ensure a stable system. Freudenberg and Looze have derived some interesting relationships which quantify the effect of RHP-poles and RHP-zeros. These are summarized in Hovd and Skogestad (1992a). If there are RHP zeros and RHP-poles in the same direction, it is important that the RHP-pole at p is located at a lower frequency than the RHP-zero at z , i.e., $|p| < |z|$.

2.4.5 Singular value analysis

The singular value decomposition of any matrix G is $G = U\Sigma V^H$ where the diagonal matrix Σ has as elements the singular values σ_i . There will be $rank(G)$ singular values different from zero. The singular values are directly related to the vector 2-norm. Specifically, we have for $y = Ax$ that

$$\underline{\sigma}(A) \leq \frac{\|y\|_2}{\|x\|_2} \leq \overline{\sigma}(A) \quad (2.4)$$

where $\overline{\sigma}(A)$ is the maximum singular value, and $\underline{\sigma}(A)$ the minimum singular value of A . We may choose the directions for x such that either the lower or upper bound in (2.4) is tight.

The singular values give the gain in the corresponding input and output directions (columns in V and U respectively). An SVD on G and G_d is useful for examining which manipulated input combinations have the largest effect and which disturbances give the largest output variations. For example, applied to distillation (Skogestad *et al.*, 1988) the singular value analysis shows that much less control action is needed to move top and bottom compositions in the *same* direction (i.e., mole fraction of light component x increases or decreases in distillate and bottoms simultaneously) as the opposite.

Minimum singular value and input magnitudes. $\underline{\sigma}(G)$ was introduced as a controllability index by Morari (1983). From (2.3) and (2.4) we get that the input needed for tracking at a sinusoidally varying reference signal $r(j\omega)$ is given by (Perkins, 1989)

$$\frac{1}{\bar{\sigma}(G)} \leq \frac{\|u\|_2}{\|r\|_2} \leq \frac{1}{\underline{\sigma}(G)} \quad (2.5)$$

Here we have used the fact that $\underline{\sigma}(G^{-1}) = 1/\bar{\sigma}(G)$ and $\bar{\sigma}(G^{-1}) = 1/\underline{\sigma}(G)$. Since r may have any direction, we see that a small value of $\underline{\sigma}(G)$ implies that large input magnitudes may be needed, and such plants are undesirable (Morari, 1983). If the variables have been scaled in accordance with the recommendations above then a requirement for avoiding input constraints for unit setpoint changes is approximately (since we are looking at the 2-norm and not infinity-norm of u) that $\underline{\sigma}(G(j\omega)) > 1, \forall \omega$. This can be generalized for a control problem with i outputs and j manipulated variables. Then at most k , such that $\sigma_k > 1.0$, independent variables can be controlled. This is an upper limit since the singular directions involve combinations of u 's which may not always be possible.

The measure $\underline{\sigma}(G)$ is useful also at steady-state. For SISO plants it simply corresponds to requiring $|g| > 1$, and otherwise preferring designs where the steady-state gain is as large as possible. For decentralized control it is desirable to pair on elements with $|g_{ij}| > 1$ to avoid input constraints.

For perfect disturbance rejection of square plants we need $u = -G^{-1}G_d d$. If we have several disturbances that all are less than 1 in magnitude (i.e., $\|d\|_\infty \leq 1$), then the input magnitude (measured in terms of the infinity-norm) needed for perfect rejection of the worst disturbance is given by

$$\|u\|_\infty = \|G^{-1}G_d\|_\infty \quad (2.6)$$

which is equal to the largest row-sum of the matrix $G^{-1}G_d$. A frequency dependent plot of the elements in $G^{-1}G_d$ give useful information about the possibility for reaching input constraints, and which disturbances that cause problems.

2.4.6 Condition number

The ratio between the largest singular value ($\bar{\sigma}$) and the smallest nonzero singular value ($\underline{\sigma}$), is often denoted the condition number, $\gamma(G) = \frac{\bar{\sigma}(G)}{\underline{\sigma}(G)}$. Plants with a large condition number are called ill-conditioned, and require widely different input magnitudes depending on the direction of the desired output. Note that $\gamma(G)$ depends on the

scaling of the inputs and outputs, and it is important that these are scaled properly. There is a close relationship between the optimally scaled condition number, $\gamma^*(G)$, (minimize $\gamma(G)$ with respect to input and output scaling) and the magnitude of the RGA-elements (e.g., Skogestad and Morari, 1987).

If γ is large, then the plant is sensitive to unstructured (uncorrelated) input uncertainty (Skogestad *et al.*, 1988). However, unstructured uncertainty is often unrealistic.

2.4.7 Relative gain array (RGA)

The most widespread controllability measure is probably the RGA which was introduced by Bristol (1966). Skogestad and Hovd (1990) give a thorough survey of the frequency-dependent RGA and its properties. For a square plant $G(s)$ the relative gain is defined as the ratio of the “open-loop” and “closed-loop” gains between input j and output i . It is defined at each frequency as

$$\lambda_{ij}(s) = \frac{(\partial y_i / \partial u_j)_{u_{i \neq j}}}{(\partial y_i / \partial u_j)_{y_{i \neq i}}} = g_{ij}(s)[G^{-1}(s)]_{ji} \quad (2.7)$$

and a RGA-matrix is computed from

$$\Lambda(j\omega) = G(j\omega) \times (G^{-1}(j\omega))^T \quad (2.8)$$

where \times denotes element-by-element multiplication. It is worth noting that the RGA is independent of scaling, and must only be rearranged (*not* recomputed) when considering different control pairings.

Plants with large RGA-values are ill-conditioned ($\gamma(G)$ is also large) irrespective of input and output scaling. Triangular plants yield $\Lambda = I$, and plants where Λ is different from I are called interactive (G has significant offdiagonal elements). It is established that plants with large RGA-values, in particular at high frequencies, are fundamentally difficult to control. In particular, it is known that one should never use decouplers in such cases because of a strong sensitivity to (structured) input uncertainty in each channel, i.e., one should never use a controller with large RGA-values (Skogestad and Morari, 1987).

The relative gains λ_{ij} give a direct measure of the sensitivity of the plant to independent element-by-element uncertainty (which actually occurs relatively rarely): $G(j\omega)$ becomes singular (and the plant impossible to control at this frequency) if any element $g_{ij}(j\omega)$ changes by $-1/\lambda_{ij}(j\omega)$, thus large RGA-elements imply that $G(j\omega)$ is close to singularity.

For interactive plants which do not have large RGA-elements, a decoupler may be useful. In particular, this applies to the case where the RGA-elements vary in magnitude with frequency (e.g., between 0 and 2), and it may be difficult to find a good pairing for decentralized control (see below). A steady-state decoupler may be used if the directions do not change too much with frequency.

2.4.8 Disturbance sensitivity

We will only give a short presentation of measures for evaluating disturbance sensitivity, as they are treated in more detail in the paper “Controllability measures for disturbance

rejection” by Skogestad and Wolff (1992).

Open-loop disturbance sensitivity. For one disturbance i the open-loop disturbance sensitivity is directly given by the i 'th element of the vector g_d , that is $\left(\frac{\partial y_i}{\partial d}\right)_{u_j} = g_{di}$. If appropriately scaling has been applied and any of the elements in G_d are larger than 1 then control is needed to get acceptable performance.

Consider a SISO plant. Typically, $|g_d|$ is larger than 1 at low frequencies and drops to zero at high frequencies. The frequency ω_d where $|g_d(j\omega)|$ crosses 1 is then of particular interest, since it yields the minimum bandwidth requirement for feedback control, i.e., $\omega_B > \omega_d$. ω_d is thus a measure of the controllability. If the plant has a RHP-zero at $s = z$ then we must require $z > \omega_d$ (It is stressed that all these relationships involving RHP-zeros and RHP-poles are approximate).

For MIMO plants we have a bandwidth region ranging from ω_B (worst direction, $\underline{\sigma}(GC)$) to ω'_B (best direction, $\bar{\sigma}(GC)$). For a single disturbance consider the frequency ω_d where $\|g_d\|_2$ crosses 1. Then we *must* require that $\omega'_B > \omega_d$ and we *may* have to require $\omega_B > \omega_d$ (depending of the direction of the disturbance).

Disturbance condition number. To study specifically the *direction* of a disturbance, Skogestad and Morari (1987) introduced the disturbance condition number of the matrix A

$$\gamma_d(A) = \frac{\|A^{-1}g_d\|_2}{\|g_d\|_2} \bar{\sigma}(A) \quad (2.9)$$

where A may be G or $L = GC$. The disturbance condition number of G , $\gamma_d(G)$, tells us for a particular disturbance how much larger the input magnitude needs to be to reject a unit disturbance, compared to if the disturbance was in the best possible direction of the plant (corresponding to the direction of $\bar{\sigma}(G)$). $\gamma_d(G)$ is thus bounded by 1 and $\gamma(G)$, with 1 indicating the disturbances are in the “easy” plant direction. $\gamma_d(G)$ depends on scaling as it is based on the condition number.

2.4.9 Partial disturbance sensitivity

The following measure is useful when considering if one may let one of the outputs be uncontrolled, for example, if the original control problem is difficult. Recall, that the open-loop disturbance sensitivity for an output i and disturbance k is $\left(\frac{\partial y_i}{\partial d_k}\right)_{u_j} = g_{dik}$. The corresponding disturbance sensitivity with all the *other* outputs $l \neq i$ perfectly controlled can be expressed as

$$\left(\frac{\partial y_i}{\partial d_k}\right)_{u_j, y_{l \neq i}} = [G^{-1}G_d]_{jk} / [G^{-1}]_{ji} \quad (2.10)$$

We denote this measure the partial disturbance gain (PDG). The term partial is used since the system is only partially controlled. For simultaneous disturbances we should evaluate the worst overall effect of them by taking the 1-norm (sum of element magnitudes). This gives rise to a combined PDG-matrix, denoted G_{PDG} with elements

$$[G_{PDG}]_{ij} = \sum_k |[G^{-1}G_d]_{jk}| / |[G^{-1}]_{ji}| \quad (2.11)$$

It is desirable to find an “uncontrolled pairing” $u_j - y_i$ for which the G_{PDG} -element is less than 1. Note that also the steady-state values of G_{PDG} are important.

For the case $j = i$ (that is, we have paired up the uncontrolled output with the output we want in manual), the PDG is equal to the ratio between the CLDG (see below) and the corresponding RGA-element:

$$\left(\frac{\partial y_i}{\partial d_k} \right)_{u_i, y_l \neq i} = \delta_{ik} / \lambda_{ii} \quad (2.12)$$

2.4.10 Novel “range” based disturbance rejection measures

Most measures for evaluating disturbance rejection properties are either based upon (perfect) feedback control or open loop behavior. The results pertain to disturbance gain, bandwidth or input signal for accomplishing $y = 0$. None of the available techniques can place the input and output signals within a 0-1 scaled limit and look at the best possible control given the worst possible disturbances. This work gives one solution in this direction.

Minimum control error. If perfect control is not possible (for example with more disturbances than manipulated variables or input constraints) the issue can be to minimize the offset in y . This corresponds to minimizing $\| y \|_\infty$. The resulting problem may then be stated as (at each frequency):

$$\begin{aligned} \max_d \quad & (\min_u \quad \| y \|_\infty) & (2.13) \\ \text{s.t.} \quad & \| d \|_\infty \leq 1 \\ & \| u \|_\infty \leq 1 \\ & y = Gu + G_d d \end{aligned}$$

The answer provides the offset given the worst disturbance direction and the best possible input direction. We can look at this condition at steady state or frequency-by-frequency.

Comment: One may alternatively evaluate for one disturbance at a time, then the \max_d is not needed and the optimization problem is much simpler:

$$\begin{aligned} \min_u \quad & \| y \|_\infty & (2.14) \\ & d = 1 \\ & \| u \|_\infty \leq 1 \\ & y = Gu + G_d d \end{aligned}$$

This has the additional advantage of yielding information about which disturbances are most difficult to reject. The individual effect of each disturbance is not additive because of the constraints; one can have perfect control of each single disturbance, but together they may cause the manipulated inputs to meet the constraints. Conversely, multiple disturbances may cancel each other while the individual effects exceed the counteracting effect of the manipulated variables.

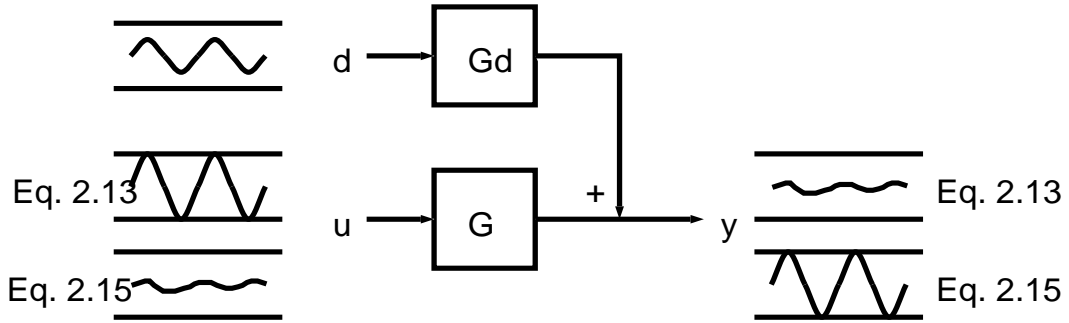


Figure 2.1: Comparison of disturbance rejection measures given by Eq. 2.13 and Eq. 2.15.

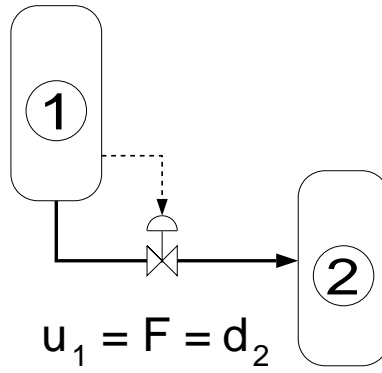


Figure 2.2: Illustration of how a manipulated input to one unit is a disturbance to another unit.

Disturbance rejection with minimum use of control inputs. Alternatively, one may minimize the inputs needed to satisfy a specified offset in y :

$$\begin{aligned} \max_d \quad & (\min_u \quad \| u \|_\infty) & (2.15) \\ \text{s.t.} \quad & \| d \|_\infty \leq 1 \\ & \| y \|_\infty = \| Gu + G_d d \|_\infty \leq 1 \end{aligned}$$

The difference between the two measures given by Eq. 2.13 and Eq. 2.15 are illustrated in Fig. 2.1. We see that Eq. 2.13 corresponds to "optimize your subproblem", that is, to use the inputs to their fullest extent, whereas Eq. 2.15 corresponds to "meet your specification, but minimize the effect on the environment (through actuator use). The last statement follows since manipulated inputs in one subproblem often are disturbances to another subproblem of the overall process as shown in Fig. 2.2.

Maximum disturbance rejection. The last problem that can be described in this way is determining how large disturbances can be rejected given $\| u \| < 1$ and $\| y \| < 1$:

$$\begin{aligned} \max_d \quad & (\min_u \quad \| d \|_\infty) & (2.16) \\ & \| u \|_\infty \leq 1 \\ & \| y \|_\infty = \| Gu + G_d d \|_\infty \leq 1 \end{aligned}$$

This problem is a generalization of the Resiliency Index (RI) of Morari *et al.* (1985). Eq. 2.16 may for example be solved through Eq. 2.15 by varying the limit on d until $\|u\|=1$.

It should be noted that all these problem descriptions are related, in that given two constrained variables (out of u , y and d), the problem is to find the magnitude of the third variable. Thus, the different solutions are comparable to viewing the control problem from complementary viewpoints.

2.4.11 Relative order and phase lag

The relative order is sometimes used a controllability measure (e.g., Daoutidis and Kravaris, 1992). The relative order may be defined also for nonlinear plants, and for linear plants it corresponds to the high-frequency rolloff, that is, the pole excess of the transfer function. Of course, we want the inputs to directly affect the outputs, and the relative order should be small. However, the usefulness of the concept of relative order is rather limited since it depends on the modeling detail. In fact, a more useful measure to consider is the phase lag of the model at the bandwidth frequencies; for decentralized control we want to pair on variables where the phase lag is as small as possible, and it should be less than -180° (see Balchen, 1988).

2.4.12 Special measures for decentralized control.

Pairing and use of RGA. For decentralized control of stable plants one should always try to pair on positive steady-state RGA-elements. Otherwise one will with integral control get instability of either 1) the overall system, 2) the individual loop, or 3) the remaining system when the loop in question is removed. Hovd and Skogestad (1992b) have extended the use of the steady-state RGA to unstable plants.

However, also for decentralized control the most important frequency region is around the closed-loop bandwidth, and we usually prefer pairings corresponding to relative gains close to 1 (with the other elements close to zero) in this frequency region.

It can be difficult to find pairings for large systems with the RGA. Since the row and column sums equal one, many possible pairings can exist with $n \geq 3$. In the worst case the number of possible pairings can increase as $n!$, corresponding to positive and small λ_{ij} . Appendix A gives computational evidence for a method that allows choosing a single pairing from a large possible set.

PRGA. One inadequacy of the RGA (eg., McAvoy, 1983, p. 166) is that it may indicate that interaction is not a problem, but significant one-way coupling may exist. This follows since the RGA is equal to the identity matrix (I) when $G(s)$ is triangular. To overcome this problem Hovd and Skogestad (1992a) introduced the performance relative gain array (PRGA). The PRGA-matrix is defined as

$$\Gamma(s) = G_{diag}(s)G(s)^{-1} \quad (2.17)$$

where $G_{diag}(s)$ is the matrix consisting of only the diagonal elements of $G(s)$, i.e., $G_{diag} = \text{diag}\{g_{ii}\}$. Note that the diagonal elements of RGA and PRGA are identical,

but otherwise PRGA does not have all the nice algebraic properties of the RGA. For example, PRGA is independent of *input* scaling, but it depends on output scaling. This is reasonable since performance is defined in terms of the magnitude of the outputs. Note that $\text{PRGA} = G_s^{-1}$ where G_s is obtained by input scaling of G such that all the diagonal elements are 1 (at all frequencies).

As is clear from 2.18 below, we prefer the PRGA-elements to be small at low frequencies, but at high frequency we want the PRGA-matrix to be triangular (i.e., $G(j\omega)$ triangular) with the diagonal elements (corresponding to the chosen pairings) close to 1.

CLDG and RDG. Consider decentralized control. Then at low frequencies the closed-loop response for loop i when also *all* the other loops are closed is (Skogestad and Hovd, 1990):

$$e_i \approx -\frac{\gamma_{ij}}{L_i} r_i + \frac{\delta_{dik}}{L_i} d_k; \quad \omega \leq \omega_B \quad (2.18)$$

Here $L_i = g_{ii}c_i$, γ_{ij} is the PRGA and δ_{ik} the Closed-loop Disturbance Gain (CLDG) defined by

$$\delta_{ik}(s) = g_{ii}(s)[G(s)^{-1}G_d(s)]_{ik} = [\Gamma G_d]_{ik} \quad (2.19)$$

To get a better interpretation of the RGA and CLDG consider the case when only one loop is closed at the time. Then at low frequencies the closed-loop response for loop i with all other loops *open* is

$$\hat{e}_i \approx -\frac{1}{L_i} r_i + \frac{g_{dik}}{L_i} d_k; \quad \omega \leq \omega_B \quad (2.20)$$

Comparing the closed-loop responses for loop i given in (2.18) and (2.20), we see that closing the other loops has the following effect: 1) The *change* in the effect of setpoint i is given by the relative gain, $\lambda_{ii} = \gamma_{ii}$. 2) The open-loop disturbance gain g_d is replaced by the closed-loop disturbance gain, δ_{ik} . Thus, the *change* in the effect of disturbance k is given by the ratio between δ_{ik} and g_{dik} . This ratio turns out to be identical to the relative disturbance gain (RDG) of Stanley *et al.* (1985). We have

$$\beta_{jk} \stackrel{\text{def}}{=} \frac{\left(\frac{\partial u_j}{\partial d_k}\right)_{y_i}}{\left(\frac{\partial u_j}{\partial d_k}\right)_{y_j, u_{l \neq j}}} = \frac{\delta_{ik}}{g_{dik}} \quad (2.21)$$

For decentralized control frequency-dependent plots of δ_{ik} may be used to evaluate the necessary bandwidth requirements in loop i , that is, at low frequencies the loop gain L_i must be larger than δ_{ik} in magnitude to get acceptable performance. Thus, designs with small CLDG-values are preferred. Note that the elements of CLDG may be significantly different from G_d when the PRGA-matrix is different from I .

2.5 More detailed analysis.

In some cases a more detailed analysis which includes finding the optimal controller may be desirable. A suitable tool for this is the Structured Singular Value (SSV or μ). However, this requires a careful definition of the model uncertainty and performance specification and will not be treated here.

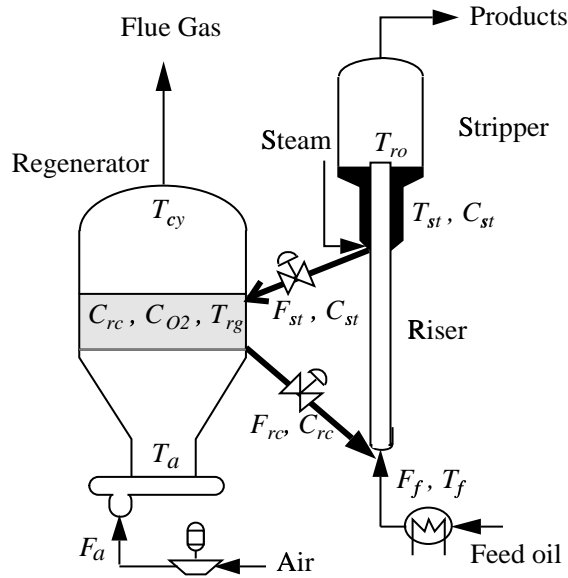


Figure 2.3: FCC reactor.

	Variable	Name	Unit	Value	Scaling
u	F_a	Air rate	kg/min	1521	180
	F_{rc}	Regenerator product flowrate	kg/min	17640	1800
	k_c	Coke production rate factor	s^{-1}	0.019	$4.75 \cdot 10^{-4}$
y	T_{ro}	Riser exit temperature	K	777	3
	T_{cy}	Regenerator cyclone temperature	K	988	2
	T_{rg}	Regenerator bed temperature	K	966	3
d	T_f	Feed temperature	K	478	5
	T_a	Air temperature	K	320	5
	F_f	Feed flowrate	kg/min	2438	240

Table 2.2: Variable notation and scaling range for the FCC process.

2.6 Example: FCC

We will use a model of a Fluid Catalytic Cracker, which is illustrated in Fig. 2.3, to illustrate the principles above. A plant model with 5 states based on the model of Lee & Groves is given by Hovd and Skogestad (1991). The FCC reactor operates in the partial combustion mode. The model has three inputs, three outputs and also three disturbances. The linearized model is given in appendix.

The manipulated variables u , the measurements y and disturbances d are given in Table 2.2 together with their scalings. The meaning of the variables should be clear from Fig. 2.3, except for k_c which is the rate constant for coke formation and is a direct function of feed composition. The feed composition can be adjusted with the recycle to the reactor (not shown).

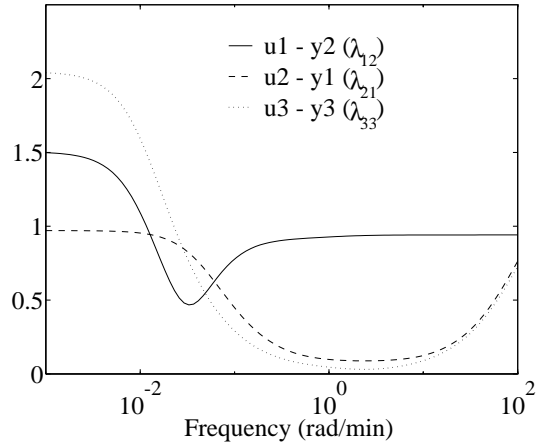


Figure 2.4: RGA-elements, $|\lambda_{ij}(j\omega)|$, for proposed pairings.

The steady-state elements of the disturbance matrix G_d (appropriately scaled) are

$$G_d(0) = \begin{pmatrix} 1.66 & 0.36 & -13.61 \\ 0.47 & 0.23 & -3.89 \\ 1.86 & 0.56 & -15.30 \end{pmatrix} \quad (2.22)$$

indicating that feedback is necessary to reject the disturbances 1 and 3 at least. The plant has no poles in the RHP; open loop stability is thus not a problem at this operating point. The steady-state gain matrix (appropriately scaled) is

$$G(0) = \begin{pmatrix} 10.16 & 5.59 & 1.43 \\ 15.52 & -8.36 & -0.71 \\ 18.05 & 0.42 & 1.80 \end{pmatrix} \quad (2.23)$$

and the steady state RGA becomes

$$\Lambda(0) = \begin{pmatrix} 0.98 & \mathbf{1.49} & -1.48 \\ \mathbf{0.96} & -0.41 & 0.45 \\ -0.94 & -0.08 & \mathbf{2.03} \end{pmatrix} \quad (2.24)$$

An objective is to control this plant using decentralized control, and we see that there is only one possible set of pairings ($u_1 - y_2$, $u_2 - y_1$ and $u_3 - y_3$) that corresponds to pairing on positive RGA-elements. The magnitude of these three elements as a function of frequency is shown in Fig. 2.4. Two of these elements are close to zero in the bandwidth region (approximately 1 rad/min). so this choice of pairings will display serious interactions at intermediate frequencies.

Consequently, decentralized control is difficult. Another simple controller is a static decoupler combined with decentralized control. However, as can be expected from the large variations in the RGA with frequency, this does not work well. For example, with a steady-state decoupler $G(0)^{-1}$ the interactions, as seen from $\Lambda(G(j\omega)G(0)^{-1})$ (not shown), are extremely large at frequencies above 0.1 rad/min.

From the SVD analysis, we find that the interactions lie mainly in the *outputs* of the plant, while the inputs are reasonably decoupled in the directions of the different

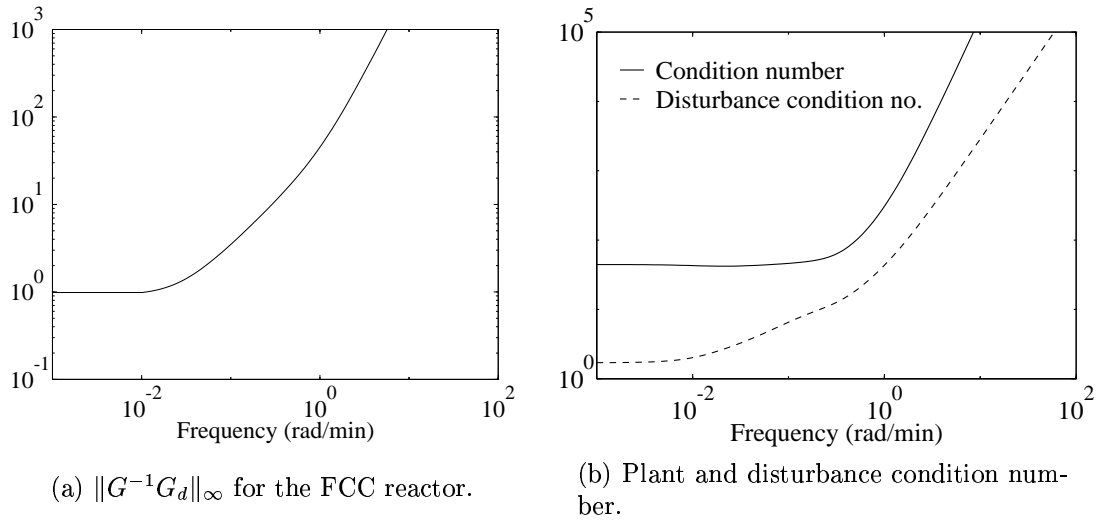


Figure 2.5: Necessary control action for perfect control and plant/disturbance alignment.

singular values $\Sigma = [26.1 \quad 9.88 \quad 0.59]$. The condition number γ equals 44.4 at low frequencies, increasing logarithmically from around 0.5 rad/min. However, since the RGA and (thus) the optimally scaled condition number are close to 1.0, we can deduce that the FCC process is not ill-conditioned.

Turning to the necessary input magnitudes for perfect control as described by Eq. 2.6, we find that $\|G^{-1}G_d\|_\infty$, as shown in Fig. 2.5a, corresponds to d_3 being most difficult to reject (perfect control not possible) and that u_3 holds too little power for handling high frequency disturbances. The disturbance condition number γ_d in Fig. 2.5b shows that the disturbances are well aligned with the plant directions.

Next, we consider the range based criteria, where we have at steady state that $\max_d \min_u \|y\| = 0$, i.e. perfect control is possible with the given scalings. This is in line with Fig. 2.5, which gives the control action needed for perfect disturbance rejection. Indeed, the other measures confirm this; $\max_d \min_u \|u\| = 0.86$ and $\max_d \min_u \|d\| = 1.16$ tell us that we can scale down the actuators by 14% or handle up to 16% larger disturbances. (This does not consider how much the *individual* disturbances can increase, only their combined maximum value.)

The CLDG shown in Fig. 2.6a indicates that disturbance 3 (feed oil flowrate) gives the largest bandwidth requirement for all loops and will be most difficult to reject. (This follows the results from the elements of G_d and $G^{-1}G_d$). In comparison, disturbance 2, T_a , will not require feedback at any frequencies, i.e. the CLDG elements are below 1 at all frequencies. The mentioned effects result from the disturbances being differently aligned with the directions of the plant; disturbance 2 is well aligned, disturbance 3 not so. Fig. 2.6a also shows that decentralized control with the pairing found by Λ will display a direct effect from disturbances d_3 to measurements y_1 and y_2 at high frequencies. This is not a desirable property, although the real degradation depends on $\|\delta_{dik}/g_{ii}c_i\|$ as shown in Eq. 2.18.

Fig. 2.6b includes the two worst CLDG elements for the case when inputs and

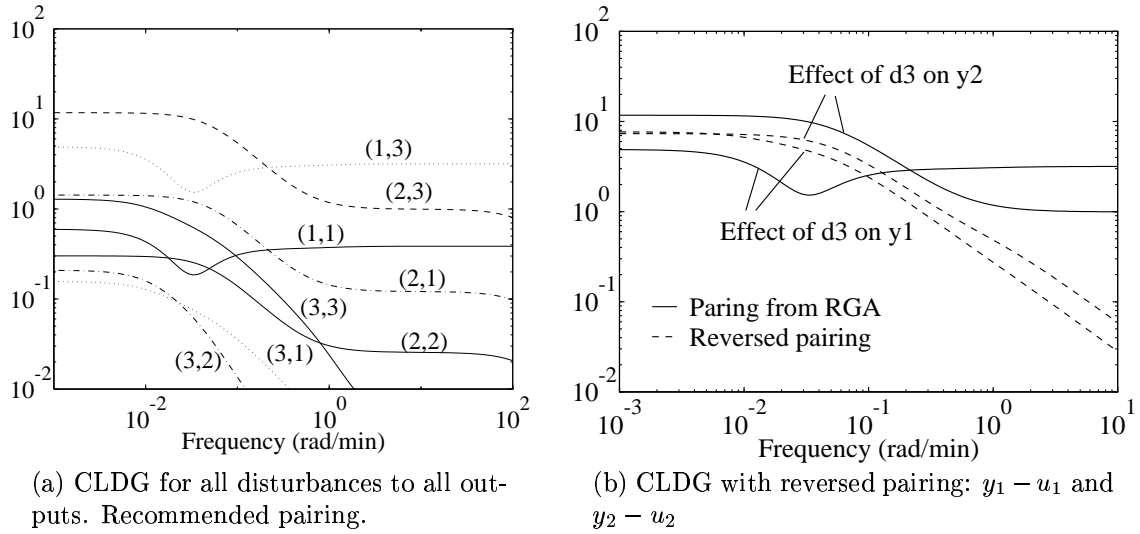


Figure 2.6: CLDG for FCC process. Comparison of two different pairings.

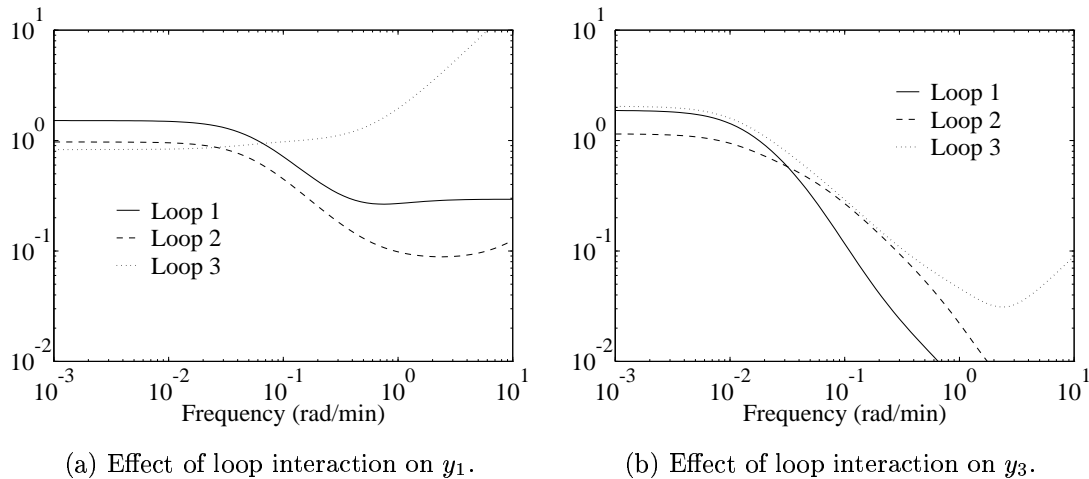


Figure 2.7: PRGA for output y_1 and y_3 .

outputs are paired corresponding to the diagonal values in $\Lambda(0)$ above, i.e. $y_1 - u_1$ and $y_2 - u_2$. Note that the disturbance rejection properties are seemingly better for all frequencies; the direct effect is removed. Pairing on negative λ is not advisable though, since the closed loop system will either be unstable or become unstable for some controller (actuator) failures (Grosdidier and Morari, 1985).

We then investigate how the decentralized control loops will interact with each other using the PRGA. In Fig. 2.7 we show the effect of the other control loops on output y_1 and y_3 . Remember here that the diagonal elements of the PRGA equals the RGA. We see that loop 3 has a significant effect on y_1 for all frequencies. y_3 on the other hand does not show any large high frequency effect of the other loops. The PRGA for y_2 (not shown) is comparable to y_1 , but with large effects from both loop 1 and 3. The advice to extract from this is that loop 3 should tunes loosely (low high frequency

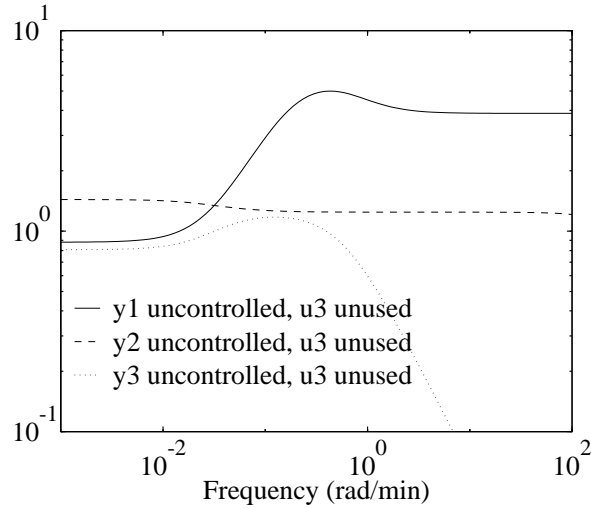


Figure 2.8: Combined PDG-matrix, G_{PDG} for u_3 in manual and $y_1 - y_3$ uncontrolled

effect) so that it does not disturb y_1 and y_2 too much. Loop 1 is not very sensitive to loop 2, while the opposite is true. In all, a preferred “speed of response” would be loop 2 fastest, loop 1 slower and loop 3 slow. Of course demands on disturbance rejection may limit this.

Since control using simple controllers seems difficult we next consider the matrix G_{PDG} of combined partial disturbance gains, to see if there are any measurements that may be left uncontrolled, and still get acceptable control performance - this will be the case if there is one element in G_{PDG} which is less than 1 at all frequencies. At steady-state we get

$$G_{PDG}(0) = \begin{pmatrix} 8.97 & 3.69 & \mathbf{0.87} \\ 14.00 & 20.00 & \mathbf{1.42} \\ 16.56 & 5.11 & \mathbf{0.80} \end{pmatrix}$$

The corresponding frequency-dependent plot is shown in Fig. 2.8 for the three lowest (best) curves (at least for $\omega < 1$ rad/min) corresponding to having u_3 in manual. Of these, the best choice of uncontrolled output is y_3 , followed by y_1 uncontrolled. The frequency dependent PDG for u_1 and u_2 in manual are significantly worse and are omitted for brevity.

For the case with output y_3 uncontrolled and input u_3 in manual, we get a 2×2 system that will reject disturbances in the uncontrolled output y_3 for virtually all frequencies. The RGA for this 2×2 system, denoted Hicks control structure, shows that interaction is significantly reduced with $\lambda_{11}(0) = 0.5$ and $\Lambda \approx I$ at frequencies above $\omega = 0.2$ rad/min. Hovd and Skogestad (1991) have looked at this process in detail and it is interesting to note that they reached the same conclusion with respect to the best 2×2 subsystem. It is important to note that our analysis has not required any controller design or simulation.

2.7 Evaluation

The example has illustrated how the different controllability measures focus on different aspects of plant operation. More specifically, they can be divided into areas covering interaction, disturbance rejection and decentralized control feasibility. The last area is more important than it may seem at first sight. The feasibility of decentralized control also reveals how manual control may cope in case of partial or full controller failure.

Combining controllability measures increases the value of the analysis information and may help avoid bad control strategies. Examples of possible conflicts that may otherwise be undiscovered are:

- Neglecting high frequency interaction may give “unstable” control and “ruin” the effect of a decoupler.
- Interaction may worsen or also alleviate the effect of disturbances.
- Disturbances with direct effect may need feedforward control.
- Conflicting bandwidth requirements may demand redesign.
- Weak manipulated variables may be recommended.
- Redundant measurements may be controlled.

2.8 Conclusion

This work has illustrated how different controllability measures complement each other, creating a whole in which the best control strategy is identified. Implementing control based solely upon the gain or condition number may fail to identify practical redundancy (unnecessary control loops) and potential trouble spots where design should be reconsidered.

We have introduced new controllability measures that gives the (controller independent) limiting performance. This measure shows some promise in evaluating control strategies based on worst case disturbance effect.

The most important conclusions for the FCC example are that T_{rg} may be left uncontrolled for the specified disturbances and that disturbance 3, F_f , is most difficult to reject.

References

- [1] Balchen, J. G. and K. Mumme, 1988. “Process Control. Structures and Applications,” Van Nostrand Reinhold, New York.
- [2] Bristol, E.H., 1966, “On a new measure of interactions for multivariable process control,” *IEEE Trans. Automat. Control*, **AC-11**, 133-134.
- [3] Daoutidis, P. and C. Kravaris, 1992. “Structural Evaluation of Control Configurations for Multivariable Nonlinear Processes,” *Chem. Eng. Sci.*, In press.

- [4] Downs, J.J. and E.F. Vogel, 1990. "A Plant-Wide Industrial Process Control Problem," *AIChE Annual Mtg.*, Chicago, USA.
- [5] Grosdidier, P., M. Morari and B.R. Holt, 1985. "Closed-Loop Properties from Steady-State Gain Information," *Ind. Eng. Chem. Fundam.*, **24**, p. 221-235.
- [6] Holt, B.R. and M. Morari, 1985. "Design of Resilient Processing Plants-VI. The effect of Right-Half-Plant Zeros on Dynamic Resilience," *Chem. Eng. Sci.*, **27**, 59-74.
- [7] Hovd, M. and S. Skogestad, 1991. "Controllability Analysis for The Fluid Catalytic Cracking Process," Paper at *AIChE Annual Mtg.*, Los Angeles, USA.
- [8] Hovd, M. and S. Skogestad, 1992. "Simple Frequency-Dependent Tools for Control System Analysis, Structure Selection and Design," *Automatica*, **28**, 5, 989-996.
- [9] Hovd, M. and S. Skogestad, 1992. "Controllability Analysis for Unstable Processes," *Proc. IFAC Workshop on Interactions Between Process Design and Control*, London, Great Britain.
- [10] Lee, E. and F. R. Groves, 1985. "Mathematical model of the fluidized bed catalytic cracking plant," *Trans. Soc. Comp. Sim.*, **2**, 219-236.
- [11] Mathisen, K.W. and S. Skogestad, 1992. "Bypass Selection for Control of Heat Exchanger Networks," *Proc. ESCAPE-1*, Elsinore, Denmark, May 1992.
- [12] McAvoy, T. J., 1983. *Interaction Analysis*, ISA Monograph, Research Triangle Park, North Carolina.
- [13] Morari, M., 1982. "Integrated plant control: A solution at hand or a research topic for the next decade?" *Proc. CPC-2*, Sea Island, Georgia, USA.
- [14] Morari, M., 1983. "Design of resilient processing plants III, A general framework for the assessment of dynamic resilience," *Chem. Eng. Sci.*, **38**, 1881-1891.
- [15] Morari, M., W. Grimm, M.J. Oglesby and I.D. Prosser, 1985. "Design of Resilient Processing Plants VII. Design of Energy Management System for Unstable Reactors - New Insights," *Chem. Eng. Sci.*, **40**, 187-198.
- [16] Morari, M. and E. Zafrou, 1987. "Design of Resilient Processing Plants. New Characterization of The Effect of RHF-Zeros," *Chem. Eng. Sci.*, **42**, 10, 2425-2428.
- [17] Morari, M., 1992, "Effect of Design on the Controllability of Chemical Plants," *Preprints IFAC workshop on Interactions between process design and process control*, London, Sept. 1992.
- [18] Perkins, J.D., 1989. "Interactions between process design & Process Control," *Preprints IFAC-symposium DYCORN+'89*, Maastricht, Netherlands, 349-357.
- [19] Rosenbrock, H.H., 1970. "State-space and Multivariable Theory," Nelson, London.
- [20] Silverstein, J.L. and R. Shinnar, 1982, "Effect of Design on the Stability and Control of Fixed Bed Catalytic Reactors with Heat Feedback. 1. Concepts," *Ind. Eng. Chem. Process. Des. Dev.*, **21**, 2, 241-256.
- [21] Skogestad, S. and M. Morari, 1987. "Implications of Large RGA Elements on Control Performance," *Ind. Eng. Chem. Res.*, **26**, 2323-2230.

- [22] Skogestad, S., M. Morari and J.C. Doyle, 1988. "Robust Control of Ill-Conditioned Plants: High-Purity Distillation," *IEEE Trans. Autom. Control*, **33**, 12, 1092-1105. (Also see correction to μ -optimal controller in **34**, 6, 672.)
- [23] Skogestad, S. and M. Hovd, 1990. "Use of Frequency-Dependent RGA for Control Structure Selection," Proc. *American Control Conference (ACC)*, 2133-2139, San Diego, USA.
- [24] Skogestad, S., E.W. Jacobsen and M. Morari, 1990. "Inadequacy of steady-state Analysis for Feedback Control: Distillate Bottom Control of Distillation Columns," *Ind. Eng. Chem. Research*, **29**, 2339-2346.
- [25] Skogestad, S. and E.A. Wolff, 1992. "Controllability Measures for Disturbance Rejection," Proc. *IFAC Workshop on Interactions Between Process Design and Control*, London, Great Britain.
- [26] Stephanopoulos, G., 1982. "Synthesis of Control Systems for Chemical Plants - A Challenge for Creativity," Proc. *Process Systems Engineering (PSE)*, Kyoto, Japan.

Appendix 1. 5-state FCC model

The linear 5 state models has been obtained by linearization of the nonlinear equations given in Hovd (1991). Scaling has not been included in the matrices below. Note that the columns of B and D are rearranged to correspond with the preferred pairings for the decentralized control analysis.

$$\frac{dx}{dt} = Ax + Bu + Ed \quad (2.25)$$

$$y = Cx + Du + Fd \quad (2.26)$$

$$A = \begin{bmatrix} -3.8942 \text{ E-03} & -2.7395 \text{ E-03} & -2.2854 \text{ E-07} & 1.6730 \text{ E-03} & 0 \\ -1.8294 \text{ E+00} & -2.3002 \text{ E+00} & -1.9125 \text{ E-04} & 0 & 0 \\ 8.2468 \text{ E+01} & 1.0171 \text{ E+02} & 6.8383 \text{ E-03} & 0 & 1.6729 \text{ E-03} \\ 1.2952 \text{ E-02} & 0 & 2.6114 \text{ E-07} & -1.6800 \text{ E-02} & 0 \\ 2.2131 \text{ E+01} & 0 & 9.3904 \text{ E-03} & 0 & -1.6800 \text{ E-02} \end{bmatrix} \quad (2.27)$$

$$B = \begin{bmatrix} 0 & 3.8030 \text{ E-08} & 0 \\ 3.6309 \text{ E-04} & 0 & 0 \\ -3.9243 \text{ E-03} & -1.0727 \text{ E-03} & 0 \\ 0 & 1.6884 \text{ E-07} & 5.9056 \text{ E-03} \\ 0 & 6.0789 \text{ E-03} & 0 \end{bmatrix} \quad (2.28)$$

$$C = \begin{bmatrix} 1.3173 \text{ E+03} & 0 & 5.5895 \text{ E-01} & 0 & 0 \\ 0 & 5.5555 \text{ E+03} & 1.0000 \text{ E+00} & 0 & 0 \\ 0 & 0 & 1.0000 \text{ E+00} & 0 & 0 \end{bmatrix} \quad (2.29)$$

$$D = \begin{bmatrix} 0 & 3.6185 \text{ E-01} & 0 \\ 0 & 0 & 0 \\ 0 & 0 & 0 \end{bmatrix} \quad (2.30)$$

$$E = \begin{bmatrix} 0 & 0 & 0 \\ 0 & 0 & 0 \\ 0 & 1.5404 \text{ E-}04 & 0 \\ 1.1494 \text{ E-}07 & 0 & -1.1812 \text{ E-}06 \\ 4.1337 \text{ E-}03 & 0 & -4.2474 \text{ E-}02 \end{bmatrix} \quad (2.31)$$

$$F = \begin{bmatrix} 2.4606 \text{ E-}01 & 0 & -2.5282 \text{ E+}00 \\ 0 & 0 & 0 \\ 0 & 0 & 0 \end{bmatrix} \quad (2.32)$$

Chapter 3

Controllability of Integrated Plants applied to Recycle Systems

Erik A. Wolff* and Sigurd Skogestad†
Chemical Engineering
University of Trondheim - NTH
N-7034 Trondheim, Norway

Revised version of paper presented at
AIChE Spring National Mtg., New Orleans, March/April 1992

Abstract

This paper examines the effect of mass recycle on dynamics and control of chemical plants with focus on actuator choice and effects of disturbance redirection. The use of analysis tools has been examined and suitable control structures have been evaluated. A plant consisting of reactor, separator, purge splitter and mixing tank is used as example. Results show that the choice of purge control actuator give fundamentally different dynamic properties. How the results depend on model complexity is also examined.

*Present Address: ABB Environmental, Box 6260 Etterstad, N-0603 Oslo, Norway

†Address correspondence to this author. Fax: 47-7-591410, E-mail: skoge@kjemi.unit.no.

3.1 Introduction

The control system for a complete plant must address many objectives, including, but not limited to safety, performance, disturbance rejection, economically optimal operation, operational discontinuities and tracking. The increased integration of process plants that has taken place in the last decades creates obstacles in fulfilling all these requirements. One important integration topic is mass (or energy) recycle.

Several articles have looked at control of recycle systems and related topics. Much attention has been given to control level decomposition, merging the design and control phase and solving specific control problems, to mention some areas. Little work has focused on controllability and inherent limitations within such complex plants.

Gilliland *et al.* (1964) examined a system consisting of a reactor and a distillation column with recycle and found that instability may occur even with a stable reactor design. Increased disturbance sensitivity was also noted. The tendency to instability and disturbance sensitivity increased with the recycle fraction.

Verykios and Luyben (1978) claimed that in a reactor/distillation system with recycle, the damping depends on the separation dynamics and that process time constants decrease with increasing recycle.

Denn and Lavie (1982) looked into the effects of large time-delay in the recycle loop and also assessed how the steady state gain may be drastically increased by recycle. They found that a large recycle loop deadtime compared to reactor time constant may trigger recurring phenomena similar to pulses.

Rinard and Benjamin (1982) primarily considered the dynamic dependence on the recycle loop deadtime. They found that continuous control was difficult when loop deadtime is the predominant dynamic characteristic.

Taiwo (1986) designed control systems for plants with recycle based upon a “recycle compensator”. This compensator (causal only when the measurement delay is longer than the recycle delay) “times” the manipulated input to the delayed response of the recycle loop.

Papadourakis *et al.* (1987) considered the multivariable recycle control problem with a CSTR followed by a distillation column and a liquid recycle stream back to the reactor. By looking at the column interaction, they conclude that analysis results for individual units do not necessarily hold when recycle is added.

Luyben (1993) looked into dynamics of recycle systems with emphasis on the effect of design changes. Also, the steady state economic dependence on the size of the reactor and separation system were analyzed. The described “snowball effect” is mainly related to reactant buildup when changes in operating conditions render the reactor holdup insufficiently large.

This article primarily looks into recycle dynamics and effects of using purge for control purposes. Pairing and actuator choice are important elements of the investigation. We also examine the effect of various modeling assumptions on the results of the controllability analysis.

There is almost a void in looking at control of recycle systems from a multivariable point of view, especially when including accumulation of non-reactive components and the use of purge flow as actuator. We hope this work will promote better understanding

on control of recycle systems.

3.2 Analysis tools

We will first give a brief description of the analysis tools that will be applied later in this paper. Consider a plant model of the form

$$y = Gu + G_d d \quad (3.1)$$

where y are the controlled variables, u are the manipulated inputs and d are the disturbances to the system. All variables are scaled to be within the interval -1 to 1, that is, their desired or expected magnitudes should be normalized to be less than 1. Recommended scalings:

- Inputs (u): An u_i of magnitude 1 should correspond to the maximum allowable input signal (eg., the input reaching its constraint).
- Outputs (y): An y_j of magnitude 1 should correspond to the largest allowed controlled output.
- Disturbances (d): A d_k of magnitude 1 should correspond to the largest expected disturbance.

3.2.1 Measures of interaction

Singular value analysis. The singular value decomposition of any matrix G is $G = U\Sigma V^H$ with the matrix Σ having the singular values σ_i on the main diagonal. There will be $r = \text{rank}(G)$ nonzero singular values, and the ratio between the largest ($\bar{\sigma}$) and smallest ($\underline{\sigma}$) nonzero singular value is often denoted the condition number, $\gamma(G) = \frac{\bar{\sigma}(G)}{\underline{\sigma}(G)}$. A plant with a large condition number is called ill-conditioned. Note that $\gamma(G)$ depends on the scaling of the inputs and outputs.

Relative gain array. The relative gain array (RGA) is calculated from the plant gain matrix (G) and gives valuable information about the interaction between the different control loops. Skogestad and Hovd (1990) give a thorough survey of the RGA and its properties. It is defined at each frequency as

$$\Lambda = G \times [G^{-1}]^T \quad (3.2)$$

where \times denotes element-by-element multiplication. It is worth noting that the RGA is independent of scaling, and must only be rearranged (not recomputed) when considering different control pairings. Plants with large RGA-values are both ill-conditioned ($\gamma(G)$ is large) and strongly interactive (G has significant offdiagonal elements).

3.2.2 Measures of disturbance rejection

Open-loop disturbance gain. When no feedback is applied the effect of disturbances on the outputs is given as:

$$y = G_d d \quad (3.3)$$

If the magnitude of G_d (i.e. $\|G_d\|$) is greater than one, feedback is required to counteract the disturbance. In the frequency domain this will give the minimum bandwidth requirements of the control system.

Closed-loop disturbance gain for decentralized control. Under closed-loop control we have:

$$e = y - r = Sr - SG_d d \quad (3.4)$$

where $S = (I + GC)^{-1}$ is the closed loop sensitivity. At low frequencies this may be written in terms of the individual loops, S_{diag} , as follows:

$$e = y - r \approx -S_{diag} G_{diag} G^{-1} r + S_{diag} G_{diag} G^{-1} G_d d \quad (3.5)$$

where G_{diag} consists of the diagonal elements (g_{ii}) of G and S_{diag} is defined as $(I + G_{diag} C)^{-1}$, i.e. has elements $1/(1 + g_{ii} c_i)$ (Skogestad and Hovd, 1991). We define the closed-loop disturbance gain (CLDG) as:

$$\Delta = [\delta_{ij}] = G_{diag} G^{-1} G_d \quad (3.6)$$

The elements δ_{ik} represent the apparent disturbance gain from disturbance k to output i when the other loops are closed, and should be used instead of G_d when we want to consider the influence of disturbances using decentralized control.

Since G_d and G are scaled the magnitude $|\delta_{ik}|$ at a given frequency directly gives the necessary loop gain $|g_{ii} c_i|$ at this frequency needed to reject this disturbance. The frequency where $|\delta_{ik}(j\omega)|$ crosses 1 gives the minimum bandwidth requirement for this disturbance. It should be less than the bandwidth that can be achieved in practice, which will be limited by time delays, RHP zeros etc.

Perfect disturbance rejection. Assuming perfect control is possible ($y = 0$), the required magnitude of the manipulated variable is:

$$u = G^{-1} G_d d \quad (3.7)$$

Correspondingly for non square plants, $u = G^+ G_d d$ where G^+ denotes the pseudoinverse of G .

“Range” based criteria. We also make use of criteria related to the “range” of offset, input magnitude and disturbance. These criteria consider the worst disturbance direction and the best use of manipulated inputs. These measures are posed as optimization problems and are formulated as

$$\max_d \min_u \|s\|_\infty \quad (3.8)$$

where s is y (offset), u (input magnitude) or d (disturbance range). See Chapter 2 for a closer description.

Numerical issues. Finding the solutions to Eq. 3.8 are not straightforward since it combines a maximization and minimization in one. The solution is thus a saddle-point and the solution may involve solving a semi-infinite optimization problem.

The most straightforward procedure is to grid for example d , then perform a minimization over u . To make the solution of Eq. 3.8 more manageable, the optimization can be performed over *real* d and u , while the constraint on y is complex. This corresponds to having no phase in the input signals. Since G and G_d are complex for $\omega > 0$, the problem may not be feasible for some ω . In order to fully deal with this deficiency, complex u and d would be needed in the optimization, increasing the set of optimization variables. Using also $\| \text{RE}(y) \| < 1$ as a constraint will secure a possible solution, although this will further limit the interpretation of the results. The tightness of the real d and u approximations have not been thoroughly checked, while the approximation of real y seems tight at low and intermediate frequencies. This is reasonable, since the phase addition is generally low at low frequencies.

If the 2-norm were used instead of the ∞ -norm, analytical solutions to Eq. 3.8 would have been available through Lagrange multipliers. This would, however, give potentially conservative results compared to the ∞ -norm. Consider a set of disturbance variables of size 2. For variables equal in size, the 2-norm will limit the average size to $\sqrt{2}/2$. Thus, the 2-norm is conservative when no single variable is dominating. A solution could have been to use for example $\| d \|_2 \leq \sqrt{n}$ to alleviate this. However, the solution using the ∞ -norm was seen as more appropriate. A development using the 2-norm may enable useful approximations though.

In the calculations, using the ∞ -norm gives the optimization poor numerical convergence properties. The reason for this is that changing minor elements of a signal vector may not influence the solution, making elements of the jacobian become zero. A solution is then to approximate the ∞ -norm with the p -norm where p is some large number, i.e:

$$\| u \|_p = [\sum |u|^p]^{(1/p)} \quad (3.9)$$

The choice of p depends on how well behaved the problem is. Later in the paper $p=99$ has been used to aid the solution.

The problem (for example Eq. 2.13) can be rewritten on the form

$$\begin{aligned} \min_{d,u,z} \quad & z & (3.10) \\ \text{s.t.} \quad & z \geq \| y(u, d) \|_\infty \\ & \| u \|_\infty \leq 1 \\ & \| d \|_\infty \leq 1 \end{aligned}$$

to give an optimization problem of lower ‘‘dimension’’. This reformulation has not been studied further for time reasons. A discussion on such reformulations can be found in Geoffrion (1982).

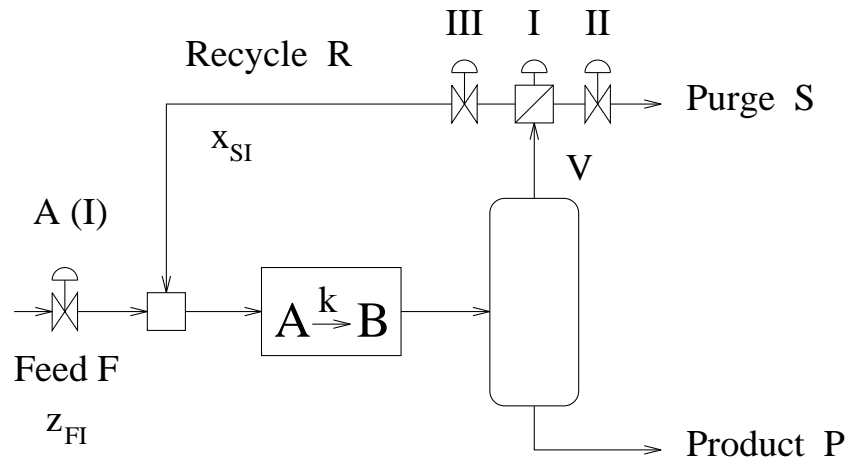


Figure 3.1: Recycle example with alternative purge control configurations.

3.3 Case study

3.3.1 Problem description

This work focuses on problems relating to control of mass recycle systems, that is, a product stream is returned to join a feed stream. This is commonly used to improve process economics (conversion), to dilute feedstocks, to reduce unwanted effects such as coking or even provide enhanced catalytic activity (autocatalytic processes).

Recycle is done on a number of scales, from large refinery units to small flotation units. This work looks at the generic features of recirculating product to the entrance of the process. One can imagine recycle processes without reaction. However, no reaction is just a special case; the reaction system is more generic.

In this paper, the examined system includes a non-reactive component (inert) in the feed. This important property makes the results also applicable to cases where the reactant composition does not quite match the stoichiometry.

To investigate closer the effect of recycle on controllability, a small example was designed. The system consists of a mixer, reactor, flash tank and splitter and is shown in Fig. 3.1. The reaction is $A \rightarrow B$ and some inert (I) is present in the feed in addition to the reactant. The reaction constant k (in the rate expression $r = kC_A$) was chosen to give a conversion of approximately 50% per pass. Additional information is given in appendix 1. The model is based on material balances only for simplicity.

- Controlled outputs are $y_1 = P$ (product flowrate) and $y_2 = x_{SI}$ (purge inert content).
- Manipulated variables are $u_1 = F$ (feed flow) and $u_2 =$ variable related to purge or recycle rate.
- Disturbances are $d_1 =$ feed composition (feed inert fraction, z_{FI}) and $d_2 =$ reaction rate constant (e.g., caused by temperature disturbances).

On a more compact form this becomes:

$$y = \begin{pmatrix} x_{SI} \\ P \end{pmatrix} \quad u = \begin{pmatrix} F \\ u_2 \end{pmatrix} \quad d = \begin{pmatrix} z_{FI} \\ k \end{pmatrix}$$

There are several choices of manipulators u_2 for controlling the split between recycle and purge:

- I. Split fraction $\alpha = S/V = S/(R+S)$
- II. Purge stream flow S ("S" denotes side stream or secondary product)
- III. Recycle stream flow R

This problem also appears in control discussions for other equipment types; for distillation S may be the product (D or B) and R the reflux or boilup. Important questions related to these alternatives are:

- Is there any difference between the alternatives I, II and III?
- Which manipulator is best?

At first it may seem like there is no difference, as a change in S will immediately give a change in R . More precisely, let V denote the flow leaving the flash tank and entering the splitter, then a material balance yields:

$$V = R + S \tag{3.11}$$

However, some more careful thinking and use of intuition will probably lead us to use the smallest stream as the manipulator (at least for the case when there is a large difference in flow rate between R and S). For example, assume the purge stream is small and that we select R as our manipulator which we fix at some desired value. Now if there is a disturbance such that V suddenly drops, then V may become smaller than R , which would require a negative S which is impossible. Consequently, it is better to use S as the manipulator when S is small.

These simple arguments are mainly related to constraints, However, there are actually other differences between the three options I, II and III. These are related to 1) the fact that disturbances in V are redirected differently as just noted, and 2) that changes in R or S yield changes in V through the recycle.

Other considerations may be the need for "small variations" in recycle or purge stream for purposes such as dilution of feed prior to reaction or use of purge as subsequent feed stock. To evaluate more carefully the alternatives we shall look at the dynamic behavior.

3.3.2 Analytical results

Starting with the differential equations for the reactor and the algebraic relations given in appendix 1, a nonlinear model is generated. For the analytical analysis we assume that a perfect split is performed in the flash. By use of the steady-state relations we may substitute all flowrates with feedrate, feed mole fractions and the desired manipulated

variable (u_2), and the following model equations arise for the different configurations, respectively:

$$I \quad (u_2 = \alpha) \quad \begin{aligned} \frac{dx_A}{dt} &= \frac{1}{M} \left[F(1 - z_{FI}) - \frac{F\alpha x_A}{1 - (1 - \alpha)(x_A + x_I)} \right] - kx_A \\ \frac{dx_I}{dt} &= \frac{1}{M} \left[Fz_{FI} - \frac{F\alpha x_I}{1 - (1 - \alpha)(x_A + x_I)} \right] \end{aligned} \quad (3.12)$$

$$II \quad (u_2 = S) \quad \begin{aligned} \frac{dx_A}{dt} &= \frac{1}{M} \left[F(1 - z_{FI}) - \frac{Sx_A}{x_A + x_I} \right] - kx_A \\ \frac{dx_I}{dt} &= \frac{1}{M} \left[Fz_{FI} - \frac{Sx_I}{x_A + x_I} \right] \end{aligned} \quad (3.13)$$

$$III \quad (u_2 = R) \quad \begin{aligned} \frac{dx_A}{dt} &= \frac{1}{M} \left[F(1 - z_{FI}) + R \frac{x_A}{x_A + x_I} - (R + F)x_A \right] - kx_A \\ \frac{dx_I}{dt} &= \frac{1}{M} \left[Fz_{FI} + R \frac{x_I}{x_A + x_I} - (R + F)x_I \right] \end{aligned} \quad (3.14)$$

Equations 3.12-3.14 relate the states of the system x_A and x_I (molefractions of A and I in the reactor) to the disturbances and actuators. The effect on the measurements, $y_1 = P$ and $y_2 = x_{SI}$ (not to be confused with x_I in the reactor) will also be interesting to evaluate for the three configurations:

$$I \quad (u_2 = \alpha) \quad \begin{aligned} P &= \frac{F(1 - x_A - x_I)}{1 - (1 - \alpha)(x_A + x_I)} \\ x_{SI} &= \frac{x_I}{x_A + x_I} \end{aligned} \quad (3.15)$$

$$II \quad (u_2 = S) \quad \begin{aligned} P &= F - S \\ x_{SI} &= \frac{x_I}{x_A + x_I} \end{aligned} \quad (3.16)$$

$$III \quad (u_2 = R) \quad \begin{aligned} P &= (R + F)(1 - x_A - x_I) \\ x_{SI} &= \frac{x_I}{x_A + x_I} \end{aligned} \quad (3.17)$$

We see that there are differences both in the internal dynamics and the response of the measurements. We can see quite immediately that the initial response of x_{SI} to a disturbance in z_{FI} will be equal for configurations I-III, whereas this is not true for P in which configuration II is independent of both disturbances (z_{FI} and k). Eq. 3.12-3.17 will give added understanding to the simulations in the next chapter.

It is of interest to establish how the behavior of the system changes through adding a recycle stream. Looking at the linearized plant will allow us some conclusions on stability and agility (speed of response). A linearization of the system described by Eq. 3.12 gives the following system matrix A :

$$A = \begin{pmatrix} \frac{-F\alpha(1 - x_I + \alpha x_I)}{M(1 - (1 - \alpha)(x_A + x_I))^2} - k & \frac{F\alpha x_A(-1 + \alpha)}{M(1 - (1 - \alpha)(x_A + x_I))^2} \\ \frac{F\alpha x_I(-1 + \alpha)}{M(1 - (1 - \alpha)(x_A + x_I))^2} & \frac{F\alpha(1 - x_A + \alpha x_A)}{M(1 - (1 - \alpha)(x_A + x_I))^2} \end{pmatrix} \quad (3.18)$$

The eigenvalues of the approximated system can then be studied for different recycle rates. Considering the limiting cases of zero recycle ($\alpha = 1$) and total recycle ($\alpha = 0$):

$$A(\alpha = 1) = \begin{pmatrix} -\frac{F}{M} - k & 0 \\ 0 & -\frac{F}{M} \end{pmatrix} \quad A(\alpha = 0) = \begin{pmatrix} -k & 0 \\ 0 & 0 \end{pmatrix} \quad (3.19)$$

(Configurations II and III give the same results.) We see that the recycle removes the tank eigenvalue at $\tau = F/M$, making the system slower. At total recycle we also have

a pure integrator since there is no outlet for the inert component. Thus, the “positive” feedback will slow down the speed of response. Morud and Skogestad (1993) cover several other effects resulting from feedback of this kind.

In Eq. 3.12-3.17 there is a lower limit on the purge flow. Below this limit, the internal flows will increase rapidly due to a buildup in the inert component. This derivation starts with the overall mass balance $P = F - S$, $x_{SI} = \frac{z_{FI}F}{S}$ and the steady state production of B : $P = kx_A M$ where M is the reactor molar holdup. The steady state values of the states then become

$$x_A = \frac{F - S}{kM} \quad \text{and} \quad x_I = \frac{x_{SI}x_{SA}}{1 - x_{SI}} \quad (3.20)$$

When the flows increase towards infinity we have $x_B \rightarrow 0$, giving the limiting condition $x_A + x_I \leq 1$ in the reactor. Combining the equations give

$$S^2 + (kM - F)S - kMz_{FI}F \geq 0 \quad (3.21)$$

The solution to this is (with some rearrangement)

$$S_{min} = \frac{F}{2} + \frac{kM}{2} \left(-1 + \sqrt{1 + \frac{2F(2z_{FI} - 1)}{kM} + \left(\frac{F}{kM}\right)^2} \right) \quad (3.22)$$

For the given example, a reduction in S from 0.2 to $S = 0.1596$ yields the limiting case when the recycle flowrate increases rapidly towards infinity. The choice of operating point may seem very close to the purge limit, but the derivation applies only to the steady state case (and with the perfect separation assumption). Running the problem under control will reduce this sensitivity to the purge flow value. This result does, however, indicate the nonlinearities that exist in recycle systems, in that the flowrates and thus reaction rates quickly change towards the limiting operating point.

3.3.3 Open loop simulations

Let us first consider the disturbance responses for the following three cases:

- I. Fixed $u_1 = F$ and $u_2 =$ recycle ratio α
- II. Fixed $u_1 = F$ and $u_2 =$ purge S
- III. Fixed $u_1 = F$ and $u_2 =$ recycle R

The dynamic responses of $y_1 = P$ and $y_2 = x_{SI}$ to step disturbances in $d_1 = z_{FI}$ (0.10→0.20) and $d_2 = k$ (0.05→0.07) are shown in Fig. 3.2. Initially, the responses are identical (apart from the effect of z_{FI} on P when S is fixed, as described in Eq. 3.16). The reason for the difference in dynamic response is that the change in z_{FI} or k changes the composition in the reactor, which subsequently changes the vapor flow rate V . Now depending on the control configuration, this change in V is redirected back to the reactor (II), out of the plant (III) or is distributed (I). For case II the response to a step in feed composition causes a build-up in the recycle stream R , with a subsequent

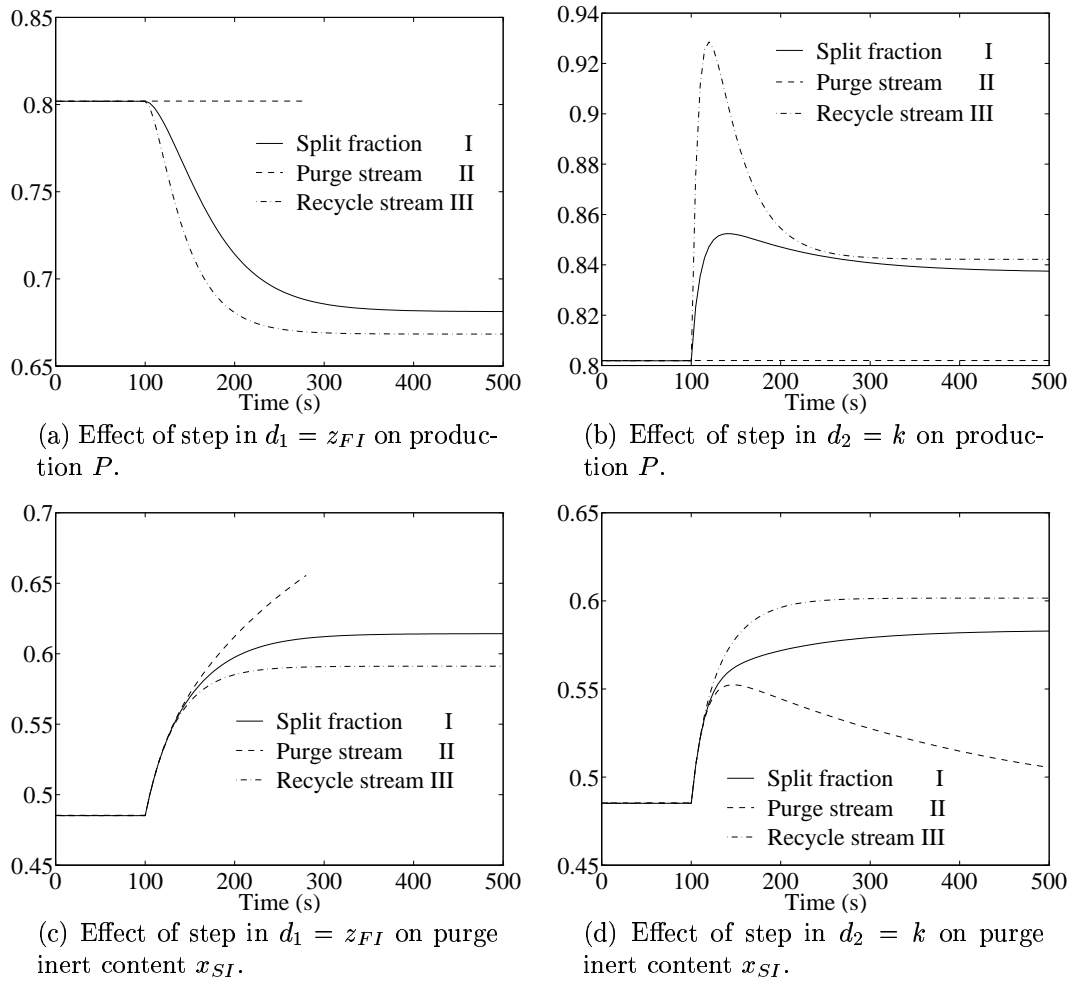


Figure 3.2: Open-loop step responses of disturbances to measurements. $\Delta z_{FI} = 0.10$. $\Delta k = 0.02$. Actuator name and configuration number indicated in legend.

decrease in reaction rate (extinction). This is readily seen from Eq. 3.22. The increase in z_{FI} give a new $S_{min} > S$ and the system becomes unstable.

Now let us consider changes in the manipulated variable $u_1 = F$ and $u_2 = \alpha, S$ or R . The applied steps in u_2 ($\Delta\alpha = +0.1$, $\Delta S = +0.2$ and $\Delta R = -0.2$) all give the same initial change in R and S . Initially, for a real system, all three configurations would respond in the same manner (this is not the case for our example where we have not included dynamics in the flash etc., so that there is some direct effect), but there will then be a secondary change in V that will be redirected differently for the three alternatives.

The secondary change in V is caused both by a direct effect on the flow rates and an indirect effect caused by changes in the reactor conditions (compositions). The responses in Fig. 3.3 show that when using the recycle stream as a manipulator (configuration III), then the secondary change in V dominates and the resulting effect

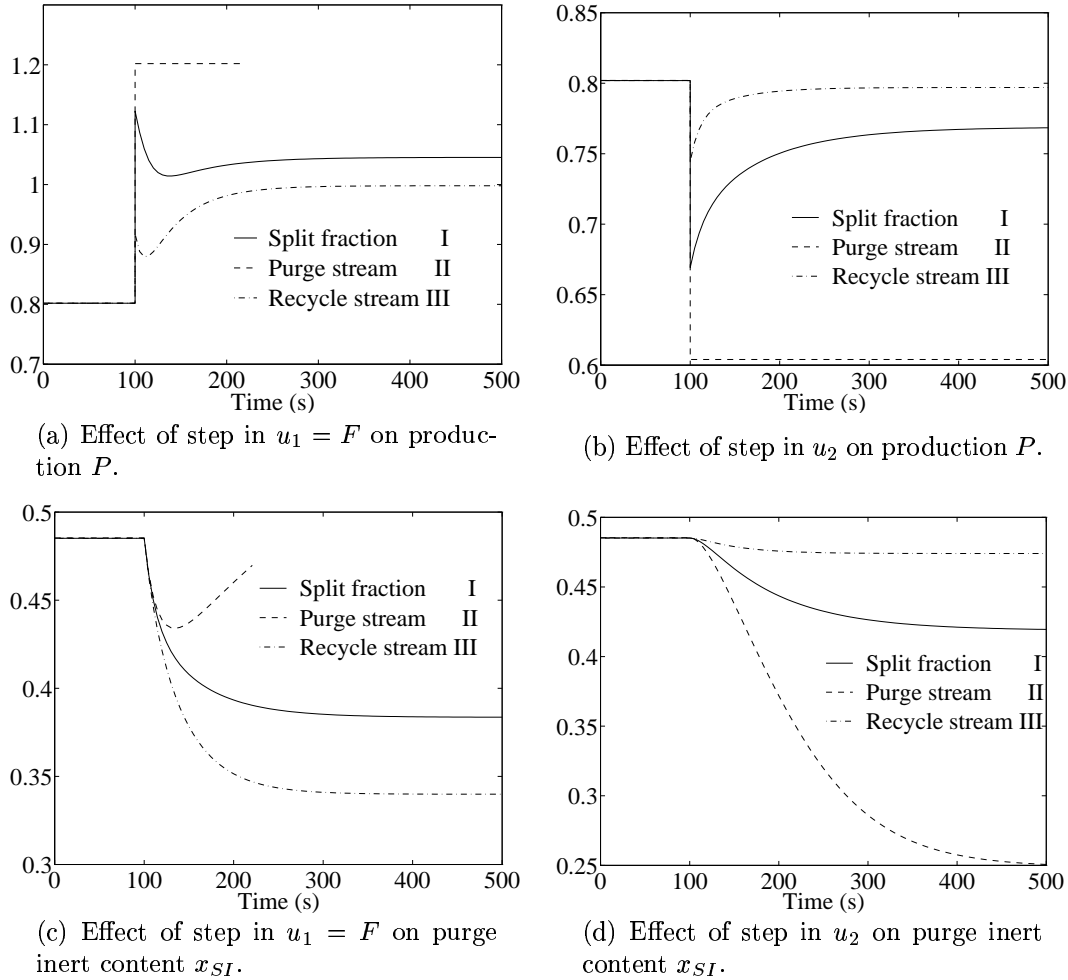


Figure 3.3: Open-loop step responses of manipulated inputs to measurements. $\Delta \text{Purge} = 0.20$ for different actuator configurations. $\Delta F = 0.4$. Actuator name and configuration number indicated in legend.

is small. In general we want the effect of the manipulated variable to be large and direct.

Investigating the effect of a step in input u_1 (the feed flow F increases from 1.0 to 1.4), the secondary effect of changing vapor flow V will also here influence the response. In case II with constant purge (S), the reactor effluent product fraction decreases towards zero due to an inert build-up as for the open loop response to a change in feed inert content. Additionally, in case II one may get an inverse response as shown more clearly in Fig. 3.4 where a smaller feed flowrate change has been imposed ($\Delta F = 0.1 \text{ m}^3/\text{s}$).

To summarize the criteria for judging the different configurations; we want the manipulated inputs to give a large and direct response and the disturbances to have a slow and small effect. Note that in all simulations case I lies between cases II and

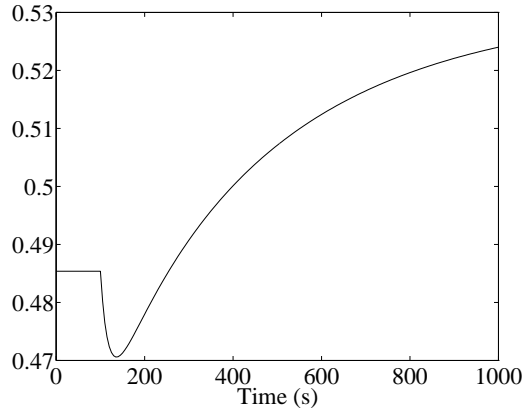


Figure 3.4: Inverse response from step in feed flow, $\Delta F = 0.1 \text{ m}^3/\text{s}$. Configuration II.

III. We will therefore below consider which of cases II and III should be preferred. From the *disturbance* simulations we see that II is the best except for the effect of a change in feed inert content on purge inert content (Fig. 3.2c), where S drops below the minimum needed to prevent inert buildup. The same conclusions are recommended from the open loop *actuator* responses. I would prefer configuration II and use $u_2 = S$ to control $y_2 = x_{SI}$ and $u_1 = F$ to control $y_1 = P$.

3.3.4 Controllability analysis

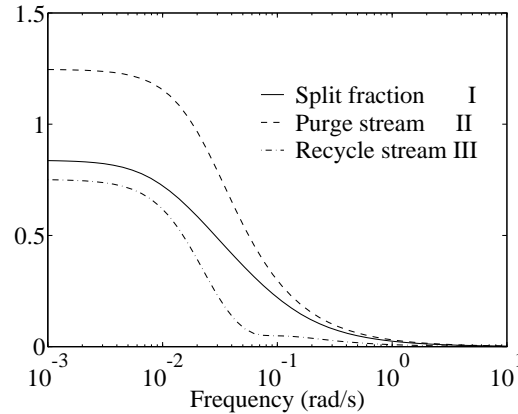
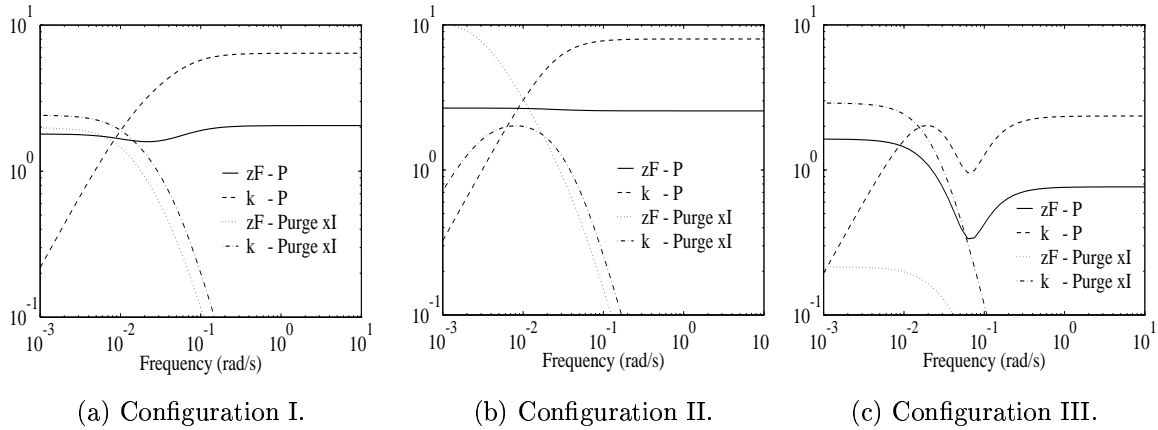
After this preliminary time domain analysis, we will perform a more careful analysis using RGA, CLDG and the range based controllability measures. Scaling is essential for both the CLDG and the range based criteria. The following scalings are used for measurements, actuators and disturbances, respectively; $y_1 : P = 0.80 \pm 0.05$, $y_2 : x_{SI} = 0.48 \pm 0.05$, $u_1 : F = 1.0 \pm 0.4$, $u_2 : S = 0.2 \pm 0.2$, $d_1 : z_{FI} = 0.1 \pm 0.1$ and $d_2 : k = 0.05 \pm 0.02$.

Directionality A singular value decomposition of the steady state gain matrices

$$G^I(0) = \begin{pmatrix} 5.38 & -0.73 \\ -2.42 & -1.71 \end{pmatrix} \quad G^{II}(0) = \begin{pmatrix} 8.00 & -4.00 \\ 3.69 & -9.33 \end{pmatrix} \quad G^{III}(0) = \begin{pmatrix} 4.82 & 0.09 \\ -3.65 & 0.22 \end{pmatrix}$$

indicate that only configuration III, using the recycle stream flow rate for control, will experience problems from constraints due to the smallest singular value $\underline{\sigma} < 1$. This is in line with the open loop simulations of this configuration, where u_2 did not have much effect on y_1 or y_2 . This can also be seen from Eq. 3.14, where the two terms in dx_i/dt involving R almost cancel.

Pairing Intuitively, one will expect to pair feed rate with product rate (u_1 with y_1) and the manipulator for recycle/purge with purge composition (u_2 with y_2). However a more careful analysis reveals that there is considerable interaction, and at high frequency the best pairing is the opposite. The 1,1-RGA-element (for the pairing u_1 to y_1) is shown as a function of frequency in Fig. 3.5. We note that it changes from close to 1 at low frequencies to 0 at high frequencies, indicating serious interaction in the

Figure 3.5: 1,1-RGA-element (for the pairing u_1 to y_1)

(a) Configuration I.

(b) Configuration II.

(c) Configuration III.

Figure 3.6: Closed loop disturbance gain CLDG for all three configurations. Loops are paired $u_1 - y_1$ and $u_2 - y_2$.

intermediate frequency range and also that the preferred pairing changes from low to high frequency. This results from changes in u_2 changing both the reactor feed flowrate and reactor feed inert fraction. The two changes have an opposite effect on x_{SI} , thus cancelling each other and giving the opposite preferred pairing at high frequencies.

Disturbance rejection Fig. 3.6 shows the closed loop disturbance gain for configuration I, II and III. The sensitivity of the production P to both disturbances does not roll off at high frequencies, i.e. there is a direct effect to this measurement. This is natural since both disturbances will affect the reactor feed flowrate and feed composition immediately. Without any variable holdups in the process, there will be no damping of transients to P . Thus, the analysis tool CLDG suffers from the low level of model detail. Results in section 3.4.2 will address this and give results for a more detailed system description of the flash tank.

It is worth noting that the reaction constant has a negligible closed loop steady state effect on the production for all configurations. The initial change in production

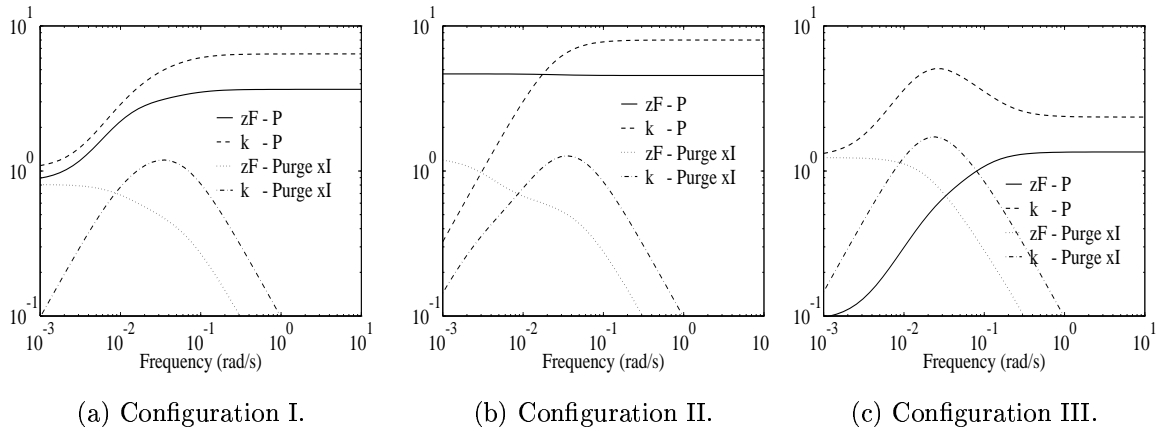


Figure 3.7: CLDG for all three configurations, **reversed** pairing.

from a change in k is later cancelled out by the secondary change in the recycle stream and thus the amount of component A in the reactor feed.

In Fig. 3.7 is shown the closed loop disturbance gain for the same three configurations, but with reversed pairing. All configurations have comparable disturbance rejection properties with the reversed pairing. The low frequency CLDG is somewhat different, although this is anyway where control works well. In addition, there is a slight increase in the effect of z_F on P when using u_2 to control P . This comes from $u_1 = F$ and u_2 having opposite effect on the reactor feed inert fraction when used to counter a change in P .

In Fig. 3.8a we show the minimum control error given constraints on the input variable. Fig. 3.8b shows the minimum input signal for constrained outputs ($\|y\| < 1$). The maximum disturbance range is not shown. As mentioned in section 3.2.2, several approximations exist that may enhance the solution procedure. Fig. 3.8a and b employ real u and d , while Fig. 3.8b also uses a real constraint on y . The latter approximation made the solution easier, removing the high spikes in $\|u\|$ that stem from the real-complex mismatch.

From the curves above it seems the best configuration is II, followed by I and III, as found by the open loop simulations.

The model used for calculating $\max_d \min_u \|y\|_\infty$ is linear, but through the constraints the effects of the two disturbances are not additive. In Fig. 3.9 we show the minimum control error decomposed into the effects of the individual disturbances for configuration II. The sum of the single disturbance effects does not equal the result as calculated by Eq. 2.13, although the difference is small. The figure illustrates the problems using only single loop gain and single step responses to evaluate disturbance rejection. It is interesting to note that the individual disturbance effects are dominating at different frequencies. For the best configuration II above, disturbance 1 (z_{FI}) contributes most to the offset at low frequencies, while disturbance 2 (k) is most dominant at high frequencies.

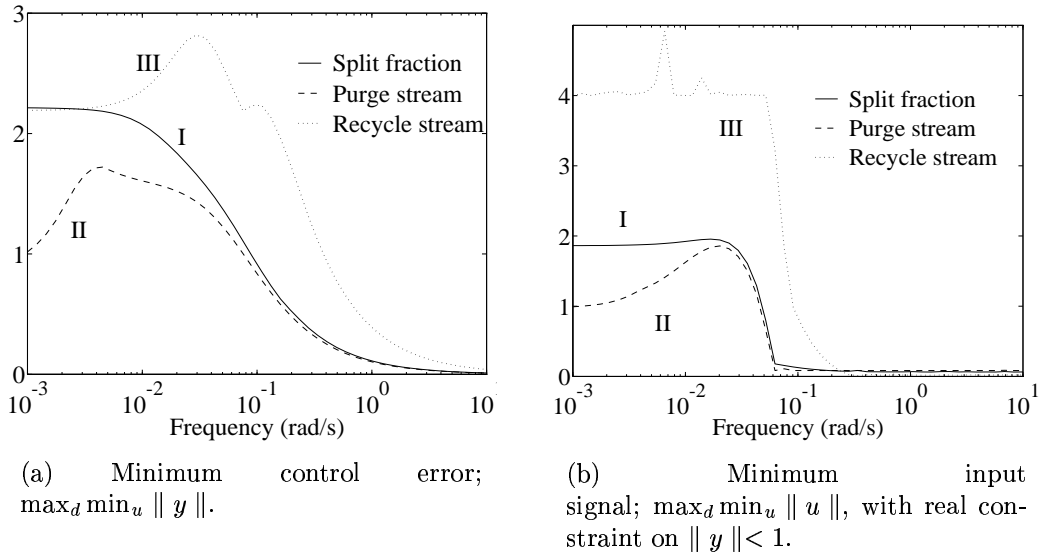


Figure 3.8: $\max_d \min_u y$ and $\max_d \min_u u$ for recycle problem.

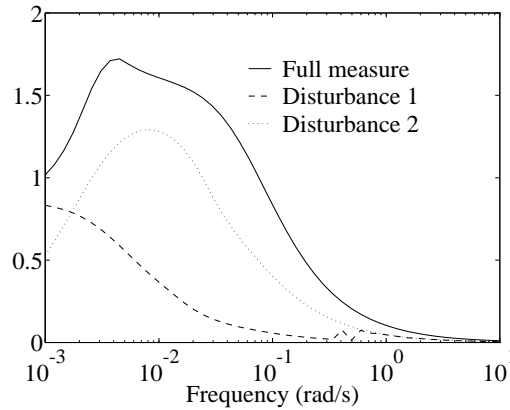


Figure 3.9: Minimum control error decomposed into effect of separate disturbances. Configuration II.

It is possible to use these measures to establish at which frequency the system is most sensitive to disturbances. By investigating the effect of the different disturbances at this frequency, limits for open-loop disturbance amplitude may be found for control failure.

To conclude the controllability analysis; configuration III is worst with respect to interaction with the given pairings. The three configurations are not very different in terms of closed loop disturbance gain. The direct effect of disturbances on P is not very large and will in any case be at frequencies where interaction prohibits good control. The minimum control error and minimum input signal measures both favor configuration II over I and III.

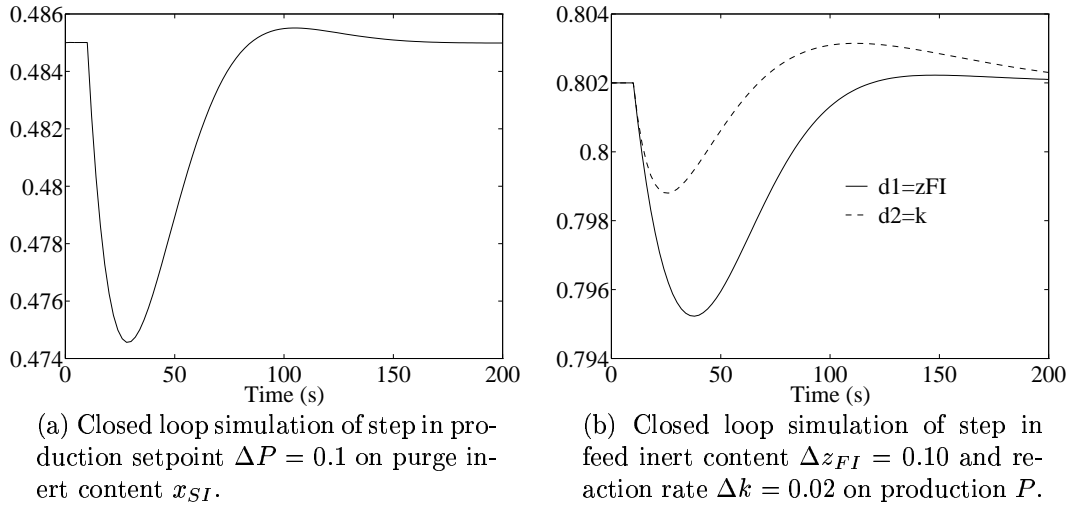


Figure 3.10: Effect of P on x_{SI} and k on P , controlled system, configuration I .

3.3.5 Closed loop simulations

We will subsequently look at the closed loop properties of this recycle system. Attention is given to decentralized controllers, although the much of the controllability analysis results are also applicable to systems with more complex controller types, for example a multivariable controller or including a decoupler.

We first look at the intuitive pairing ($y_1 - u_1$ and $y_2 - u_2$), which showed little steady state interaction, but all the more at higher frequencies. Two proportional-integral controllers are used in the following. Because of the low order of the model, ordinary frequency domain tuning rules were not applicable. We therefore tuned the controllers to give use of manipulated variables around the scaling range. The following controller tunings were found suitable:

Loop	K	τ_I	
P	20	20	(3.23)
x_{SI}	-2	20	

Configuration I (ratio control) is examined. Fig 3.10a shows how the control of x_{SI} displays high frequency interaction to a setpoint change in P . Fig 3.10b shows the closed loop effect on P of disturbances in z_{FI} and k . The CLDG predicted no significant steady state effect of k on P and indeed u_1 returns to its initial value. However, the control of x_{SI} shows a slow settling, which in turn effects P .

Turning towards the reversed pairing, that is, $y_1 - u_2$ and $y_2 - u_1$, the results were considerably worse. The low gain from α to P together with low and intermediate frequency interaction gave large overshoots in P as well as a slower settling (not shown). Although this is not clearly indicated by the CLDG above, the gain matrix and the RGA give this rather straightforward.

3.4 System dependencies

This section will examine some of the possible changes to the system and how they affect the conclusions, without leaving the simple concept. The alterations that are discussed relate to reaction type, separation system dynamics and varying dynamics in the recycle loop. We primarily consider configuration I in the following.

3.4.1 Reaction type

The reaction has so far been assumed to be of first order, which is not uncommon. Reactions with nonlinear dependencies (i.e. $r \propto C_{reactant}$) may display other effects to the different actuator configurations. In cases where multiple reactions occur, varying reactor conditions may favor one reaction over another, creating several distinct operating regions, which in turn may favor different actuator configurations.

Looking first at the simple extension of having a second order reaction, $r = kC_A^2$, the changes are not very dramatic. The reaction constant is reduced by C_A to give an equal steady state operating point. λ_{11} , which describes the interaction properties, is slightly increased over all frequencies, for example is $\lambda_{11}(0) = 0.91$ versus 0.84 for the base case. The change in disturbance rejection properties, as described by the CLDG, are also small (when remembering to change the scale of the reaction constant disturbance).

3.4.2 Separation system dynamics

For some reaction systems, reactants and products may be easily separated. In many cases though, a complicated purification process is needed. For example in the production of MTBE (a motor fuel additive), the difficult separation of isobutane from butane can be an integral part of the recycle loop.

As long as normal operation is assumed in the separation system (product compositions are kept within prescribed bounds), changes in the amount of reactant in the reactor effluent will generally propagate through the separation system. With this assumption, the principle differences in configuration I, II and III should apply. To get an indication of the effect of the separation system dynamics, we introduce holdup in the flash tank.

Introducing variable holdup into the flash tank model is not straightforward with no energy balance. We therefore choose to use proportional controllers to regulate the liquid and vapor level to allow a comparison. Separation systems can have large holdups, so a holdup of 10 times the reactor holdup (i.e. $20 m^3$) is used, of which 75% is in the liquid. The interaction properties (in terms of RGA) are very similar to the base case as depicted in Fig. 3.11.

A complex separation system, where product compositions are also controlled, will introduce additional complexity to the analysis. For example, assume a distillation column instead of the proposed flash tank. Controlling the bottoms composition with, say, the boilup rate will also be affected by the recycle as mentioned by Papadourakis *et al.* (1987).

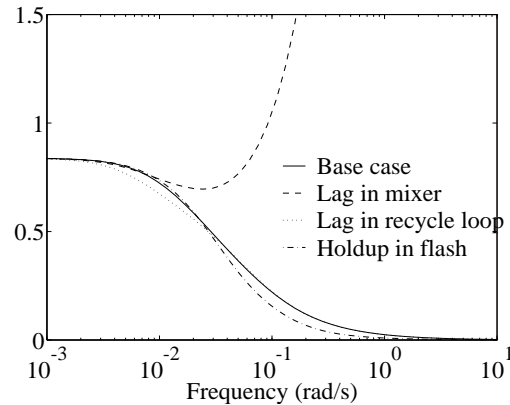


Figure 3.11: 1,1-RGA element with dynamics introduced to various units. Ratio control, configuration I.

3.4.3 Recycle loop dynamics

The recycle loop in our case includes no dynamic elements or deadtime. Both these effects will change the overall dynamics. However, assuming the recycle loop dynamics does not change the recycle composition (i.e. pure lag components), it will primarily affect the high frequency dynamics. The effect of this can be seen by including a tank in the feed/recycle mixer. We assume this tank (for example, for evening out fluctuations) to be 50% of the reactor tank size. We also look at having a similar lag element in the recycle loop only. The relative gain array for these cases are given in Fig. 3.11.

Looking at the first two cases (base case and lag in mixer), the interaction properties are similar at low frequencies, but with a marked difference above 0.1-1 rad/s . This frequency is related to the residence time in the mixer, $\tau = V/q = 1/0.109 \approx 9s$. Smaller or larger residence time in the mixer gives different frequencies where the interaction changes from the base case. The limiting case with an infinitely small mixer lag corresponds to the base case.

Having a lag element *only* in the recycle loop is almost identical to the 'base case' in terms of interaction, with only minute differences at intermediate frequencies, $\lambda_{11}(0)$ and $\lambda_{11}(\infty)$ are equal to the simplest base case. Further investigations show that all process configurations with a lag element in the mixer show high frequency interaction. The reason is as follows. An increase in the recycle flow R will immediately increase the reactor feed flow F_i . When a tank (lag) is present in the mixer, the corresponding inert fraction in the reactor feed (denoted x_i here) will at first *not* increase. When, on the other hand, the lag is in the recycle loop, then the reactor feed inert fraction will increase, due to the larger inert fraction in the recycle loop than in the fresh feed. So, there are two different effects; an increase in F_i and an increase in x_i . These two changes will (separately) give opposite effects in the purge inert fraction, x_{SI} . To summarize; a lag in the feed recycle mixer will dampen the change in x_i which competes with a change in F_i . This characteristic leads to the difference in high frequency interaction.

3.4.4 Unit time constants

The residence time (or time constant) of both reactors (τ_R) and the separation system (τ_S) can display large variations. Oil crackers, for example, do their reaction in around a second, while catalytic reforming and alkylation may take 30 minutes or more. Similar variations exist in separation systems. The difference in dominating time constant will determine which dynamics that will be most important for controlling the system as a whole (the exit point for the product is of course also important). For plants with $\tau_R/\tau_S \in < 0.1, 10 >$ one may anticipate that the dynamics of both plants are important, while plants with values outside this approximate range will be dominated by the slowest dynamics.

3.5 Conclusion

- Choosing manipulators on the regulatory control level must take into account the disturbance propagation. When recycles are present secondary effects must be evaluated.
- The correct use of combinations of analysis tools enhances the possibility of finding the best control configuration.

Specific to recycle systems:

- Using purge (configuration II) for control is bad due to the sensitivity to feed composition. Ratio control is better than using the recycle flow for control.
- Investigating controllability as a function of model complexity reveals that the simple model is able to capture the most significant effects.

Nomenclature

- A - Component, [-]
 B - Component, [-]
 C - Concentration, [$kmol/m^3$]
 d - Plant disturbance, [-]
 e - Control error, [-]
 F - Feed, [$kmol/s$]
 G - Plant transfer matrix, [-]
 G_d - Disturbance plant transfer matrix, [-]
 I - Inert component, [-]
 k - Reaction rate constant, [s^{-1}]
 K - Vapor liquid equilibrium constant, [-] or controller gain
 M - Reactor holdup, [$kmol$]
 P - Product, [$kmol/s$]
 R - Recycle stream, [$kmol/s$]
 S - Sensitivity function, [-]
 S - Purge, or side product, [$kmol/s$]

u - Plant input, [-]
 U - Output directions from SVD decomposition, [-]
 V - Flash vapor product, [$kmol/s$] and reactor volume, [m^3]
 V - Input directions from SVD decomposition, [-]
 x - Liquid mole fraction, [$kmol/s$]
 y - Plant output, [-]
 y - Vapor mole fraction, [-]
 z - Feed mole fraction, [-]

greek

α - Split fraction, [-]
 γ - Condition number, [-]
 Δ - Closed loop disturbance gain, [-]
 Λ - Relative gain array, [-]
 Σ - Matrix of singular values, [-]
 σ - Singular value, [-]
 τ - Controller reset time or unit time constant, [s]

subscripts

i - Component index (molefractions) or input/output index (u, y)
 ij - Stream and component index or matrix position index

References

- [1] Denn, M.M. and R. Lavie, 1982, "Dynamics of Plants with Recycle", *Chem. Eng. Journal*, **24**, 55-59.
- [2] Geoffrion, A.M., 1972, "Generalized Benders Decomposition", *JOTA*, **10**, 4, 237-260.
- [3] Georgiou, A. and C.A. Floudas, 1989, "Structural Analysis and Synthesis of Feasible Control Systems - Theory and Applications", *Chem. Eng. Res. Des.*, **67**, p. 600-618.
- [4] Gilliland, E.R., L.A. Gould and T.J. Boyle, 1964, "Dynamic Effects of Material Recycle", *Preprints JACC, Stanford, Ca.*, 140-146.
- [5] Govind, R. and G.J. Powers, 1982, "Control System Synthesis Strategies", *AIChE J.* **28**, 60-73.
- [6] Luyben, W.L., 1993, "Dynamics and Control of Recycle Systems", *Ind. Eng. Chem. Res.*, **32**, 466-486.
- [7] Mathisen, K.W., S. Skogestad and E.A. Wolff, 1991, "Controllability of Heat Exchanger Networks", Paper 152n at *AIChE Annual Mtg.*, Los Angeles, USA.
- [8] J. Morud and S. Skogestad, 1994, "Effects of recycle on dynamics and control of chemical processing plants", *Computers and Chem. Engng.*, **18**, Suppl., S529-S534. (Supplement from symposium ESCAPE-3, Graz, Austria, July 5-7, 1993).

Stream name	Flow	x_A	x_B	x_I
Feed, F	1.00	0.90	0.00	0.10
Reactor feed, F_i	2.78	0.64	0.01	0.35
Reactor effluent, F_o	2.78	0.35	0.30	0.35
Flash bottoms, B	0.80	0.006	0.989	0.005
Flash top, V	1.98	0.50	0.02	0.48
Purge, S	0.20	0.50	0.02	0.48
Recycle, R	1.78	0.50	0.02	0.48

Table 3.1: Stream data.

- [9] Papadourakis, A., M.F. Doherty and J.M. Douglas, 1987, "Relative Gain Array for Units in Plants with Recycle", *Ind. Eng. Chem. Res.*, **26**, 1259-1262.
- [10] Rinard, I.H. and B.W. Benjamin, 1982, "Control of Recycle Systems. Part 1. Continuous Control", *Preprints ACC 82*, Session WA5.
- [11] Shinskey, F.G., 1984, "Distillation Control", McGraw-Hill, New York, USA.
- [12] Skogestad, S. and M. Hovd, 1990, "Use of Frequency-Dependent RGA for Control Structure Selection", *Proc. American Control Conference (ACC)*, 2133-2139, San Diego, May 1990.
- [13] Taiwo, O., 1986, "The Design of Robust Control Systems for Plants with Recycle", *Int. J. Control*, **43**, 2, 671-678.
- [14] Verykios, X.E. and W.L. Luyben, 1978, "Steady-state Sensitivity and Dynamics of a Reactor/Distillation Column System with Recycle", *ISA Transactions*, **17**, 2, 31-41.

Appendix 1. Model for Recycle example.

The system consists of a mixer, reactor, separator and a tee. The conditions in the reactor are described by three ordinary differential equations:

$$\begin{aligned}
 \frac{dC_A}{dt} &= \frac{F_i}{V}(C_{A_i} - C_A) - kC_A \\
 \frac{dC_B}{dt} &= \frac{F_i}{V}(C_{B_i} - C_B) + kC_A \\
 \frac{dC_I}{dt} &= \frac{F_i}{V}(C_{I_i} - C_I)
 \end{aligned} \tag{3.24}$$

The volume of the reactor is constant; $V = 2 \text{ m}^3$. The nominal feed to the mixer $F = 1 \text{ kmol/s}$ consists of 90 % A and 10 % I. The nominal values of the full stream set are given in Table 3.1.

The reaction constant $k = 0.05$. The flash is essentially an ideal separator between components A and I (top product) and component B (bottom product). The equations

are

$$\begin{aligned}y_i &= K_i x_i \\F &= V + L \\Fz_i &= Vy_i + Lx_i \\ \Sigma x_i &= 1\end{aligned}\tag{3.25}$$

Remark: In the analytical expressions a perfect split is assumed such that $V = F_o(x_A + x_I)$, $P = F_o x_B$ where x_A , x_B and x_I are the molefractions in the reactor.

The K-values used in the flash calculations were $K_A = 80$, $K_B = 0.02$ and $K_I = 100$. A density of 900 kg/m^3 and an average moleweight of 40 kg/kmol were used in the conversion between mole flow and volume flow. The mixer, splitter and flash all consist of algebraic equations, giving a total problem of index 1.

Chapter 4

Control Configuration Selection for Distillation Columns Under Temperature Control

Erik A. Wolff* and Sigurd Skogestad†
Chemical Engineering
University of Trondheim - NTH
N-7034 Trondheim, Norway

Extended version of paper
presented at
ECC '93, Groningen, June/July 1993

Abstract

This paper examines how difficult control tasks are enhanced by introducing secondary measurements, creating control cascades. Temperature is much used as secondary measurement because of cheap implementation and quick and accurate response. Distillation is often operated in this manner due to slow or lacking composition measurements, although the benefits have hardly been investigated closely, especially for multivariable control applications. We therefore use distillation as example when quantifying improvements in interaction and disturbance rejection. We also give analytical expressions for the secondary controller gain. The improvements are reached through simple cascade operation of the control system and requires no complicated estimator function.

*Present Address: ABB Environmental, Box 6260 Etterstad, N-0603 Oslo, Norway

†Address correspondence to this author. Fax: 47-73594080, E-mail: skoge@kjemi.unit.no

4.1 Introduction

In most process control applications, the structural issues which precede the actual controller design are the most important. The problem of *control structure selection* involves the following decisions:

1. Selection of control objectives, actuators and measurements.
2. "Control configuration selection": Selection of controller structure (e.g., pairing of actuators for decentralized control).

Note that we define the last step as the "control configuration selection", whereas the combination of the two steps is denoted the "control structure selection".

In practice, control systems are implemented in a hierarchical manner, with a regulatory ("basic") control system at the lowest level. The two main objectives for the regulatory control system are:

1. Take care of control tasks where fast response is needed.
2. Make the control problem, as seen from the levels above, simple.

The higher levels in the control system may include a supervisory and optimizing control system or simply the operator. In any case, the issue of control structure selection is usually most important for regulatory control. This is because the main control objective at this level is to facilitate good operation, that is, to implement a simple control system that makes it easy for the operators to operate the plant. Thus, the control objectives are not clearly defined at this level, and since the control system should be simple we generally want to implement decentralized SISO controllers.

Specifically, one often has extra measurements which are not particularly important to the control of the plant from an overall (or economic) point of view. However, at the regulatory control level one often uses these variables as *secondary control objectives* by closing local loops. Typically, such variables may include selected temperatures and pressures. The setpoints for these loops may be adjusted from the higher levels giving rise to a *cascaded control system*. Effectively, by closing secondary control loops, we replace the original independent variables (typically, flows and valve positions in process control applications) by some new independent variables (the setpoints for the secondary control variables). The idea is then that the control problem in terms of these new independent variables is simpler, and at least that they need not be adjusted so frequently, that is, the "fast control" is taken care of by the secondary control loops implemented at the regulatory level.

A block diagram is shown in Fig. 4.1. Here u_2 represents the original independent variables which are used to control the secondary ("extra") outputs, y_x . After closing the secondary control loops the setpoints for the secondary loops y_{xs} become the new control variables, $u_x = y_{xs}$.

Some work has been done on comparing ordinary feedback control with cascade control (see for example Krishnaswamey *et al.*, 1990). These results mainly recommend

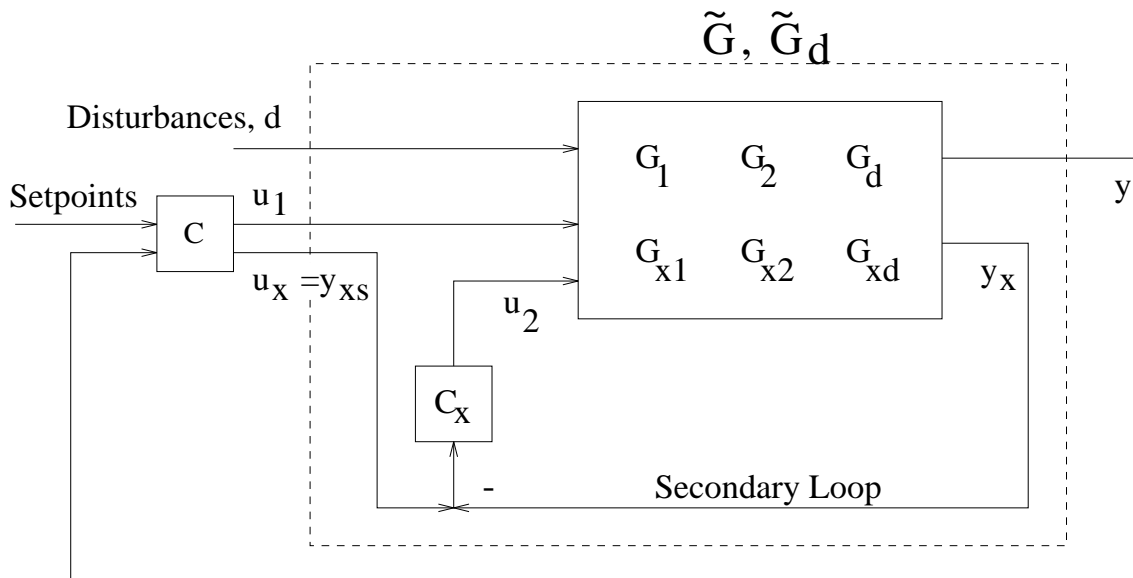


Figure 4.1: Block diagram with secondary loop closed.

using cascades when the deadtime in the secondary loop is much smaller than in the primary loop.

In most practical cases it is desirable to have the secondary loops as fast as possible. Thus, when the operator or higher levels in the control system change u_x , this results in an almost immediate change in y_x , i.e., $y_x \approx u_x$. Also, in this case the tuning of the secondary loops does not matter much for the overall system (provided they are sufficiently fast). However, the distillation example presented in this paper illustrates that in some cases it may be better to *not* tune the secondary loop as fast as possible and use, for example, a proportional controller in the secondary loop.

Simple proportional controllers are normally used as secondary controllers, the reason being that the primary loop will have integral action and remove stationary error anyway. In some applications PI secondary loop controllers may be beneficial, most notably when the primary loop is very slow compared to the secondary loop (e.g. Krishnaswamey *et al.*, 1992).

In this paper we use distillation column control as an application. The main control problem here is the strong coupling between the two loops as indicated, for example, by the large RGA-values. In the paper, we study how the use of temperature cascades, in addition to improving the operation, may help reduce this interaction.

4.2 Distillation control

Control of distillation columns is a challenging problem due to strong interactions, nonlinear behavior and the large number of possible control structures. A simple distillation column (Fig. 4.2) may, from a control point of view, be considered a 5×5 problem with L, V, D, B and V_T as the manipulated inputs (actuators) and x_D, x_B (product quality), M_D, M_B (levels) and p (pressure) as the controlled outputs (control

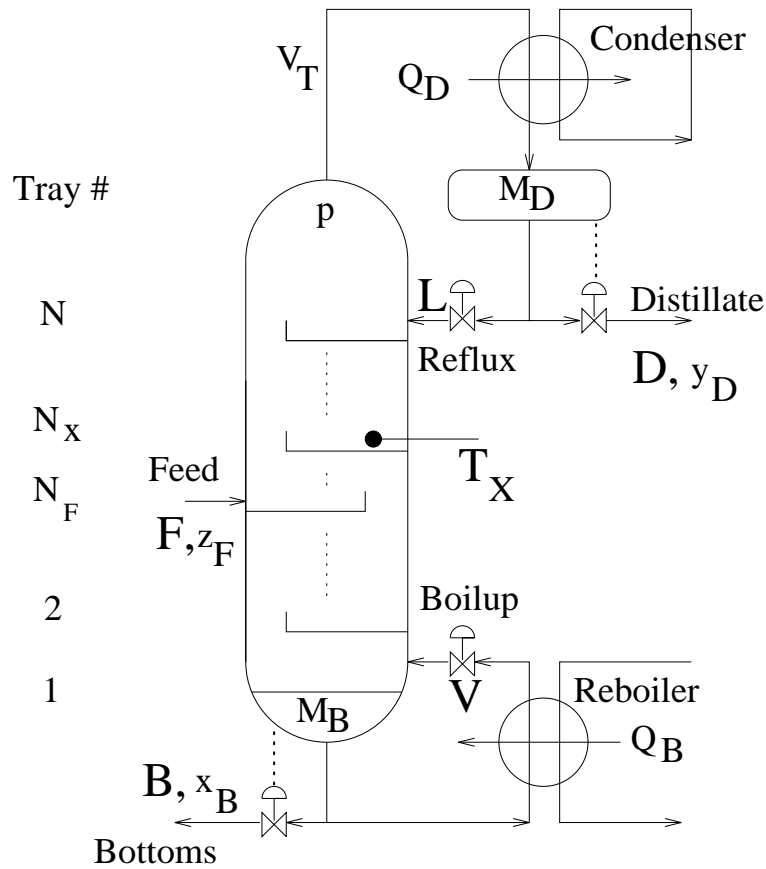


Figure 4.2: Typical distillation column using LV-configuration.

objectives). Typical disturbances (d) include feed composition (z_F), feed flowrate (F) and feed enthalpy (q_F).

In practice, distillation columns are usually controlled in a hierarchical manner with the three loops for level and pressure control implemented at the regulatory control level. The “conventional” distillation control configuration selection problem, which addresses which of the five inputs should be used for control in these three loops, has been discussed by a number of authors (e.g., Shinskey, 1984, Skogestad *et al.*, 1990). By convention, the resulting configuration is named by the two independent variables which are left for composition (quality) control, for example, the LV-configuration uses reflux L and boilup V for composition control. In this paper the LV and $(L/D)(V/B)$ configuration are considered.

The quality control is often implemented at some higher level or left for manual control by the operators. However, this approach has several problems:

- Unless very fast control is used, the use of $u_1 = V$ and $u_2 = L$ to control the $y_1 = x_B$ and $y_2 = x_D$ yields a very difficult control problem with strong interactions and large RGA-values.
- There is often a long delay associated with measuring the product compositions which makes fast control impossible.

- There is a need to close at least one loop with relatively fast control in order to "stabilize" the compositions in the distillation column, which otherwise behave almost as a pure "integrator".

To deal with at least the last problem one often implements a secondary temperature loop at the regulatory control level (e.g., Kister, 1991). This loop makes it possible for the operators to operate the column when the composition loops are not closed.

Remark. An alternative approach is to use multiple temperature measurements along the column to estimate the compositions (e.g., Mejdell and Skogestad, 1991ab). This avoids the measurement delay and makes it easier to have fast control. However, even in this case one may for operational reasons want to close one temperature loop at the regulatory control level as described above.

4.3 Closing secondary loops

4.3.1 General results.

From Fig. 4.1 we have with the secondary loops open ($C_x = 0$)

$$y = G_1 u_1 + G_2 u_2 + G_d d \quad (4.1)$$

(Note that we have assumed that some regulatory loops, e.g., the pressure and level loops for distillation columns, have been closed). Similarly, with $C_x \neq 0$, the model for the secondary output is

$$y_x = G_{x1} u_1 + G_{x2} u_2 + G_{xd} d \quad (4.2)$$

Closing the secondary loops, effectively means that we replace the inputs u_2 by the setpoints $u_x = y_{xs}$, and for the cascaded system, we get,

$$y = \tilde{G}_1 u_1 + \tilde{G}_2 u_x + \tilde{G}_d d \quad (4.3)$$

where

$$\tilde{G}_1 = G_1 - G_2 C_x (I + G_{x2} C_x)^{-1} G_{x1} \quad (4.4)$$

$$\tilde{G}_2 = G_2 C_x (I + G_{x2} C_x)^{-1} \quad (4.5)$$

$$\tilde{G}_d = G_d - G_2 C_x (I + G_{x2} C_x)^{-1} G_{xd} \quad (4.6)$$

In most cases we use decentralized control for the cascade loops and C_x is a diagonal matrix. The use of the cascade clearly changes the "effective" plant as seen from the disturbances and inputs. Specifically, if the cascade loops are slow ($C_x \rightarrow 0$) we have

$$\tilde{G}_1 = G_1, \quad \tilde{G}_2 = G_2 C_x, \quad \tilde{G}_d = G_d \quad (4.7)$$

and as expected the system behaves as without the cascade except that the inputs u_2 are scaled by C_x . At the other extreme, tight control of the secondary variables ($C_x \rightarrow \infty$) yields $G_2 C_x (I + G_{x2} C_x)^{-1} \approx G_2 G_{x2}^{-1}$ and

$$\tilde{G}_1 = G_1 - G_2 G_{x2}^{-1} G_{x1}, \quad (4.8)$$

$$\tilde{G}_2 = G_2 G_{x2}^{-1},$$

$$\tilde{G}_d = G_d - G_2 G_{x2}^{-1} G_{xd}$$

The changes in control properties resulting from implementing the secondary loops may be analyzed by use of a number of standard measures for linear controllability evaluation, such as RHP-zeros, RGA-analysis for interactions, disturbance sensitivity and sensitivity to model uncertainty.

4.3.2 Analysis tools

In this paper we mainly use the relative gain array (RGA or Λ) to look at interaction in the distillation column with an added temperature control loop. The properties of the RGA are well known (e.g., Grosdidier *et al.*, 1985). The most important for our purpose are: 1) No two-way interaction is present when $\Lambda = I$, 2) The RGA is independent of scaling in inputs or outputs, and 3) The rows and columns both sum up to 1. For 2×2 systems the RGA is especially easy to compute; because of the third property mentioned, we only have to compute the (1,1) element of the RGA which is given by $\lambda_{11} = 1/(1 - Y)$, $Y = \frac{g_{12}g_{21}}{g_{11}g_{22}}$. One deficiency of the RGA is that triangular plants (having only one way interaction) give $\Lambda = I$. Hovd and Skogestad (1992) therefore introduced the Performance relative gain array. The PRGA is defined as $\Gamma = G_{diag}G^{-1}$, where G_{diag} is the matrix consisting of only the diagonal elements of G .

To evaluate the disturbance sensitivity, we consider the closed-loop disturbance gain (CLDG) which is the appropriate measure when we use decentralized control (Hovd and Skogestad, 1992). The CLDG is defined as $G_{diag}G^{-1}G_d$, where G_{diag} consists of the diagonal elements of G .

Although the main part of the analysis is based on the RGA, we also provide detailed controller designs and simulations to confirm the predictions.

4.3.3 Temperature cascade for distillation column

We here consider composition control by manipulating the reflux L and boilup V (LV-configuration), but the following development also applies to other control configurations as well.

We use a tray temperature measurement for cascade control. Which tray to place this measurement on will be addressed in a later section. For a binary mixture with constant pressure there is a direct relationship between tray temperature (T) and composition (x). In terms of deviation variables we then have $T_x = K_{Tx}x_x$, where for ideal mixtures K_{Tx} is approximately equal to the difference in pure component boiling points. The open-loop model for the LV-configuration may be written,

$$\begin{pmatrix} x_D \\ x_B \\ x_x \end{pmatrix} = \begin{pmatrix} g_{11} & g_{12} \\ g_{21} & g_{22} \\ g_{x1} & g_{x2} \end{pmatrix} \begin{pmatrix} L \\ V \end{pmatrix} \quad (4.9)$$

where x_D , x_B and x_x are the compositions in the top, bottom and x^{th} tray of the distillation column. See also Fig. 4.3 for a description of the cascade.

We now implement a SISO controller from the temperature T_x to the reflux L : $L = c_x(T_s - T_x)$. (we could have used boilup instead). Here T_s is the setpoint for the

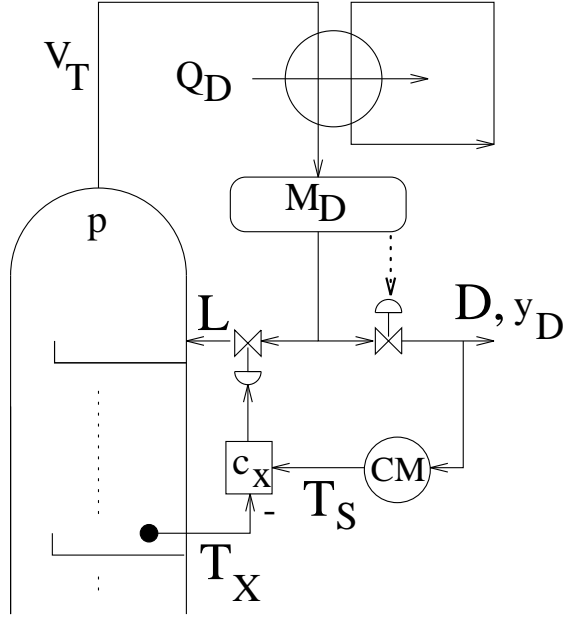


Figure 4.3: Composition control using temperature in secondary loop. CM is for composition measurement.

temperature loop which becomes the new manipulated variable instead of L . In terms of the general problem discussed above this corresponds to selecting $u_1 = V$, $u_2 = L$, $u_x = T_s$, $y_x = T_x$ and $y = [x_B \ x_D]^T$. We can now write the linear equations relating the top and bottom compositions to the new set of manipulated variables as

$$\begin{pmatrix} x_D \\ x_B \end{pmatrix} = \tilde{G} \begin{pmatrix} T_s \\ V \end{pmatrix}, \quad (4.10)$$

$$\tilde{G} = \begin{pmatrix} \frac{g_{11}c_x}{1+g_{x1}c_xK_{Tx}} & g_{12} - \frac{g_{11}g_{x2}c_xK_{Tx}}{1+g_{x1}c_xK_{Tx}} \\ \frac{g_{21}c_x}{1+g_{x1}c_xK_{Tx}} & g_{22} - \frac{g_{21}g_{x2}c_xK_{Tx}}{1+g_{x1}c_xK_{Tx}} \end{pmatrix}$$

The RGA for \tilde{G} can now be computed to study the interaction properties of the column for different temperature loop gains c_x ,

$$\lambda_{11}(\tilde{G}) = \left(1 - \frac{g_{21}g_{12} - \frac{g_{21}g_{11}g_{x2}c_xK_{Tx}}{1+g_{x1}c_xK_{Tx}}}{g_{11}g_{22} - \frac{g_{21}g_{11}g_{x2}c_xK_{Tx}}{1+g_{x1}c_xK_{Tx}}} \right)^{-1} \quad (4.11)$$

We have the two limiting cases,

$$c_x = 0: \quad \lambda_{11}(\tilde{G}) = \left(1 - \frac{g_{12}g_{21}}{g_{11}g_{22}} \right)^{-1} = \lambda_{11}(G) \quad (4.12)$$

$$c_x = \infty: \quad \lambda_{11}(\tilde{G}) = \left(1 - \frac{g_{21}(g_{12}g_{x1} - g_{11}g_{x2})}{g_{11}(g_{22}g_{x1} - g_{21}g_{x2})} \right)^{-1} \quad (4.13)$$

As expected, with sufficiently slow temperature cascade controllers the RGA is unchanged.

Ideally, we would like no two-way interaction. Setting $\lambda_{11} = 1.0$ and solving Eq. 4.11 for c_x yields the following “optimal” feedback controller,

$$c_x^* = K_{Tx}^{-1} \left(\frac{g_{12}}{g_{11}g_{x2} - g_{12}g_{x1}} \right) \quad (4.14)$$

The “optimal” loop transfer function for the temperature loop is then given by,

$$L^* = c_x^* K_{Tx} g_{x1} = - \left(1 - \frac{g_{11}g_{x2}}{g_{12}g_{x1}} \right)^{-1} = \lambda_{11}(G^s) - 1 \quad (4.15)$$

where

$$G^s = \begin{pmatrix} g_{11} & g_{12} \\ g_{x1} & g_{x2} \end{pmatrix} \quad (4.16)$$

Thus the optimal loop gain is essentially equal to the RGA involving x_D and x_x as outputs. We note that when x_D and x_x are strongly coupled (in terms of the RGA) then the loop gain should be large. Also, the bandwidth of the cascade loop should be approximately equal to the frequency where this RGA approaches 1. Since for the LV-configuration the shapes of the open-loop gains (e.g. g_{x1}) and the RGA as a function of frequency are similar (they break off at the dominant time constant, e.g., see Skogestad *et al.* (1990)), it seems that a simple proportional controller should be close to the optimal choice. Thus, in the example below we will only consider the steady-state value of $\lambda_{11}(\tilde{G})$ and primarily assume that c_x is a P controller.

4.4 Distillation example

We consider as an example high-purity binary distillation. We study the system corresponding to column A studied by Skogestad and Morari (1988) with the addition of liquid flow dynamics. The basic data are given below:

#Trays	x_D	$1 - x_B$	z_F	L/F	M_i/F [min]
41	0.99	0.99	0.5	2.71	0.5

We use a 82nd order linear model in all work in this paper. The resulting liquid lag from the top to the bottom of the column is about $\theta_L = 1.5$ min. The steady-state RGA-value of the model is $\lambda_{11}(G) = 35.5$ and approaches 1 at frequency $1/\theta_L$ (also see Fig. 4.5 with $K_c = 0$).

4.4.1 Selection of tray for temperature sensor

There are several effects that must be taken into account when choosing where to install the temperature sensor: 1) When using a secondary loop involving reflux as the input, the sensor should be placed in the top part of the column to minimize the process delay due to the liquid flow dynamics. 2) The interaction properties as expressed by the optimal loop gain in Eq. 4.15 will depend on the location. When reflux is used for the secondary temperature loop, placing the temperature close to the top will lead to

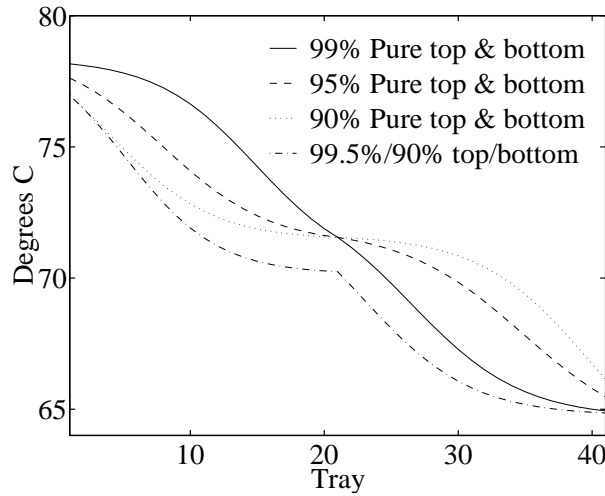


Figure 4.4: Steady-state column temperature profile at different operating points. (Bottom is Tray 1.)

an infinite loop gain and it will drop down to a value of $\lambda_{11}(G) - 1 = 34.5$ with the measurement located at the bottom of the column. 3) The temperature measurement should be sensitive such that it may be distinguished from noise (this consideration is probably the most important). Other sources of measurement uncertainty are pressure variations (typically $\pm 2\%$) and variations in content of non-product components in the multicomponent case. These considerations often translate to a minimum temperature sensitivity of 1°C .

It is important to note that the existing column profile may dictate in which end to implement a secondary measurement. This results from the column profile sometimes showing significant temperature variations in only the rectifying or stripping section depending on the design, operating point and feed composition. See also Tolliver and McCune (1980) for a further discussion on optimum temperature control trays.

Fuentes and Luyben (1983) claim that a loosely tuned (proportional only) cascade loop is best for rejecting feed composition disturbances while tight tuning takes best care of feed rate disturbances.

Fagervik *et al.* (1983) hold that one-way decoupling seems preferable to two-way decoupling in dual composition control. This is due to better or equal performance and less sensitivity to modeling inaccuracies.

Fig. 4.4 depicts different column temperature profiles as a function of operating conditions. To get high sensitivity (point 3 above) we have chosen to control the temperature at tray 34 (tray 8 counted from the top) for the remaining analysis.

4.4.2 Controllability analysis

The model in Eq. 4.9 then becomes, at steady-state,

$$\begin{pmatrix} x_D \\ x_B \\ x_{34} \end{pmatrix} = \begin{pmatrix} 0.8754 & -0.8618 \\ 1.0846 & -1.0982 \\ 6.3912 & -6.3051 \end{pmatrix} \begin{pmatrix} L \\ V \end{pmatrix} \quad (4.17)$$

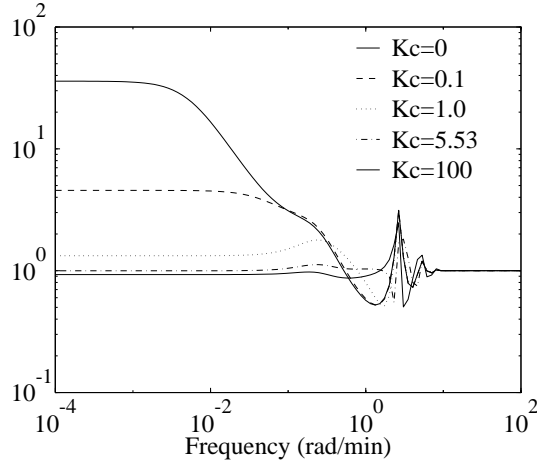


Figure 4.5: Effect on the frequency-dependent RGA, $\lambda_{11}(\tilde{G}(j\omega))$, of varying gain in the secondary loop, $c_x = K_c$.

We get

$$\lambda_{11}(G^s(0)) = \left(1 - \frac{g_{12}g_{x1}}{g_{11}g_{x2}}\right)^{-1} = 477.9 \quad (4.18)$$

and since $K_{Tx} = -13.5$ in our example, we will have no two-way interaction at steady state with the optimal P-controller having gain

$$c_x^* = K_c = \frac{1}{K_{Tx}g_{x1}}(\lambda_{11}(G^s(0)) - 1) = \frac{476.9}{-13.5 \cdot 6.3912} = -5.53 \quad (4.19)$$

To avoid misinterpretation of “larger” and “smaller” values of K_c , we will speak of $|K_c|$ (i.e. absolute value) in the rest of [this](#) section.

Frequency-dependent RGA-plots for the column, $\lambda(\tilde{G}(j\omega))$, with various gains for the temperature cascade are shown in Fig. 4.5. We note that with $K_c = 5.53$ the RGA is close to 1.0 at most frequencies (and not only at steady-state), confirming that a simple P-controller is close to the optimal. It is interesting to note that $\lambda_{11} = 1.0$ is not a limit, as for $K_c > 5.53$ the interaction becomes more pronounced again with $0 < \lambda_{11} < 1$.

The loop gain $L = K_c K_{Tx} g_{x1}$ for the cascade loop with the “optimal” controller gain $K_c = 5.53$ is shown in Fig. 4.6. The loop gain crosses 1 in magnitude at frequency $\omega_c = 3.0$ rad/min, which is the approximate bandwidth of that loop. Due to valve dynamics and measurement dynamics, a liquid lag of about 0.3 min from the top to tray 34, etc., it seems that the closed-loop bandwidth must be about 1 rad/min or less. Thus in practice, the controller gain should be reduced by a factor of about 3.0, and we will use a controller gain $K_c = 1.84$ in the following.[‡] This will not have much effect on the “decoupling” property of the secondary loop, as we note from Fig. 4.5 that the RGA-plot is rather insensitive to the value of K_c .

[‡]Alternatively, we might have introduced dynamics into c_x to avoid instability. For example, since with infinite gain the RGA at steady-state is 0.925, which is very close to 1, we might have used a PI controller.

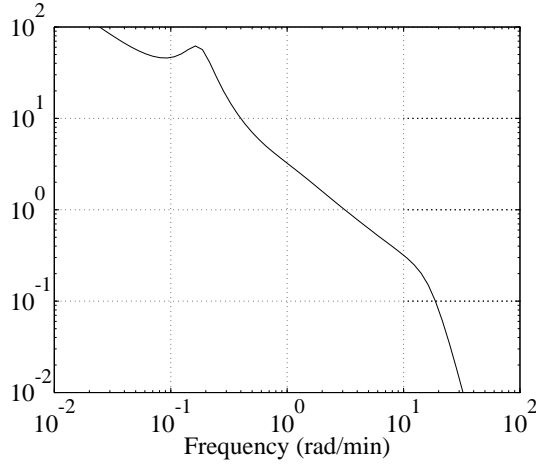


Figure 4.6: Loop gain for the secondary temperature loop with $K_c = 5.53$.

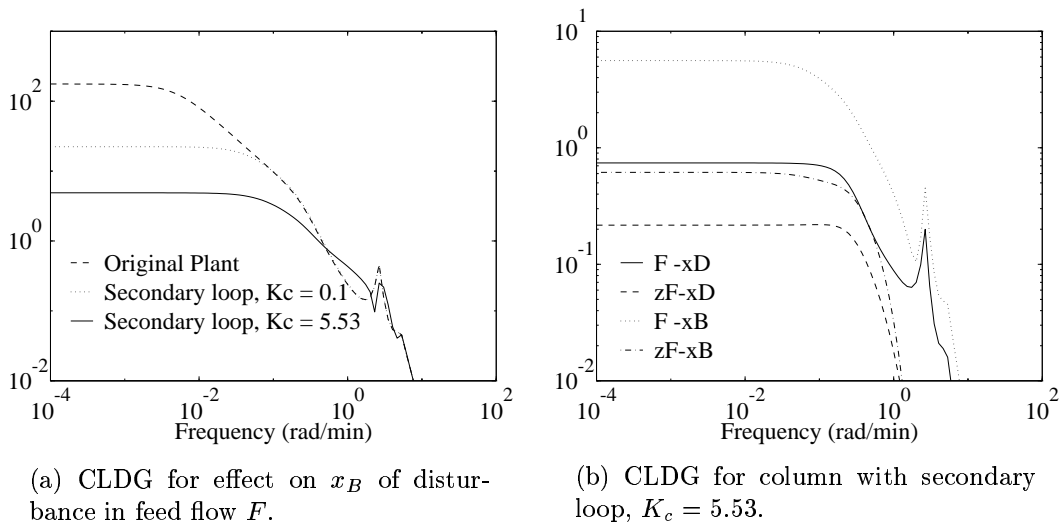


Figure 4.7: Improved disturbance rejection with temperature cascade. Note the different scales in the two plots.

No RHP-zeros are obtained for the resulting “open-loop” system $\tilde{G}(s)$ for any value of K_c .

The “closed loop” disturbance-rejection properties are also improved through use of the temperature cascade. This is seen from Fig. 4.7 which shows the Closed-Loop Disturbance Gain, $CLDG = G_{diag}G^{-1}G_d$, as a function of the secondary controller gain, K_c , for the most difficult disturbance (effect of F on x_B). All the elements are also shown for the column with a secondary loop with $K_c = 5.53$. Note that in the plots the outputs have been scaled such that an output of magnitude 1 corresponds to 0.01 mole fraction units.

The other elements of the CLDG were also improved by the temperature cascade.

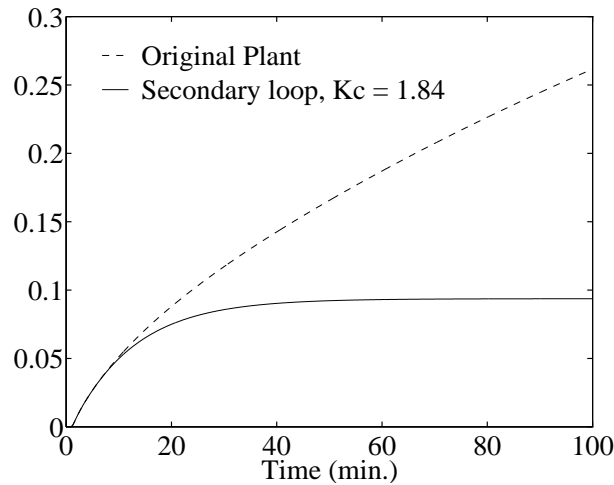


Figure 4.8: Improved open loop disturbance rejection with temperature cascade, $K_c = 1.84$. Plot shows response in Δx_B to a 1% disturbance in the feed rate, F .

This is specifically mentioned, as changes to the plant or control system may sometimes improve the disturbance rejection properties in one measurement at the expense of another. Here however, disturbance rejection was improved throughout.

4.4.3 Simulations

Similar results are obtained from Fig. 4.8 which shows a simulation of a step change in the same disturbance. We thus find that closing the secondary loop strongly reduces the sensitivity of the bottom composition to disturbances. The reason is of course that the compositions inside the column are strongly coupled, and fixing the composition at one point[§] results in small changes also at other locations. This is important because there is then less need to use fast control in the primary composition loops, and fast control in the primary loops is often impossible because of long measurement delays.

Closed loop simulations with also the two primary composition loops closed are even more interesting. A measurement delay of $\Theta = 6$ minutes for the compositions is used in both loops. For the original plant without the secondary temperature loop we use PID tunings from Skogestad and Lundström (1990):

<i>Loop</i>	K	τ_I	τ_D	
x_D	0.14	16.6	3.17	(4.20)
x_B	0.12	14.3	3.54	

For the case with a secondary temperature loop we use PID tunings based on the Ziegler-Nichols tuning rule but with the proportional gain reduced by a factor two (and again, $K_c = 1.84$),

<i>Loop</i>	K	τ_I	τ_D	
x_D	3.71	6.28	1.57	(4.21)
x_B	0.56	6.98	1.75	

[§]For a binary separation, temperature is a direct measure of composition.

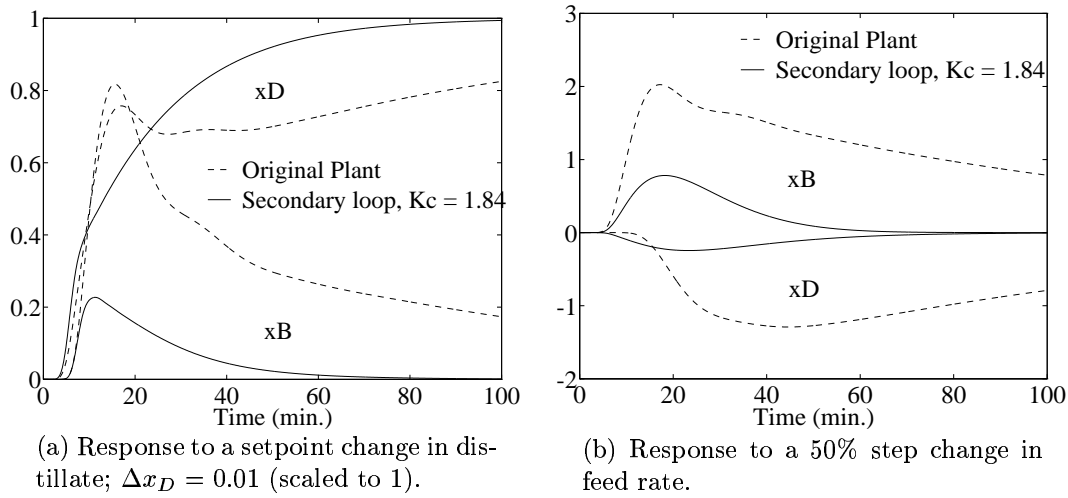


Figure 4.9: Time simulations with composition loops closed.

The temperature measurement in the latter case is passed through the filter

$$f = \frac{1}{1 + \tau_f s} \quad (4.22)$$

where $\tau_f = 0.5 \text{ min}$, to account for some sensor dynamics.

Time simulations with a comparison of the two control systems are given in Fig. 4.9. We see from the simulations that the secondary temperature loop provides for much better control of the top composition, x_D , with somewhat less improvement for the bottom composition, x_B . This is as expected since the temperature sensor is located towards the top (stage 34 or stage 8 from the top) and its setpoint is determined by the x_D -controller. In effect we have achieved a one-way decoupling: With $u_1 = V$ and $u_{2x} = T_s$ as the new inputs, we find that u_1 has an effect on $y_1 = x_B$, but very little effect on $y_2 = y_D$, whereas u_{2x} has an effect on y_1 and somewhat less effect on y_2 .

4.4.4 Actuator behavior

Including the secondary loop gives larger (and earlier) input signals (changes in reflux and boilup) than for the original plant. This is natural since the decoupling effect of the cascade allows us stable operation without detuning the composition controllers to account for the phase lag contribution of the deadtime.

It may be argued that this procedure will produce unrealistically large or oscillatory input signals, given the fast tuning of the secondary loop. Investigations show this to be of minor importance. Two aspects are evaluated: i) the actuator is too slow for this application and ii) oscillatory operation will give intolerable wear.

The effect of varying the filter time constant τ_f is evaluated with respect to composition response and actuator behavior in Fig. 4.10. The figure shows the responses in x_B and boilup V to a setpoint change in x_D for τ_f equal to 0.5, 1.5 and 5 minutes

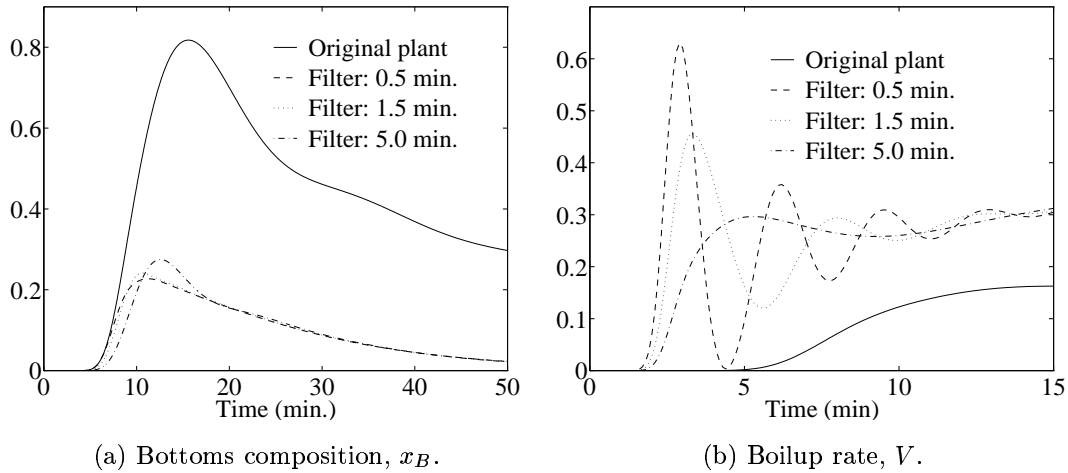


Figure 4.10: Response to a setpoint change in x_D ($\Delta x_D = 0.01$) for various filter time constants τ_f .

as well as the original plant with no secondary loop. The actuator behavior is significantly different for the varying τ_f ; the secondary loop gives an oscillatory use of the manipulated inputs with a fast secondary loop. As τ_f increases (the secondary loop becomes slower), V turns into a nicely damped almost first order curve. However, the composition responses are virtually equal to the system with short filter time constant with only a minor addition to the initial transients. The limited actuator dynamics does not remove the main effect of the temperature cascade; making the composition responses approximately as fast as the liquid lag through the column. This is quite readily observed in Fig. 4.10b, where V in the original plant is delayed by $\approx \Theta$ before counteracting changes in x_D . The column with the secondary loop, however, shows changes in V after $\approx \Theta_L$. Deadtime in the secondary loop has been neglected as this would obscure the comparison. Shorter deadtimes than in a composition measurement are however anticipated.

The conclusion is that a slower secondary loop will remove actuator oscillations with insignificant performance loss. Tuning of K_c is easily done online, confirming that removal of oscillations in the secondary loop may be a good starting point for tuning cascade control systems. Tuning of the primary loops based on a fixed K_C worked well. This solution seems robust to changing K_c values.

The benefit of including integral action in the secondary loop has also been evaluated, using the controller

$$c(s) = \frac{-1.84}{s}(1 + \tau_i s) \quad (4.23)$$

The integral time τ_i was kept high (low effect) to reveal primarily marginal effects.

Fig. 4.11 shows the response to a feed rate disturbance when integral action is included in the primary loop. We see that there is some improvement in the distillate composition control, while the overshoot in the bottoms composition becomes slightly worse. The distillate composition also shows a slightly delayed settling. The responses

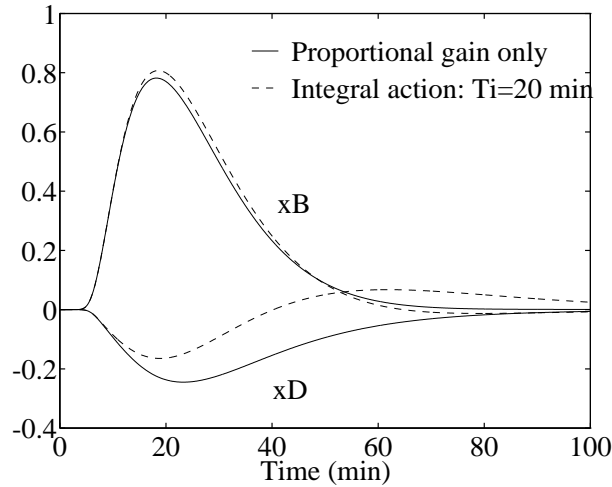


Figure 4.11: Response to a 50% step change in feed rate F with and without integral action in the secondary loop.

to changes in z_F and the setpoints behaved in largely the same manner (not shown); an improvement is in one output balanced by an increased overshoot in the other. There does not seem to be any incentive for including integral action in the secondary loop for this choice of deadtimes and time constants.

4.5 $(L/D)(V/B)$ Configuration

We will now turn our focus to the $(L/D)(V/B)$ configuration, that is, use the ratio between L and D to affect the top composition and manipulate the bottoms composition through the ratio between V and B . Shinsky (1984) claims that the $(L/D)(V/B)$ configuration is applicable over the broadest range of cases. This configuration has also been recommended by others (e.g. Rademaker, 1975). A drawback is the interdependence between level and composition control and the need for more measurements. This control configuration also depends on fast level control, without which the level and composition control will interact with each other.

The $(L/D)(V/B)$ control scheme generally has lower interaction in terms of RGA or Λ than for example the LV -configuration. Flow disturbances are also handled well. The reason for this is that the internal flows are adjusted together with the external flows when the level control responds. Despite this, a temperature cascade might be a good investment in order to make the composition control quicker.

When using L/D and V/B for control, the following relations exist between L , V , D and B and L/D , V/B when assuming perfect level control (Skogestad and Morari, 1987)

$$dL = Dd\left[\frac{L}{D}\right] + \frac{L}{D}dD \quad (4.24)$$

$$dV = Bd\left[\frac{V}{B}\right] + \frac{V}{B}dB \quad (4.25)$$

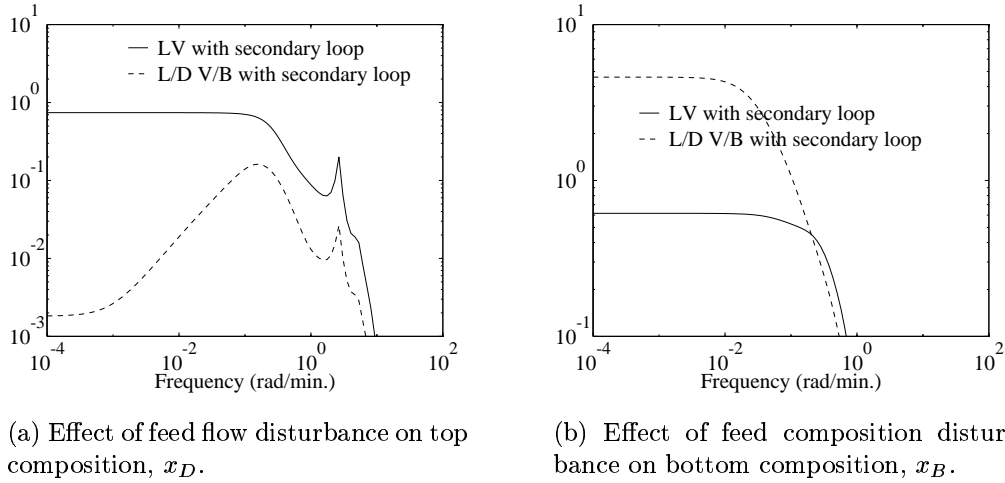


Figure 4.12: Closed loop disturbance gain of LV and $(L/D)(V/B)$ configuration with secondary loop installed.

This shows how the level control affects the internal streams and thus the product compositions. For a (diagonal) decentralized controller at a fixed operating point the LV and $(L/D)(V/B)$ configuration are interchangeable through

$$du = \begin{bmatrix} dL \\ dV \\ dD \\ dB \end{bmatrix} = \begin{bmatrix} D & (L/D)K \\ B & K \\ & (V/B)K \\ & K \end{bmatrix} \begin{bmatrix} dy_D \\ dx_B \\ dM_D \\ dM_B \end{bmatrix} = \Delta dy \quad (4.26)$$

where K is the gain in the level control loop.

The column with the $(L/D)(V/B)$ configuration has $\lambda_{11}(0) = 3.29$ for the $(L/D)(V/B)$ configuration versus 35.5 for the LV configuration. Applying a secondary control loop makes both schemes one-way interactive at steady state, so a comparison must be based upon other indices. We therefore look at the closed loop disturbance gain for these two configurations.

The CLDG reveals that the increased handling of flow disturbances of the $(L/D)(V/B)$ configuration is present also with the secondary loop installed. Fig. 4.12 shows how the $(L/D)(V/B)$ configuration is superior towards feed flow changes, while not rejecting feed composition disturbances as well as the LV case. The responses shown are representative also for the two channels not shown.

The results in Fig. 4.12 are confirmed by simulations. Using the same tuning procedure as for the LV case we get the following controller tunings:

Loop	K	τ_I	τ_D	
x_D	1.18	10.5	2.62	(4.27)
x_B	0.035	10.5	2.62	

Fig. 4.13a shows the improved feed flowrate disturbance handling with the $(L/D)(V/B)$

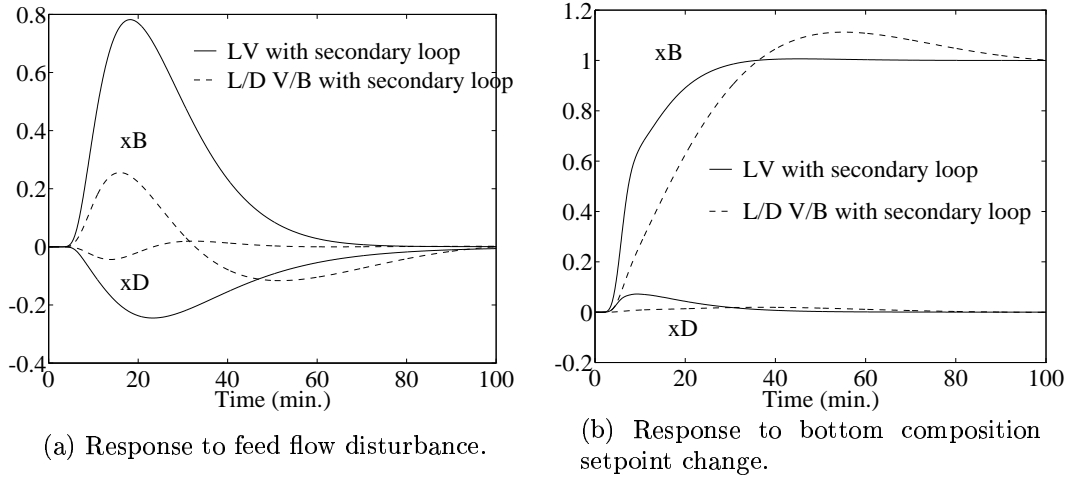


Figure 4.13: Simulations of LV and $(L/D)(V/B)$ configuration with secondary loop installed.

configuration. The response to a change in z_F (not shown) on the other hand, gives the opposite conclusion, as predicted by the CLDG. In both cases x_B is most difficult to control.

Simulated setpoint changes (as represented by x_B in Fig. 4.13b) show that the LV and $(L/D)(V/B)$ configurations behave much more similarly to setpoint changes than towards disturbances. This is reasonable since the interaction properties are almost equal (with a secondary loop) and the change in internal flows will be applied equally fast in both cases.

4.6 Using two cascades

Since using an intermediate temperature for composition control works well, why not use this scheme for controlling both top and bottom composition? We choose a tray 8 stages from the bottom ($N = 8$) for the bottom composition control cascade. Denoting the multiple temperature measurements and corresponding gains with the traynumber, we get the model:

$$\begin{pmatrix} x_D \\ x_B \\ x_{34} \\ x_8 \end{pmatrix} = \begin{pmatrix} g_{11} & g_{12} \\ g_{21} & g_{22} \\ g_{34,1} & g_{34,2} \\ g_{8,1} & g_{8,2} \end{pmatrix} \begin{pmatrix} L \\ V \end{pmatrix} = \begin{pmatrix} 0.8754 & -0.8618 \\ 1.0846 & -1.0982 \\ 6.3912 & -6.3051 \\ 10.9603 & -11.0723 \end{pmatrix} \begin{pmatrix} L \\ V \end{pmatrix} \quad (4.28)$$

Using developments similar to those in chapter 4.3, we can construct a plant \tilde{G} such that

$$\begin{pmatrix} x_D \\ x_B \end{pmatrix} = \tilde{G} \begin{pmatrix} T_{34,s} \\ T_{8,s} \end{pmatrix} \quad (4.29)$$

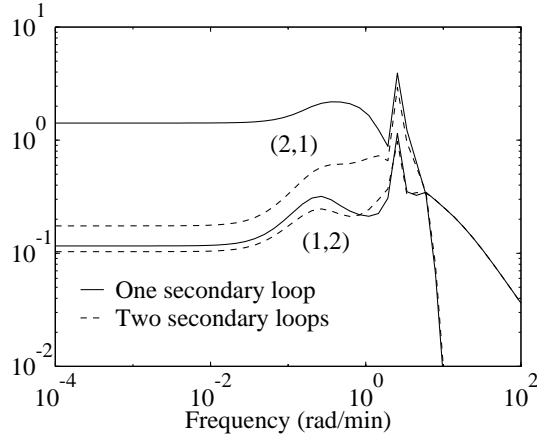


Figure 4.14: Comparison of PRGA with one and two secondary loops installed. Diagonal entries (corresponding to λ_{11}) are omitted.

The elements of \tilde{G} (which are omitted for brevity) all contain both K_1 and K_2 , the cascade proportional gains in the top and bottom respectively. The relative gain for this case is $\lambda_{11} = 1/(1 - Y)$, where

$$Y = \frac{(g_{21}(1 + K_2 K_{Tx} g_{8,2}) K_1 - g_{22} K_2 K_{Tx} g_{8,1} K_1)(g_{12}(1 + K_1 K_{Tx} g_{34,1}) K_2 - g_{11} K_1 K_{Tx} g_{34,2} K_2)}{(g_{11}(1 + K_2 K_{Tx} g_{8,2}) K_1 - g_{12} K_2 K_{Tx} g_{8,1} K_1)(g_{22}(1 + K_1 K_{Tx} g_{34,1}) K_2 - g_{21} K_1 K_{Tx} g_{34,2} K_2)} \quad (4.30)$$

Solving for K_i that will give least interaction ($\lambda_{11} = 1.0$ or $Y = 0$ in our sense) yields the following answers;

$$K_1 = K_{Tx}^{-1} \left(\frac{g_{12}}{g_{11} g_{34,2} - g_{12} g_{34,1}} \right) \forall K_2 \quad (4.31)$$

$$K_2 = K_{Tx}^{-1} \left(\frac{g_{12}}{g_{11} g_{8,2} - g_{12} g_{8,1}} \right) \forall K_1$$

We see that there exist multiple solutions for K_i in this case and that which values to choose are not so obvious. We will here choose K_1 and K_2 from Eq. 4.31, corresponding to choosing both K_i as if the cascades were independent.

The secondary loop gain K_1 is thus chosen equal to the single cascade case ($K_1 = -1.84$). The solution to the bottom secondary controller gives an optimal cascade gain of $K_2 = 2.94$. We detune the bottom cascade controller by a factor of 3 for the reasons given earlier, arriving at $K_2 = 0.98$ for the implemented controller.

At this point it is of interest to see how the *one way* interaction has changed compared to the single secondary loop case. Fig. 4.14 shows the PRGA for these two cases. The second secondary loop has reduced the one way interaction from loop 1 to measurement x_B significantly. This is in line with the corresponding improvement from the first cascade, which largely improved the interaction properties towards output 1; x_D (also seen in Fig. 4.14). Both cascades improve the interaction properties of the measurement they are closest to.

Turning towards the disturbance rejection properties, these are only slightly improved over the case with one temperature cascade. From Fig. 4.15 we see that feed

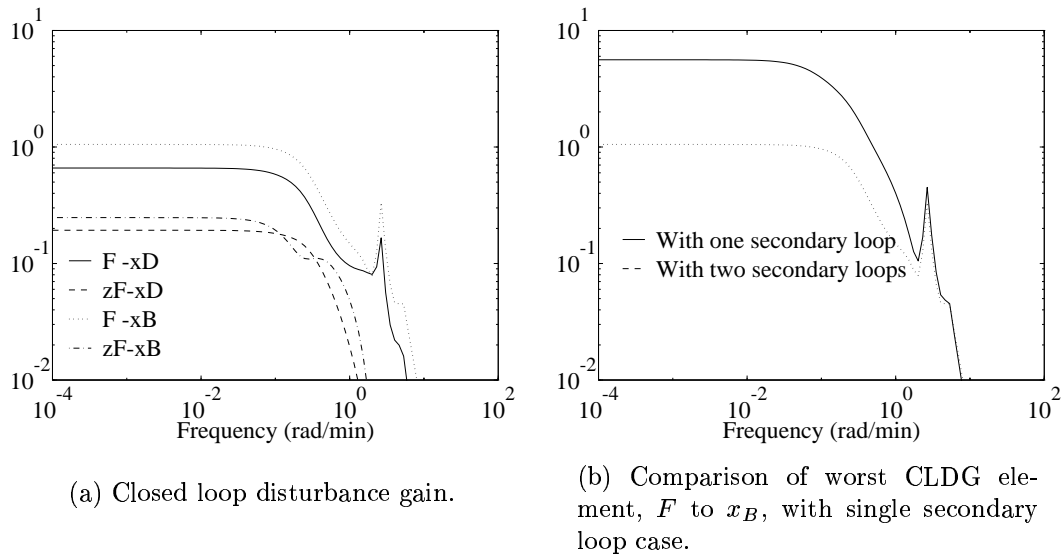


Figure 4.15: Closed loop disturbance gain for the LV configuration with two secondary loops.

flow disturbances have less influence on x_B , while the other channels are less changed.

Using the given cascade tunings, we then use Ziegler-Nichols tuning rules for the composition loops as described earlier, arriving at;

<i>Loop</i>	K	τ_I	τ_D	
x_D	2.21	6.54	1.64	(4.32)
x_B	1.82	6.16	1.54	

The simulations in Fig. 4.16 show that two temperature cascades generally give worse performance compared to using one cascade, although there is a small improvement in the initial response of the bottoms composition. This is natural since the first temperature cascade has already stabilized the column profile a great deal and any improvements should come at the end closest to the additional cascade. The overall improvement does, however, not warrant the extra cascade loop in this case.

4.7 Discussion

1. We note from the simulations that the feed flow disturbance ΔF has a rather large effect on x_B even with the secondary loop closed. The reason is that it takes some time before the temperature sensor near the top registers this disturbance. To improve this response the temperature sensor should be located in the bottom part of the column. However, in this case the top composition would become more sensitive to disturbances. The obvious conclusion is to place the temperature sensor in the top part (and close

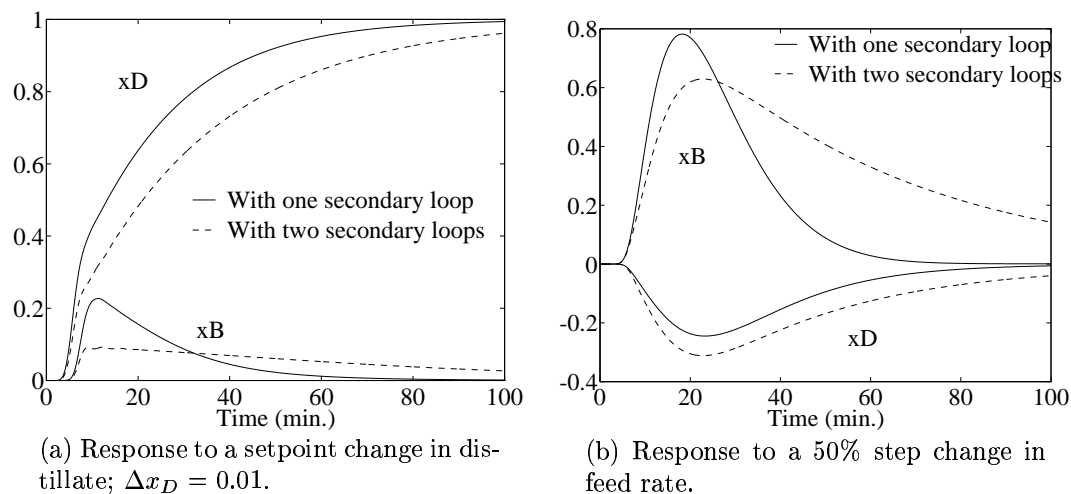


Figure 4.16: Comparison of simulation results with one and two secondary loops.

this loop using L) if the top composition is most critical, or place it in the bottom (and close this loop with V) if the bottom composition is most critical.

2. A second temperature cascade in two-point distillation control is not advised from the results shown here.

3. If large variations in the operating point of the column is expected one may choose to use the weighted average of several tray temperatures for the temperature measurement. This will avoid the problem of an insensitive measurement if the temperature profile becomes flat at the selected tray location. The outer cascade which contains integral action will in any case reset the setpoint of the average temperature to its correct value.

4. The use of “weighted average temperature” is indeed very similar to the static composition estimator of Mejdell. But, as noted before, even with such an estimator, it may be a good idea to implement an independent inner temperature cascade. Also, temperature cascades need not be updated due to the feedback nature.

5. The reason why the temperature cascade reduces interaction is essentially as follows. The distillation column is actually quite decoupled at high frequencies due to the flow dynamics. Therefore, if one can close one loop with sufficiently high gain, one can at least make the system one-way interactive and reduce the RGA. It is then possible to implement advanced controllers on top of this without regard for the robustness problems which follow when the RGA is large.

References

- [1] Fagervik, K.C., Waller, K.V. and Hammarström, L.G., 1981, “One-way and Two-way Decoupling in Distillation”, *Chem. Eng. Comm.*, **21**, 235.

- [2] Fuentes, C. and Luyben, W.L., 1983, "Control of High-Purity Distillation Columns", *Ind. Eng. Chem. Process Des. Dev.*, **22**, 361-366.
- [3] Grosdidier, P., Morari, M. and Holt, B.R., 1985, "Closed-Loop Properties from Steady-State Gain Information", *Ind. Eng. Chem. Fundam.*, **24**, 221-235.
- [4] Hovd, M. and Skogestad, S., 1992, "Simple Frequency-Dependent Tools for Control System Analysis, Structure Selection and Design", *Automatica*, **28**, 5, 989-996.
- [5] Kister, H.Z., 1990, "Distillation operation", McGraw-Hill, New York.
- [6] Krishnaswamey, P.R., G.P. Rangaiah, R.K. Jha and P.B. Deshpande, 1990, "When to use Cascade Control", *Ind. Eng. Chem. Res.*, **29**, 2163-2166.
- [7] Krishnaswamey, P.R. and G.P. Rangaiah, 1992, "Role of Secondary Integral Action in Cascade Control", *Trans. IChemE*, **70**, Part A, 149-152.
- [8] Mejdell, T. and Skogestad, S., 1991a, "Estimation of distillation composition from multiple temperature measurements using PLS regression", *Ind. Eng. Chem. Res.*, **30**, 12, 2543-2555.
- [9] Mejdell, T. and Skogestad, S., 1991b, "Composition estimator in a pilot plant distillation column using multiple temperatures", *Ind. Eng. Chem. Res.*, **30**, 12, 2555-2564.
- [10] Shinskey, F.G., 1984, "Distillation Control", 2nd Edition, McGraw Hill, New York.
- [11] Skogestad, S. and Lundström, P., 1990, "Mu-optimal LV-control of Distillation Columns", *Comp. Chem. Engng.*, **14**, 4/5, 401-413.
- [12] S. Skogestad, Lundström, P. and Jacobsen, E.W., 1990, "Selecting the best distillation control configuration", *AIChE Journal*, **36**, 5, 753-764.
- [13] S. Skogestad and Morari, M., 1987, "Control configuration Selection for Distillation Columns", *AIChE J.*, **33**, 10, 1620-1635.
- [14] S. Skogestad and Morari, M., 1988, "LV-control of a High-Purity Distillation Column", *Chem. Eng. Sci.*, **43**, 1, 33-48.
- [15] Stephanopoulos, G., 1984, "Chemical Process Control", Prentice-Hall, London.
- [16] Tolliver, T.L. and McCune, L.C., 1980, "Finding the Optimum Temperature Control Trays for Distillation Columns", *InTech*, September 1980.

Chapter 5

Dynamics and Control of Integrated Three-Product (Petlyuk) Distillation Columns

Erik A. Wolff*, Sigurd Skogestad[†] and Kjetil Havre
Chemical Engineering
University of Trondheim - NTH
N-7034 Trondheim, Norway

Presented at
AIChE Annual Mtg., St. Louis, November 1993
and
ESCAPE-4, Dublin, March 1994.

Abstract

This paper considers operation and control of the Petlyuk design. The degrees of freedom are analyzed especially at steady-state. These results together with steady-state solution curves help describe the complex plant dynamics and possible optimization strategies. We also propose control schemes for controlling three and four product compositions. The results indicate that there may be serious problems involved in operating the Petlyuk column, at least for high-purity separations.

*Present Address: ABB Environmental, Box 6260 Etterstad, N-0603 Oslo, Norway

[†]Address correspondence to this author. Fax: 47-73594080, E-mail: skoge@kjemi.unit.no

5.1 Introduction

The separation of more than two components by continuous distillation has traditionally been done by arranging columns in series. Several alternative configurations exist, most notably the direct and indirect sequence (where light or heavy components are removed first, respectively).

Almost 50 years ago Wright (1949) proposed a promising design alternative for separating a ternary feed. This design consists of an ordinary column shell with the feed and sidestream product draw divided by a vertical wall through a set of trays. As compared to the direct or indirect sequence, this implementation offers savings in investment (only one shell and two heat exchangers) as well as operating costs. Although several authors have studied the design of such columns, very little work has been done on the operation and control.

This configuration is usually denoted a **Petlyuk column** after Petlyuk *et al.* (1965) who later studied the scheme theoretically. Many authors have since predicted considerable savings in energy and capital cost with this design, but still few of these integrated columns have been built. One reason is probably that the Petlyuk column, compared to an ordinary distillation column, has many more degrees of freedom in both operation and design. This undoubtedly makes the design of both the column and its control system more complex.

A two-column implementation of the Petlyuk design is shown in Fig. 5.1a. It consists of a prefractionator with reflux and boilup from the downstream 3-product column, a setup with only one reboiler and one condenser. As proposed by Wright (1949), practical implementation of such a column can be accomplished in a single shell by inserting a vertical wall through the middle section of the column (Fig. 5.1b), thus separating the feed and side product draw. Petlyuk's main reason for this design was to avoid thermodynamic losses from mixing different streams at the feed tray location. We will hereafter denote the product streams D , S and B (and feed F), with ternary components 1, 2 and 3. Component 1 is most volatile, followed by component 2 and 3. Molefractions are denoted x_{ij} where i is the stream and j is the component.

A similar design, but with a condenser and reboiler also for the prefractionator was proposed even earlier by Brugma (1939). We will denote this a pseudo-Petlyuk design.

Cahn and Di Micelli (1962) have also proposed a Petlyuk design, although this was for separating four components by introducing *two* product sidestreams.

Stupin and Lockhart (1971) claimed that Fenske-Underwood design computations overestimated the stage requirements and found the performance of the Petlyuk column to be rather insensitive to changes in trays and internal flows.

Tedder and Rudd (1978) were among the first to study the optimal separation of a given ternary feed. The alternatives included the direct and indirect sequence, columns with sidedraws, columns with sidestrippers and siderectifiers and a pseudo-Petlyuk design. They found the pseudo-Petlyuk design to be preferable when the fraction of intermediate component 2 in the feed is large (40% - 80%).

Cerda and Westerberg (1981) derived simple methods for estimating the operating parameters at limiting flow conditions.

Fidowski and Krolkowski (1986) compared the optimal (minimum) vapor flow rates

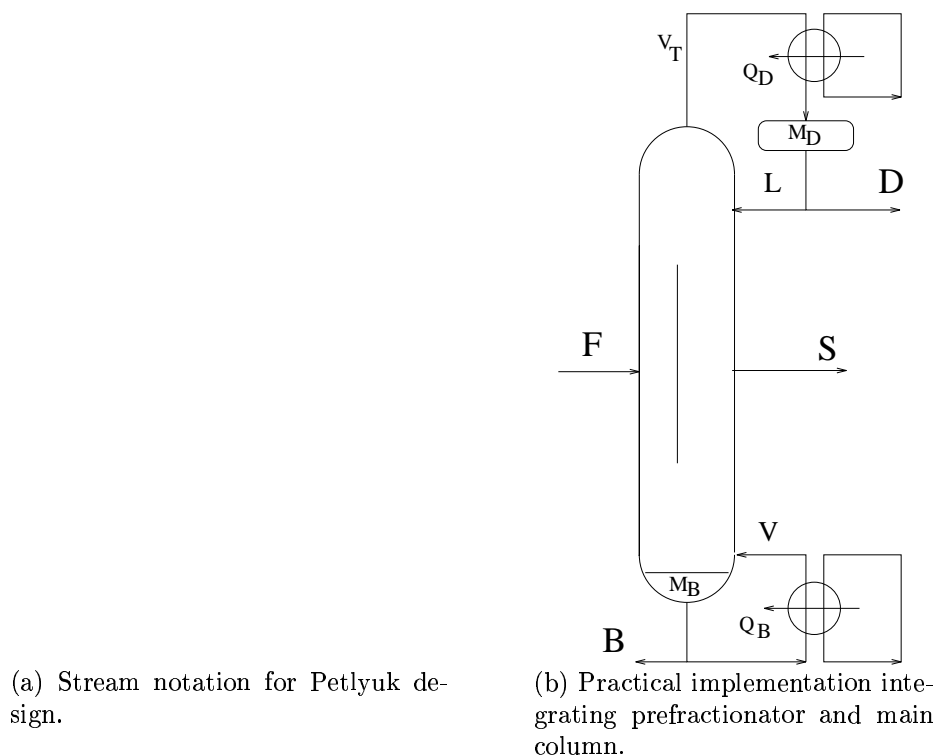


Figure 5.1: Petlyuk column representations.

for the direct and indirect sequence with both the Petlyuk and the pseudo-Petlyuk design. The Petlyuk design showed significant savings. They developed analytical expressions for the minimum vapor flowrate based on the Underwood formulas.

Chavez *et al.* (1986) discussed the possibility for multiple steady states in complex columns, concentrating their work on a Petlyuk design. They found that the Petlyuk design has five degrees of freedom at steady-state, and they found that four different steady-state solutions may occur when specifying three purities (in each of the products) plus bottom rate and reboiler duty. They explain this in terms of matching specifications in interlinked columns.

Glinos and Malone (1988) also derived analytical expression for various alternative designs, including the Petlyuk design. Their recommendations are to use the Petlyuk design when the fraction of intermediate component 2 in the feed is small, and they found that the maximum vapor savings compared to simple sequences were about 50% when $x_{F2} \rightarrow 0$. They found that columns with siderecifiers may be equally well suited when the fraction of component 2 in the feed is less than 30%. However, they concluded that Petlyuk columns may also have a significant advantage for moderate or high x_{F2} values, but that the conclusion depends on the relative volatilities.

Faravelli *et al.* (1989) build on the work of Chavez *et al.* and looked at which of the steady states are most resilient to changing internal flows. They applied “control” to the column, but only to aid in finding the steady-state solutions.

Triantafyllou and Smith (1992) presented a good overview over the design of Petlyuk columns and explained how it may be approximated as a regular column with two

sidestrippers which are joined together.

The only report of an industrial implementation of a Petlyuk design is from BASF in Germany (as reported by Rudd, 1992). The Department for Process Integration at UMIST is currently investigating operational aspects of a Petlyuk pilot plant.

In this work we will study the dynamic behavior of a Petlyuk column and propose suitable controller structures. The original motivation of this project was to study composition control of the three product streams of a Petlyuk column. The results from this study, which are presented at the end of this paper, show that from a linear point of view there are no major problems.

However, during this work it became clear that there are serious problems related to the steady-state behavior that can make practical operation very difficult. The main problem is that there exist “holes” in the operating region for which it is not possible to achieve the desired product specifications. This behavior has no equivalence in ordinary two-product distillation columns.

5.2 Degrees of Freedom

We here consider the *Degrees of Freedom* (DOF) in a given column with fixed stages, feed locations, etc. Starting with binary distillation and considering steady-state where it is assumed that the holdups (condenser level, reboiler level and pressure) are already controlled, two independent (manipulated) variables remain, for example L and V .

In a Petlyuk column we get at steady-state three additional degrees of freedom - one for each of the three additional streams leaving the column. These are the sidestream S plus the streams L_1 and V_2 sent back to the prefractionator (we will use the fractions $R_L = L_1/L$ and $R_V = V_2/V$ as DOFs in the further analysis). See also Fig. 5.2. Note that in this analysis the prefractionator itself does not have any degrees of freedom at steady state. The five DOFs for the Petlyuk design may be used to specify (control) the top and bottom composition (x_{D1} and x_{B3}) and one or two compositions in the side stream. This leaves one or two degrees of freedom for optimization purposes, which we in this paper select to be minimizing the energy consumption in terms of the boilup to feed rate, V/F .

There are also possibilities for increasing the DOFs, for example, by taking off several sidestreams (e.g., a vapor and liquid sidestream, S_V and S_L) and by using a triple-wall solution as suggested in the figure in the paper of Petlyuk *et al.* (1965).

In a usual two-product distillation column one can at most control one specification for each product (two-point control). Simpler alternatives are no control (relying on self-regulation) or one-point control. Since in high purity distillation columns it is critical that the overall product split is adjusted correctly (such that D/F is approximately equal to the fraction of light component), one generally finds that no control is unacceptable. However, due to strong interactions one-point control, with the composition in the other end being self-regulated, is usually satisfactory if some over-refluxing (increased energy consumption) is allowed for.

For a Petlyuk scheme one must at least adjust two product splits correctly (e.g. D/F to match the light component and S/F to match the intermediate component),

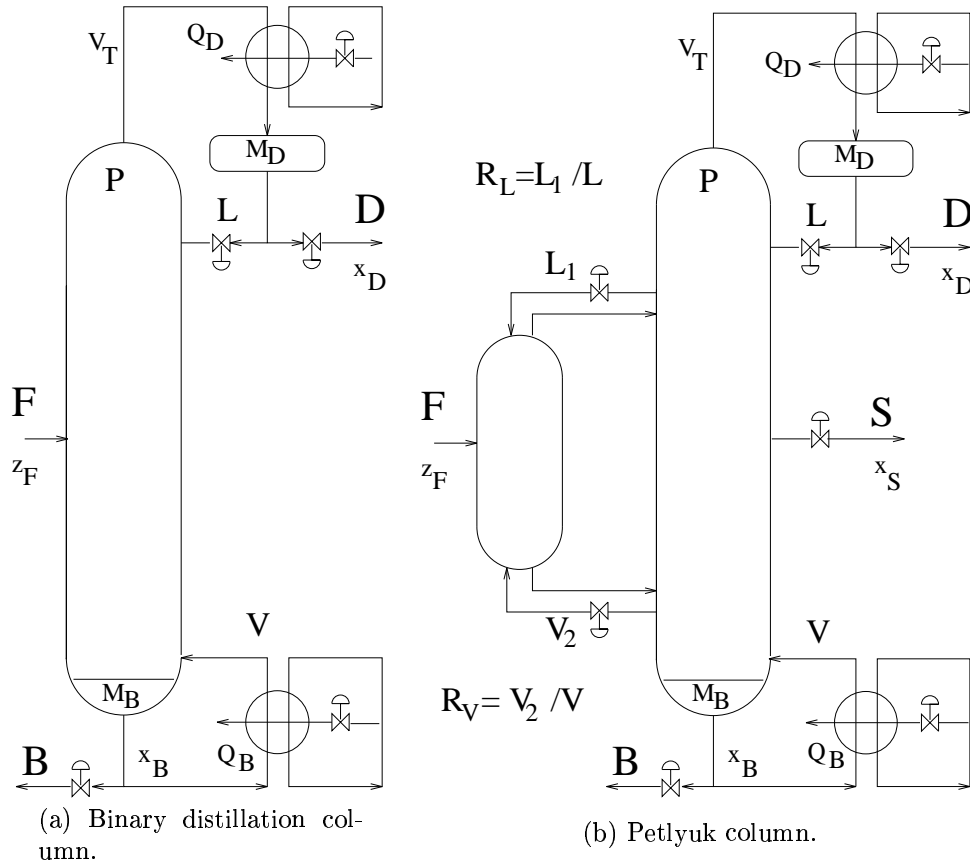


Figure 5.2: Degrees of freedom in distillation (indicated by valve position).

thus at least two-point control is required. Such a control scheme is not treated in detail here, but again it is clear that it will at least require increased energy consumption. Additionally, there will be no way to adjust the separation in the prefractionator, as determined by the recycle fractions R_L and R_V .

In this paper we first study three-point control where one composition in each product is controlled, for example x_{D1} , x_{S2} and x_{B3} . This may be an adequate control scheme. However, with only one degree of freedom to control the sidestream composition, we will not be able to adjust the ratio between the sidestream impurities, x_{S1} and x_{S3} , which may constitute an additional product specification. Thus, we finally consider four-point control with four product composition specifications (two in the sidestream).

5.3 Case Study

Previous authors have looked at a variety of ternary systems, from close boiling C_4 isomers to component sets spanning C_1 to C_6 . We have chosen the system ethanol, propanol and butanol for the examples. The model description considers only the

Design	Boilup
Direct	100 %
Indirect	110 %
Rectifier	92 %
Stripper	91 %
Pseudo-Petlyuk	96 %
Petlyuk	87 %

Table 5.1: Relative energy consumption.

material balance of the system, assuming constant molar flows and constant relative volatility. A relative volatility of 4:2:1 was used for the three components, based on the geometric average of ASPENPLUS data for the top, feed and bottom tray. The model incorporates linearized flow dynamics with a time constant of 3.6 minutes. The results are primarily generated with SPEEDUP, an equation based solver. This enabled optimization, linearization and dynamic simulations to be performed within the same environment. Steady state simulations were also done with ASPENPLUS, a steady-state flowsheet simulator, to check the integrity of the results. Here we used the Redlich-Kwong-UNIFAC thermodynamic property set and no pressure drop.

We have used the same number of trays in the center sections of the “main” column as in the prefractionator. This is in line with the assumed industrial implementation with a dividing wall in the shell. The “main” column consists of 40 stages and there are 20 stages in the prefractionator. The feed is liquid at its boiling point with a flowrate of 60 *kmol/min.* and feed composition $x_F = [0.333, 0.333, 0.334]$. We demand 99% pure products in the top and bottom and the design purity in the sidestream is around 99%. When having four specifications, we also demand $x_{S1} = x_{S3}$.

Comments on model structure and calculations. SPEEDUP is an equation-oriented solver, i.e. all model equations are solved simultaneously and not in a modular fashion. This makes it easy to change specifications, but the solution (often) depends on good start estimates. This, together with the fact that including pressure makes distillation an even more difficult (stiff) problem to solve, largely determined the level of complexity of the model.

Economic gain in Petlyuk design. Earlier work has showed that the Petlyuk design often is more energy efficient. This was confirmed for our mixture, the savings in energy compared to the standard “direct sequence” with two columns was 13% (Calculations performed with ASPENPLUS). Table 5.1 give an economic comparison with other ternary separation schemes and shows the Petlyuk column operates most economically for the given components and feed composition. The other schemes were the **Indirect** sequence, removing the heaviest component first, **Pseudo-Petlyuk**, as described earlier and a binary column with a side-**Rectifier** or side-**Stripper** attached, respectively. All designs consist of 60 stages, optimally distributed between the different column sections to give the least boilup.

How to determine the number of trays in a Petlyuk column for an economic compar-

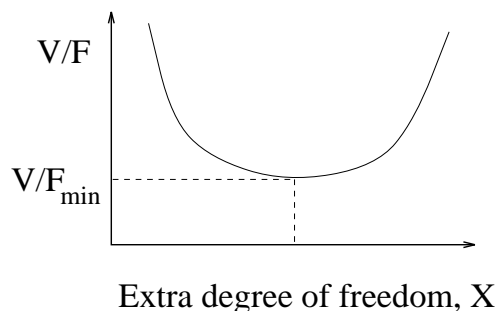


Figure 5.3: Energy use (Boilup rate, V/F) as function of extra DOF.

ison may be disputed. Here we have chosen to include all trays according to the model structure derived from Fig. 5.1. This should be a conservative estimate. Counting only the trays in the main column section (assuming the prefractionator to be an integral part) leads to a relative boilup of 69% with an optimally distributed prefractionator. Both implementations (dividing wall or separate prefractionator) may be preferred at hitherto unknown operating conditions. Without going into detail, it seems reasonable to prefer one shell at high pressure where shell costs constitute more of the total.

5.4 Steady state optimal operating point

This section is concerned with exploiting any extra DOF to achieve optimal economic operation in terms of boilup rate. Three and four compositions are specified in the optimization problem.

5.4.1 Four compositions specified

As noted above the column has five degrees of freedom at steady-state. We first study the steady-state behavior with four compositions specified: $x_{D1} = 0.99$, $x_{B3} = 0.99$, $x_{S2} = 0.99$ and $x_{S1}/x_{S3} = 1$ (equal distribution of the impurities in the sidestream). The purity of the sidestream (x_{S2}) is nominally 0.99, but the results are also given for other values.

One degree of freedom (DOF) then remains to be specified (denoted X in the following). For operation it is important to make a good choice of X since this variable will be kept constant or changed only slowly to minimize the operation costs, which is here selected to be given by the boilup rate (V/F). At first we expected to find a relationship as given in Fig. 5.3, where V/F has a minimum as a function of X . Ideally, we would like the plot to be as “flat” as possible such that the exact value of X was not too important.

Unfortunately, the picture is not quite as simple in practice. This is illustrated in Fig. 5.4a which shows boilup V/F as a function of $X = R_L$ (the internal reflux ratio to the prefractionator) for two values of x_{S2} . The first thing to note is that there are two possible solutions for some values of R_L . One of these corresponds to a higher value of V/F and should be avoided. These results are similar to those of Chavez (1986). Thus, if R_L is used as the DOF to be kept constant, the first challenge for operation and

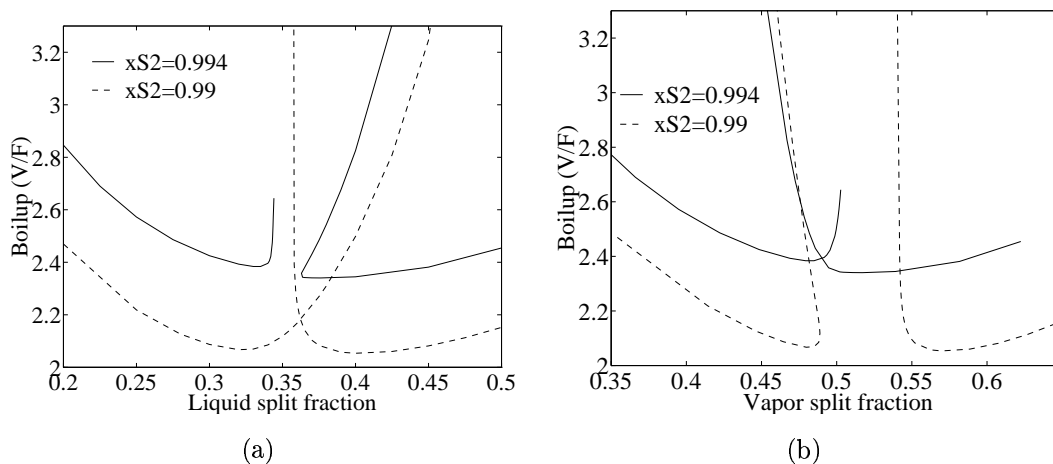


Figure 5.4: Boilup V/F as a function of internal stream splits R_L and R_V . Four product compositions specified. (SPEEDUP calculations.)

control would be to stay at the “lower” solution corresponding to the smallest V/F . Assuming that this could be done, we find for $x_{S2} = 0.99$ that keeping R_L at about 0.35 would be a good choice, and that V/F would not depend too strongly on the exact value. However, for increased sidestream purity, $x_{S2} = 0.994$, there is a “hole” in the operating region, and for $R_L = 0.35$ it is not possible to achieve the desired product specifications even with infinite reflux.

It is then clear that R_L is not a good choice for the remaining DOF. To see if other choices are better we prepared similar plots for other choices ($X = R_V$ or compositions within the prefractionator) shown in Fig. 5.4b, 5.5a and 5.5b. However, we find that none of these are acceptable. For example, with R_V fixed we find a hole in the operating range for *low* values of x_{S2} . We also find similar problems when specifying compositions in the prefractionator.

When x_{S2} is increased slowly from 0.99 and upwards, we see that the “hole” in Fig. 5.4a *develops*, while a “hole” simultaneously *closes* in Fig. 5.4b. A “hole” is present for all values of x_{S2} , either for $V/F(R_V)$ or $V/F(R_L)$.

The data have been compared with results generated with ASPENPLUS. As we see from Fig. 5.6, we get a behavior very similar to the results from SPEEDUP, with holes for different x_{S2} specifications. ASPENPLUS uses more complex thermodynamics (Redlich-Kwong-UNIFAC was chosen here) with for example composition dependent K-values. This and other more rigorous aspects in the ASPENPLUS calculations lead to the difference in x_{S2} values for which the holes appear. The difference in V/F between the two programs is approximately 4% for equal specifications. Slight changes to the relative volatilities in SPEEDUP would probably give better correspondence, both in terms of V/F and the specifications for which the holes develop.

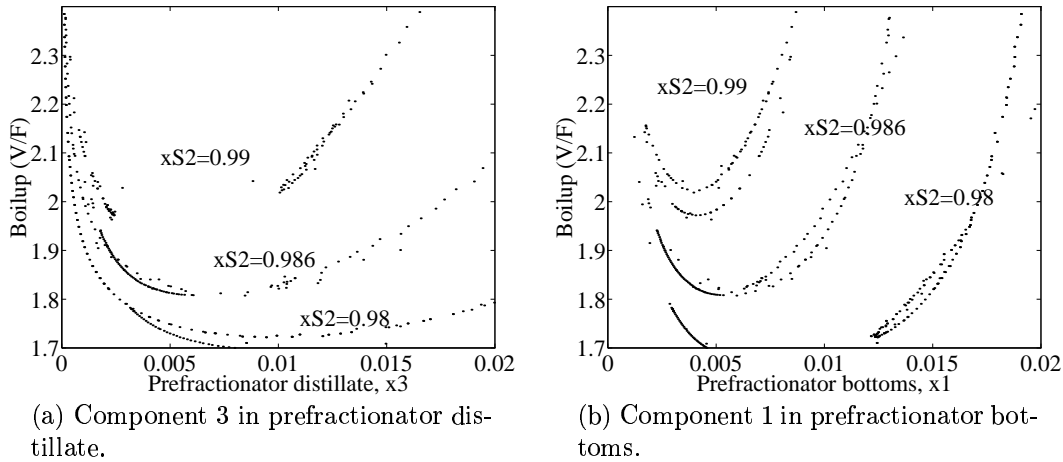


Figure 5.5: Boilup V/F as a function of prefractionator compositions. Four compositions specified. (ASPEN calculations.)

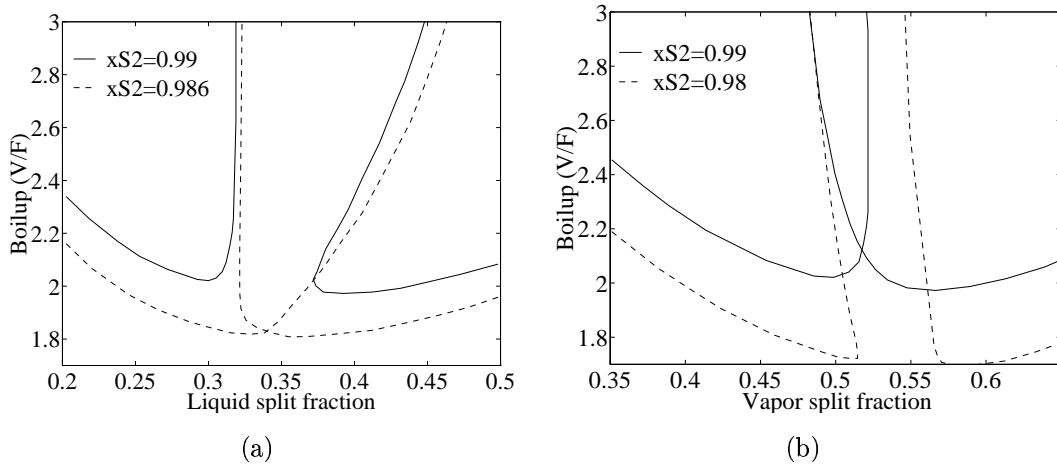


Figure 5.6: Boilup V/F as a function of internal stream splits R_L and R_V . Four product compositions specified. (ASPEN calculations.)

5.4.2 Three compositions specified

The conclusion from the above plots is that “holes” in the operating range will make it very difficult to control four compositions. A possibly better alternative is to control only three compositions, that is, to let the ratio of the impurities in the sidestream vary freely (and not specify $x_{S1}/x_{S3} = 1$ as above). This yields another DOF that must be specified, for example, one may select $X_1 = R_L$ and $X_2 = R_V$. This is the choice made in the control part later.

Obviously the removal of one specification “loosens up” the problem somewhat,

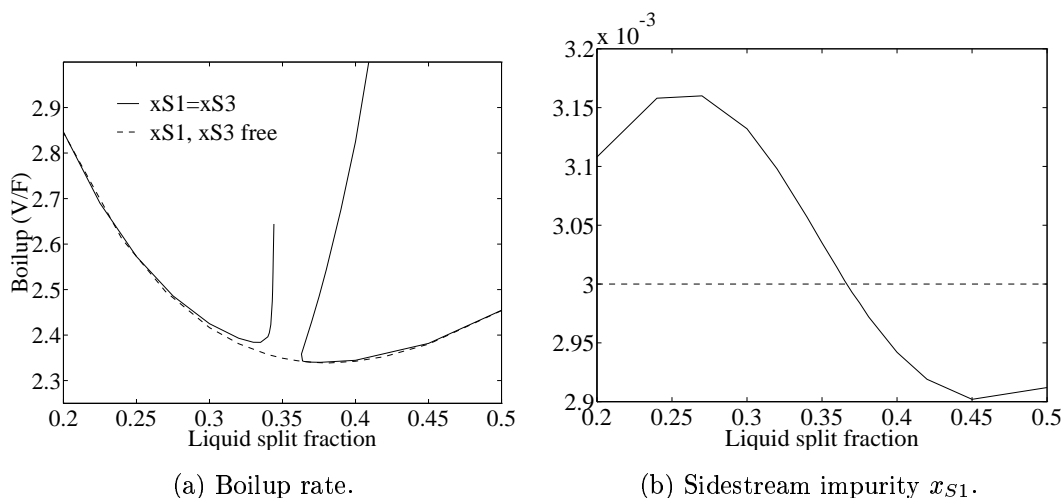


Figure 5.7: Boilup rate V/F and x_{S1} as a function of R_L when relaxing the constraint $x_{S1} = x_{S3}$.

letting the column profile vary more freely. For example, while it was impossible to achieve $x_{S2} = 0.994$ with $R_L = 0.35$ and $x_{S1}/x_{S3} = 1$, we find that we can achieve $x_{S2} = 0.994$ with $R_L = 0.35$ and $R_V = 0.49$, for example, giving $x_{S1}/x_{S3} = 1.02$ and $V/F = 2.35$. Fig. 5.7a shows how the hole has disappeared when relaxing the constraint $x_{S1} = x_{S3}$. No solutions corresponding to another branch were found. Fig. 5.7b shows how one of the sidestream impurities x_{S1} has varied to accomplish the minimum boilup in Fig. 5.7a.

Specifying three compositions gives a lower minimum boilup than with four compositions specified. The difference between the two cases in Fig. 5.7a is small. This results from the column “naturally” preferring $x_{S1} \approx x_{S3}$ with the given tray distribution and sidestraw position (also evident from Fig. 5.7b).

To summarize; the Petlyuk column exhibits holes in the operating space when four product compositions, including two in the sidestraw, are specified. The location of these holes in terms of values of R_L and R_V varies with design and specifications. The lower bound on the boilup for the 4-specification set is given by the 3-specification solution.

5.5 Control of the Petlyuk column

In the remaining part of the paper we consider control of the column using decentralized control. The reflux (L) is used to control the top composition (x_{D1}), boilup (V) is used to control the bottom composition (x_{B3}), and the sidestream flowrate (S) is used to control sidestream composition (x_{S2}). For “three-point” control R_L and R_V are fixed. For “four-point” control R_L is used to control the impurity ratio (x_{S1}/x_{S3}) with R_V fixed. We also consider using multiple side draws in control of four compositions.

5.5.1 Linear Analysis Tools

In the following we will use a plant description of the form

$$y(s) = G(s)u(s) + G_d(s)d(s) \quad (5.1)$$

where G and G_d denote the process and disturbance plant model and y , u and d are the measurements, manipulated inputs and disturbances, respectively.

In this paper we mainly use the relative gain array (RGA or Λ) to study interaction in the distillation column. The properties of the RGA are well known (e.g., Grosdidier *et al.*, 1985). The most important for our purpose are: 1) No twoway interaction is present when $\Lambda = I$, 2) The RGA is independent of scaling in inputs or outputs, and 3) The rows and columns both sum up to 1. To evaluate the disturbance sensitivity, we consider the closed loop disturbance gain (CLDG) which is the appropriate measure when we use decentralized control (Hovd and Skogestad, 1992). The CLDG is defined as $\Delta = G_{diag}G^{-1}G_d$, where G_{diag} consists of the diagonal elements of G . For decentralized control frequency-dependent plots of $\Delta = \delta_{ik}$ are used to evaluate the necessary bandwidth requirements in loop i , that is, at low frequencies the loop gain $L_i = g_{ii}c_i$ must be larger than δ_{ik} in magnitude to get acceptable performance. We also look at the singular value decomposition $G = U\Sigma V^T$ and examine the elements of G .

The disturbances considered are changes in the feed flow and feed composition. All variables have been scaled with respect to the maximum allowed change for judging performance: $\Delta L = \Delta V = 30\%$, $\Delta R_L = \Delta R_V = 0.2$, $\Delta S = 25\%$, $\Delta x_{ij} = 0.01$, $\Delta F = 17\%$ and $\Delta z_{Fi} = 20\%$.

5.5.2 Analysis of three-point control, LVS-configuration

In this case R_L and R_V are fixed and the outputs and inputs are

$$y = \begin{pmatrix} x_{D1} \\ x_{B3} \\ x_{S2} \end{pmatrix} \quad u = \begin{pmatrix} L \\ V \\ S \end{pmatrix} \quad (5.2)$$

The Petlyuk column at the operating point with minimum energy use ($R_L = 0.376$, $R_V = 0.517$) has transmission zeros in the right half plane (RHP). The most dominant zero is at a frequency of 2.53 rad/min. Thus, there may exist fundamental problems with instability, inverse responses or inherent bandwidth limitations.

A RHP zero occurs between S and x_{S2} at this operating point for the following reason; changes in S will behave towards x_{S3} almost as an integrator through changes in S initially only affecting the liquid below the tray. The initial change in x_{S1} is larger than for x_{S3} , but it will then level off after a short time. The relation between these two responses will determine if an inverse response occurs or not. The subsequent analysis will reveal that these RHP zeros will only slightly impair the high frequency behavior and not prove a control problem.

The steady state gain matrix G is

$$G(0) = \begin{pmatrix} 153.45 & -179.34 & 0.03 \\ -157.67 & 184.75 & 21.63 \\ -4.80 & 6.09 & -2.41 \end{pmatrix}$$

We see that the sidestream S mainly affects the middle and bottom product, while both L and V have a large effect on x_{S2} . We see quite readily that there will be interaction between the top and bottom composition, in line with ordinary binary distillation.

The singular value decomposition $G = U\Sigma V^T$ (at steady-state) will allow us some conclusions on the high and low gain directions of the plant. The output and input directions are given (as the columns) in U and V , respectively and the singular values are $\Sigma = \text{diag}[339.12 \quad 15.33 \quad 0.34]$.

$$U = \begin{pmatrix} 0.70 & -0.70 & 0.14 \\ -0.72 & -0.69 & 0.11 \\ -0.02 & 0.18 & 0.98 \end{pmatrix}$$

$$V = \begin{pmatrix} 0.65 & -0.04 & 0.76 \\ -0.76 & 0.03 & 0.65 \\ -0.05 & -1.00 & -0.01 \end{pmatrix}$$

We see that the high gain output direction (column 1 of U) corresponds to moving the top and bottom compositions in opposite directions, or moving the column composition profile up or down. (Remember that we look at three compositions, not only the composition of light component in the top and bottom as in binary distillation.) x_{S2} is not affected much in this case, corresponding to trading x_{S1} with x_{S3} . The low gain direction (column 3 of U) corresponds to moving them in the same direction, i.e. making both D and B more or less pure. This is in accordance with ordinary binary distillation. The medium gain direction corresponds almost entirely to changing S (column 2 in V) and moves x_{S2} opposite to x_{D1} and x_{B3} . This is reasonable; for example reducing S will give a buildup of component 2 around the sidedraw, giving more impurities both in the top and bottom section of the column.

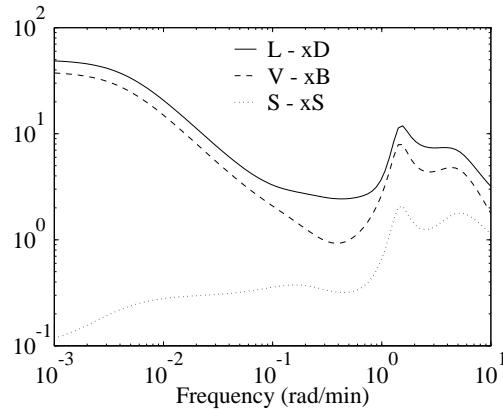
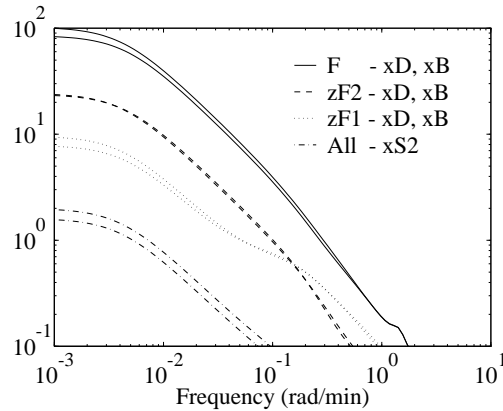
We can predict from this that using S for control will require countermeasures to keep both x_{D1} and x_{B3} at their setpoints. Moving the column profile in the high gain direction will leave x_{S2} quite immobile, whereas the low gain direction (making D and B more pure) will significantly affect x_{S2} .

We then study the interaction and disturbance rejection properties. The steady state RGA values

$$\Lambda(0) = \begin{pmatrix} 49.83 & -48.83 & 0.00 \\ -38.34 & 38.44 & 0.90 \\ -10.48 & 11.38 & 0.10 \end{pmatrix}$$

show again that the control of x_{D1} and x_{B3} interact. The same trend is evident from the frequency dependent RGA as shown in Fig. 5.8. The interaction tapers off at higher frequencies, showing that the control having effect around the bandwidth of the plant will not be much affected by interaction. Pairing on very low RGA values is generally not advisable, thus questioning a pairing on $\lambda_{33} = 0.1$. Again, however, the medium frequency values are better, giving confidence to the indicated pairing.

The RGA indicates that another feasible pairing than the one mentioned exists; using boilup to control the sidestream purity and the sidestream to control the bottom composition (denoted LSV configuration). This again indicates that changes in S , through mainly affecting the liquid flow below the sidedraw, primarily interact with the lower part of the column.

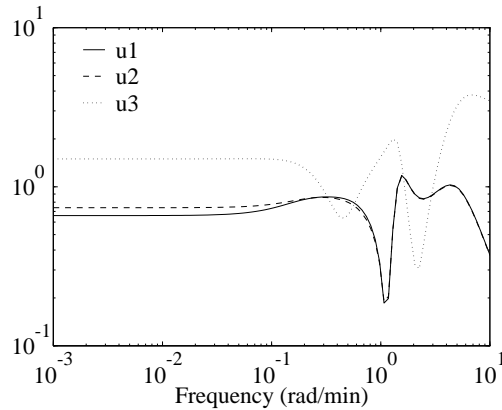
Figure 5.8: Relative gain array, λ_{ii} for LVS configuration.Figure 5.9: Closed loop disturbance gain, δ_{ij} , for LVS configuration.

The closed loop disturbance gain, CLDG, is shown in Fig. 5.9 for the pairing indicated in Eq. 5.2. The most difficult disturbance to reject is changes in F on x_D and x_B requiring a bandwidth of about 0.25 rad/min (time constant of 4 minutes) in this loops. On the other hand, the required bandwidth for controlling x_{S2} is significantly smaller (less than 0.1 rad/min). This gives us that sidedraw control loop can be tuned more loosely than the top and bottom composition loops.

Examining the CLDG for the reversed pairing mentioned above gives approximately the same bandwidth requirements (not shown). In addition, x_{S2} becomes more sensitive to disturbances in general and x_B less sensitive to changes in F .

Fig. 5.10 shows the necessary control action for perfect disturbance rejection at all frequencies. It is worth noticing that $\|G^{-1}G_d\|_\infty$ (the largest row sum) is only slightly over 1, meaning that good control is possible, following the recommendation from the closed loop disturbance gain. The curve also shows that the requirements are largest on u_3 , the sidestream flowrate.

The CLDG and $G^{-1}G_d$ complement each other nicely; the first indicates the most difficult disturbance, the other which actuator is the primary limitation to perfect control under disturbances.

Figure 5.10: Necessary control action for perfect control, $(G^{-1}G_d)_i$.

Controller	Kx100	τ_I (min)
x_{D1}	50	18
x_{B3}	50	18
x_{S2}	-5	30

Table 5.2: Controller tunings, LVS-configuration.

5.5.3 Nonlinear simulations with three point control

The conclusion is that from a linear point of view the process is easy to control at this operating point. There might even be several good pairings for control. We next perform nonlinear simulations to test these conclusions within a “normal” operating range. Frequency response based tuning rules were not applicable due to the low high frequency phase shift ($\angle G(j\omega) \leq \pi$). The controller tunings in Table 5.5.3 were found to give acceptable measurement and actuator behavior.

The simulation results in Fig. 5.11 show the closed loop response to disturbances in F ($60 \rightarrow 50$) and z_F ($[0.33, 0.33, 0.33] \rightarrow [0.33, 0.40, 0.27]$) and a distillate purity setpoint change ($0.99 \rightarrow 0.995$), respectively. The Petlyuk column handles disturbances and setpoint changes well.

Although the system seems resilient, a setpoint change in x_{S2} of $0.994 \rightarrow 0.996$ is infeasible for this operating point (L and V increase $> 100\%$), showing that three-point control may have problems for some range of R_L and R_V .

The response of x_{S1} and x_{S3} to a setpoint change in x_{S2} helps explain why the column has more difficulties with increased purity specifications in the sidestream than in the top or bottom. This is due to x_{S1} being insensitive to changes in S (which is also seen from the gain matrix $G(0)$ above). Thus, an increase in x_{S2} will primarily be at the expense of x_{S3} , which becomes increasingly difficult at low x_{S3} values. This leads to an interest in four-point control, including x_{S1} or x_{S3} as measured variable.

It is also worth noting that binary columns, using a design rule like $N_{trays} = N_{trays,min} * 2$, can handle purity increases of almost an order of magnitude, i.e. $0.99 \rightarrow$

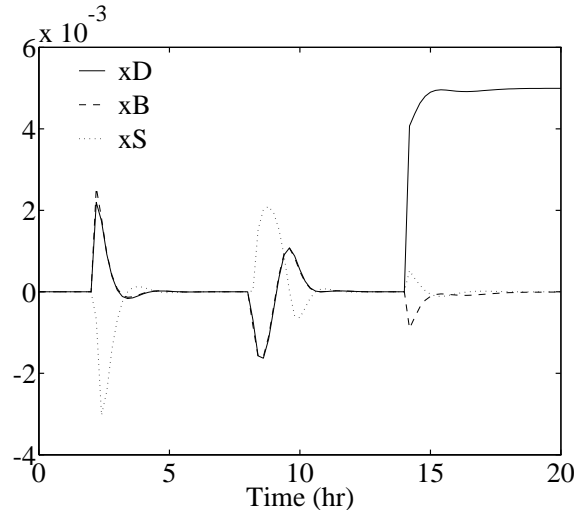


Figure 5.11: Time response to disturbances and setpoint change, LVS configuration. ΔF at $t = 2$, Δx_F at $t = 8$ and $\Delta y_{D1,s}$ at $t = 14$. Plot shows deviations from steady state values.

0.999 without reaching the limit of R_{max} . This does not look equally possible for the sidestream S in the Petlyuk column, where a near stationary x_{S1} limits the possible increase in x_{S2} to at most the absolute value of x_{S3} . This will, however, depend on the design.

The pairing with V and S actuators exchanged (LSV-configuration) seemed equally feasible from the linear analysis. However, the control system with this pairing failed against the mentioned perturbation set. The reason for this failure is the strong non-linearity from V to x_{S2} .

5.5.4 Analysis of four-point control, $LVR_L S$ configuration

R_L is added as a manipulated variable and is used to control x_{S1} . The set of measurements and manipulated variables is thus

$$y = \begin{pmatrix} x_{D1} \\ x_{B3} \\ x_{S1} \\ x_{S2} \end{pmatrix} \quad u = \begin{pmatrix} L \\ V \\ R_L \\ S \end{pmatrix}$$

The process gain and RGA at steady-state operating conditions are

$$G(0) = \begin{pmatrix} 153.45 & -179.34 & 0.23 & 0.03 \\ -157.67 & 184.75 & -0.10 & 21.63 \\ 24.63 & -28.97 & -0.23 & -0.10 \\ -4.80 & 6.09 & 0.13 & -2.41 \end{pmatrix}$$

$$\Lambda(0) = \begin{pmatrix} 23.84 & -22.95 & 0.11 & 0.00 \\ -49.01 & 49.09 & 0.02 & 0.90 \\ 39.23 & -39.31 & 1.08 & -0.00 \\ -13.06 & 14.18 & -0.21 & 0.10 \end{pmatrix}$$

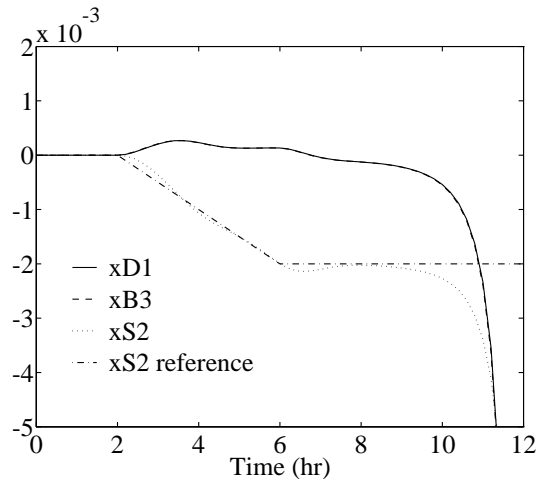


Figure 5.12: $x_{S2} = 0.994 \rightarrow 0.992$ setpoint ramp decrease from $t = 2$ to $t = 6$, LVR_LS-configuration.

We see that although a suitable pairing exists ($L \rightarrow x_{D1}$, $V \rightarrow x_{B3}$, $R_L \rightarrow x_{S1}$ and $S \rightarrow x_{S2}$) the manipulated variable R_L has a very low gain towards *all* control objectives. The largest gain is about 0.23 which means that the input signal needed to reject disturbances will be approximately 4-5 times the assigned bounds. The closed loop disturbance gain is nearly identical to the three-point control case. The additional measurement x_{S1} is insensitive to all disturbances, having values below 0.2 at all frequencies and thus not needing control at all for disturbance rejection. Conclusion: x_{S1} is insensitive to both inputs and disturbances. This confirms the steady-state analysis where we found that specifying the ratio x_{S1}/x_{S3} may not yield feasible solutions.

5.5.5 Problems with Four-point control

It was predicted earlier that four-point control may experience problems with either R_L or R_V fixed. This is indeed the case, and Fig. 5.12 shows the result of a setpoint *decrease* in x_{S2} with fixed $R_V = 0.517$; the column becomes unstable. Reflux and boilup reach the imposed constraints (+100%) without managing to hold the specifications. The reason for this is that R_L , when used for control, is reduced to comply with the specification on x_{S1} . This in turn brings R_L into the hole, causing the specifications set to become infeasible. The difficulties with operating in areas corresponding to “holes” in the $V/F(X)$ plots seriously limit four-point control, despite good disturbance rejection properties.

5.5.6 Four-point control with multiple sidestreams, LVR_SS configuration.

As mentioned in Chapter 5.2, several sidestreams can be withdrawn from the column to add degrees of freedom for optimization or control. Here two liquid sidestreams S_1 and S_2 (which are then mixed to a single side product) are considered for improved control over the sidestream impurities.

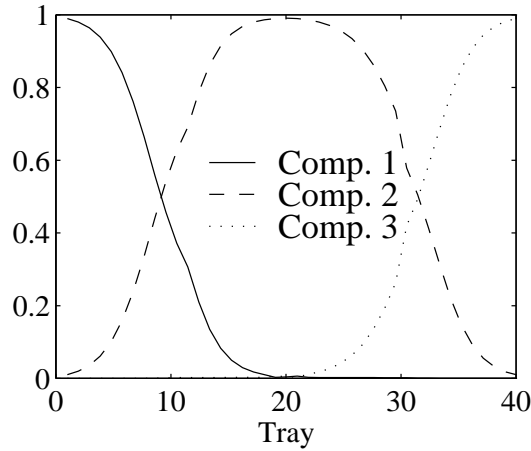


Figure 5.13: Composition profile in main column section.

Configuration	V/F	Highest x_2
Base case	2.34	0.994
1 tray separating side draws	2.44	0.995
3 trays separating side draws	2.72	0.996

Table 5.3: Economic sensitivity to placement of multiple sidedraws.

Consider the column composition profile in Fig. 5.13. We see that component 2 creates a bell-shaped curve with a maximum around the sidedraw. If it is of interest to keep the impurities at a prescribed level, having two separate product streams will increase the flexibility (through the choice of blending). Envision (for clarity) that the product streams are withdrawn from trays 15 and 25. If the blend of these two streams is to follow the specification $x_{S2} = 99.4\%$, then obviously x_2 must be equal or above 99.4% (i.e. overfractionation) over a wider span of trays around the sidedraws. The point here is that increased flexibility in the sidedraw product specification gives increased utility use through some overfractionation. This holds for the comparison with an optimal sidedraw placement, but might be reversed for bad designs where the introduction of a second drawpoint relieves a “stressed” profile.

To make the discussion conceptually simpler, the two product streams are mixed and the fractional content of the upper sidedraw, denoted R_S , is introduced. Thus, the set of actuators becomes $u = (L \ V \ R_S \ S)^T$. This is closely related to the $LVR_L S$ configuration in that a stream distribution is used to manipulate the sidestream impurities, only the streams are external, not internal to the column.

The flexibility of x_{S1}/x_{S3} is limited by the compositions of the separate draws, that is, the cases $R_S = 0$ or $R_S = 1$. Clearly, sidedraws far from each other will allow more leverage w.r.t. x_{S1}/x_{S3} than sidedraws next to each other.

We first examine the economic penalty of having separate draws (within the same total number of trays). Table 5.3 shows the added boilup from having 1 and 3 trays

between S_1 and S_2 compared with the base case data. We see that within the allotted amount of trays, attaining the required separation quickly becomes expensive. Table 5.3 also shows the highest x_2 between the sidedraws. As mentioned earlier, some overfractionation is necessary in the column for the side product to reach $x_{S_2} = 0.994$.

In the following, S_1 and S_2 are separated by one tray (combined, the total side product is again S), giving $x_{S_1} = 0.0046$ and 0.0016 , respectively, when $R_S = 0$ or $R_S = 1$ and $x_{S_2} = 0.994$ is specified. The analysis of this configuration shows that R_S resembles R_L with respect to gain and interaction and is thus not suited for control. The gain matrix G ,

$$G = \begin{pmatrix} 141.56 & -166.91 & -0.20 & 0.02 \\ -145.22 & 171.63 & 0.13 & 21.88 \\ 22.91 & -27.17 & 0.21 & -0.09 \\ -4.19 & 5.35 & -0.07 & -2.55 \end{pmatrix}$$

which corresponds to the following measurements and actuators

$$y = \begin{pmatrix} x_{D1} \\ x_{B3} \\ x_{S1} \\ x_{S2} \end{pmatrix} \quad u = \begin{pmatrix} L \\ V \\ R_S \\ S \end{pmatrix}$$

is visibly similar to the gain for the LVR_LS configuration. Thus, the $LVR_S S$ configuration can not be recommended for four-point control. The solution with multiple sidestreams will give increased flexibility, though.

5.5.7 Possible operational problems

Seider *et al.* (1990) discussed complex nonlinearities and questioned the stability of the Petlyuk column on the different solution branches (the work only uses this as an illustrative example). This work has not found any indications of this property when looking at the system eigenvalues for the linearized plant on all solution branches.

The steady state results and simulations in this paper are based on the condition that R_L , R_V or both can be measured (and manipulated) to a certain accuracy. This section discusses possible problems in view of common control limitations and current practice.

R_L and R_V are both ratios although flows are the real static or dynamic variables. As with the $(L/D)(V/B)$ control scheme for binary distillation (see for example chapter 4.5 in this thesis for a description), ratio control demands more instrumentation than corresponding single flowrate based schemes (LV -control in the binary case). For the Petlyuk column this is equivalent to controlling only one stream out of the interconnection trays. For the liquid split at the top of the prefractionator controlling only one stream is feasible, since tray overflow is selfregulating.

R_V does not easily lend itself for control since this involves manipulating vapor flows in a non-confined area (i.e. not pipes) and the current implementation at UMIST leaves R_V uncontrolled. Controlling column pressure in distillation can usually be done within 2% (Tolliver and McCune, 1980) allowing for sensor error and actuator

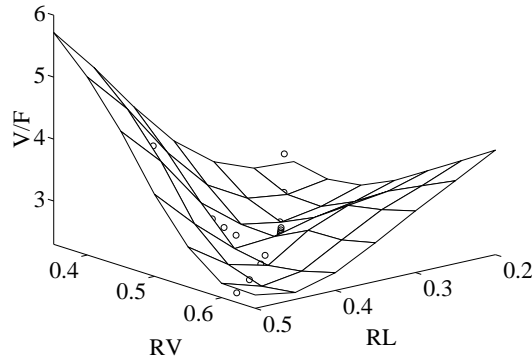


Figure 5.14: Surface plot of solution points for boilup as a function of R_L and R_V .

uncertainty. Similar results might be attainable with pressure drop “vents” given that the design is suitable.

The economic sensitivity to erroneous values for R_L or R_V is evident from tracing their optimal values in a three-dimensional plot. From the mass balance over the column the relation between R_L and R_V is found to be

$$R_L = (V/L)R_V - (1/L)D' \quad (5.3)$$

where D' is the net distillate from the prefractionator ($V_1 - L_1$ in Fig. 5.1a). Thus, the sensitivity to uncertainty in R_L and R_V depends on their mutual distribution. From Fig. 5.14 we see that the worst error is when $\Delta R_L = -\Delta R_V$ over most of the parameter space.

It is apparent that the parameter sensitivity is design dependent, varying with changes in number of overall trays, tray distribution or design vapor speed. Excessive overdesign (many more trays than optimal) may introduce “pinch zones” in the column where the composition hardly changes. This will ‘buffer’ disturbances or decouple the column sections above and below the pinch.

This work has so far evaluated direct composition control of three or four compositions. In many distillation systems, however, a single control loop is often implemented to stabilize the column composition profile, typically a tray temperature. See for example the work of Wolff and Skogestad (1993)[‡] for a discussion on the effects of using cascade control in distillation. There are more possible alternatives in the choice of which tray temperature to control in the Petlyuk column than in ordinary binary distillation. The obvious choice is to control a tray temperature close to the most critical composition measurement, giving an overall stabilization of the composition profile. Choosing a tray temperature closer to the sidestream may, however, be better since the continuous composition profile of *three* components gives a two-way temperature dependence, not only one-way.

[‡]Corresponds to chapter 4 in this thesis

5.5.8 Control comparison with conventional configurations

The Petlyuk column has been presented as a viable solution for ternary separation. This section compares the Petlyuk column with more common ternary distillation sequences.

Speed of Response. The direct and indirect designs consist of two complete distillation columns, which together with holdups and piping will certainly give a larger deadtime through the separation section. This may not be important, just like the size of the deadtime in unmeasured disturbances usually doesn't matter. However, with the increased implementation of supervisory control (in addition to for example a DCS), setpoint changes are more frequently imposed. Quicker plant settling may enable updates to be performed more often and indirectly improve economics.

Robustness of x_{S2} specification. The Petlyuk column has a continuous composition profile around the sidedraw S , while the four conventional designs have discontinuous profiles and are thus very dependent on the separation in the first (or main) column section. Consider the direct sequence; if too much light component follows into the second column, x_{S2} cannot reach its specification since the impurity x_{S1} has no exit point but S . The same argument holds for the other conventional designs. This makes the Petlyuk design more robust towards uncertainty in the side draw specification.

Flexibility. Increased product specifications are probably easier dealt with in ordinary distillation, where common design rules allow a large degree of overfractionation. In the Petlyuk design especially the sidestream is sensitive to increased purity demands. Feed disturbances are handled differently depending upon the control configuration. Using $(L/D)(V/B)$ configuration for the top and bottom composition control, for example, will probably be more resilient to feed flow disturbances than the LV -configuration. The degree of optimality to permanent changes (for example through a debottlenecking) is not clear.

Maintenance. Using a conventional arrangement includes more holdups and thus more control loops. This results in greater maintenance tasks as well as larger chances of problems such as pump failure or actuator wear. It must be noted though, that design of actuators for manipulating R_L and R_V is very uncertain.

5.6 Design suggestions

This section summarizes discoveries important in design of the Petlyuk column.

Internal flows Because of the many interconnections in the Petlyuk column, there are also many different liquid and vapor flowrates. Optimal operation will depend on the internal flow regimes so these should be investigated, also considering possible flooding and weeping. High internal flowrates in the main column section will minimize the disrupting effect on the composition profile from the prefractionator product. Conversely,

Sidedraw	V/F (4 spec.)	V/F (3 spec.)
2 up	2.93	2.67
1 up	2.55	2.43
Base case	2.34	2.34
1 down	2.60	2.35
2 down	2.66	2.45

Table 5.4: Economic sensitivity to side draw position with 3 and 4 product specifications.

very low internal flows will easily give an unbalanced system under external influences. (example: disturbance in feed enthalpy).

Sidestream placement To enable fine tuning of the sidestream composition, multiple sidedraws and blending opportunities are advised. This is especially important where a wide range of feed compositions are treated and when 4 product specifications are imposed. The side draw placement is also important for economic operation, given that wrong placement of the sidedraw can make a big difference in the boilup. Table 5.4 shows how V/F depends on the sidedraw placement for three and four specifications. The boilup is less sensitive with only three specifications since x_{S1}/x_{S3} can then vary freely. This is in line with the lower sensitivity to the internal splits R_L and R_V .

Pressure control This study has not investigated the effect on pressure control from column holdup (load). Increased liquid holdup on the trays will effect the pressure drop, such that pressure control and liquid/vapor distribution may not balance for all operating phenomena. This is not thought to be of significant importance.

Startup Equation 5.3 is also useful for determining R_L and R_V for the startup period (normally total reflux). D' is obviously zero and L and V are equal, giving $R_L = R_V$. This is reasonable since the best separation is usually when the liquid and vapor flows balance. There may be other startup issues that can significantly reduce the time it takes to establish the correct column composition profile.

5.7 Conclusion

The Petlyuk column displays complicated behavior with multiple internal distributions for given product compositions. Some product specification sets may be infeasible (“holes”) for some choices of R_L and R_V in the operating range. It has been shown that fixing R_L or R_V at values in the “hole” may give instability to x_{S2} setpoint increases *and* decreases, respectively. A better understanding of the complexities of the Petlyuk column is needed.

The results have illustrated that it is possible to control a Petlyuk column, although serious problems may arise due to the mentioned “holes”. Three-point control looks most promising. If four specifications are to be controlled, then one should choose as actuator the internal split ratio that does not give a hole for the chosen operating

range. Although the gain of R_L and R_V are not very large, the right choice should at least keep the column out of the trouble spot.

There is an abundance of DOFs when counting both design and control and all have not been exploited here. The design of the Petlyuk column is a difficult task and developments here may aid the operational problems encountered.

References

- [1] Brugma, A.J., 1937, Dutch Patent No. 41,850 (October 15, 1937).
- [2] Cahn, R.P. and A.G. Di Micelli, 1962, U.S. Patent No. 3,058,893 (October 16, 1962).
- [3] Cerda, J. and A.W. Westerberg, 1981, "Shortcut Methods for Complex Distillation Columns. 1. Minimum Reflux", *Ind. Eng. Chem. Process Des. Dev.*, **20**, 546-557.
- [4] Chavez, C.R., J.D. Seader and T.L. Wayburn, 1986, "Multiple Steady-State Solutions for Interlinked Separation Systems", *Ind. Eng. Chem. Fundam.*, **25**, 566-576.
- [5] Faravelli, T., M. Rovaglio and E. Ranzi, 1989, "Dynamic Analysis and Stability of Interlinked Multicomponent Distillation Columns", *Dechema Monographs*, **116**, p. 229-236.
- [6] Fidowski, Z. and L. Krolkowski, 1986, "Thermally Coupled System of Distillation Columns: Optimization Procedure", *AIChE J.*, **32**, 4, 537-546.
- [7] Glinos, K. and F. Malone, 1988, "Optimality Regions for Complex Column Alternatives in Distillation Systems", *Chem. Eng. Res. Des.*, **66**, 229-240.
- [8] Grosdidier, P., M. Morari and B.R. Holt, 1985, "Closed-Loop Properties from Steady-State Gain Information", *Ind. Eng. Chem. Fundam.*, **24**, 221-235.
- [9] Hovd, M. and S. Skogestad, 1992, "Simple Frequency-Dependent Tools for Control System Analysis, Structure Selection and Design", *Automatica*, **28**, 5, 989-996.
- [10] Petlyuk, F.B., V.M. Platonov and D.M. Slavinskii, 1965, "Thermodynamically optimal method for separating multicomponent mixtures", *Int. Chem. Eng.*, **5**, 3, 555-561.
- [11] Rudd, H., 1992, "Thermal Coupling for Energy Efficiency", *Chemical Engineer (Distillation Supplement)*, 27. august 1992.
- [12] Seider, W.D., D.D. Brengel, A.M. Provost and S. Widagdo, 1990, "Nonlinear Analysis in Process Design. Why Overdesign to Avoid Complex Nonlinearities?" *Ind. Eng. Chem. Res.*, **29**, 805-818.
- [13] Stupin, W.J. and Lockhart, F.J., 1972, "Thermally Coupled Distillation - A Case History", *Chem. Eng. Progress*, **68**, 10, 71-72.

- [14] Tedder, D.W. and D.F. Rudd, 1978, "Parametric Studies in Industrial Distillation: Part 1. Design Comparisons", *AIChE J.*, **24**, 2, 303-315.
- [15] Triantafyllou, C. and R. Smith, 1992, "The Design and Optimisation of Fully Thermally Coupled Distillation Columns", *Trans IChemE*, **70**, 118-132.
- [16] E.A. Wolff and S. Skogestad, "Control Configuration Selection for Distillation Columns under Temperature Control", *Preprints European Control Conference '93*, Groningen, The Netherlands, June 28-July 1, 1993.
- [17] Wright, R.O., 1949, U.S. Patent No. 2,471,134 (May 24, 1949).

Chapter 6

A Procedure for Operability Analysis

Erik A. Wolff*, John D. Perkins[†] and S. Skogestad[‡],
Imperial College of Science, Technology and Medicine
Centre for Process Systems Engineering
London, SW7 2BY, U.K.

Presented at
ESCAPE-4, Dublin, March 1994.

Abstract

The work presented here considers operability assessment and subsequent design of a (decentralized) control system for a total process plant. The work shows how operability tools perform for plant-wide applications. We also discuss in which sequence operability analysis tasks should be performed, to maximize the benefit of the available information. These guidelines are collected into a procedure for operability assessment.

*Present Address: ABB Environmental, Box 6260 Etterstad, N-0603 Oslo, Norway

[†]Address correspondence to this author.

[‡]Address: Chem. Eng., University of Trondheim-NTH, N-7034 Trondheim, Norway

6.1 Introduction

During any plant construction (design) project, the question arises of how well the finished plant will run. The answer must cover numerous issues, including “smoothness” of operation, versatility, safety, etc. In total, we want an “operable” plant. How to obtain a credible answer to this question is a difficult task. This work tries to alleviate this assessment process.

To date, a large variety of measures and techniques have been proposed to assess a plants operational characteristics and to help devise a good control system. Many of them are specific to the type of process (plant-wide or single unit operation) or the type of model (flowsheet description or differential equations, steady state or dynamic).

Considering the amount of attention each separate assessment step has received, one would expect more effort to be applied in structuring them together to maximize the benefit. Indiscriminately applying some analysis tools, but not others, may obscure the total picture and leave some aspects unresolved.

There is an incentive to increase the scope of plant analysis and control system design to include more operational effects. We will look into clarifying the relationships between the different steps of operability assessment and apply these principles to a test case; the HDA plant.

6.2 Operability and Control

A process plant and it’s control system have to attend to many different specifications during operation. These requirements can be summarized in that we want the plant to be “operable”. We thus define:

Operability: The ability of the plant (together with the control strategy) to achieve acceptable static and dynamic operation. This includes switchability, flexibility and controllability, safety and fault tolerance.

It is of interest to assess the operability to ensure that proper operation is feasible for the integrated plant as a whole. The next sections will try to clarify operability in terms of analysis tasks and decisions on the plant and operating point.

6.2.1 Elements of operability

The following is a break-down of operability into a set of properties of the plant and operating point and decisions to be made during operability assessment.

- *Stability:* The ability (of the open-loop plant) to remain at a fixed operating point.
- *Optimality:* A mode of operation which coincides to an extremal point in an objective function, usually an economic condition. We will distinguish between optimality regarding the plant structure and the subsequent choice of optimal

operating point. Optimality will in this context not treat structural decisions, only design parameter optimization.

By viewing optimality without considering the back-off needed to facilitate operation in the face of modeled or unmodeled disturbances, we are only dealing with an approximation to the optimal plant/operating conditions.

- *Measurements:* The choice of measurements to be used as controlled variables. These are closely linked with the purpose of the plant, and usually found by examination of specifications to be met and how variables perform against the constraints which are levied upon them. Often, variables at their bounds need to be controlled. Safety and other non-productive constraints also give needed controlled variables.

It may not always be possible to extract the favored output from the plant, in which case a calculated estimate or another closely linked variable is used.

- *Manipulated variables:* Finding a set of manipulated variables and assigning them to the task of controlling a choice of outputs, resulting in a feasible and suitable set of relationships for control.
- *Flexibility:* Ensuring feasible regions of steady state operation for a variety of different conditions, also denoted static resiliency. This may relate to disturbances, imposed changes or degenerate conditions such as fouling. Robustness to uncertainty is also considered part of the flexibility assessment, since some plant parameters are sometimes only known within a range.
- *Controllability:* To be able to move the plant efficiently from one operating point to another despite dynamic changes levied on the plant. We choose to include disturbance rejection properties as well as servo performance into the controllability assessment, as both are highly linked with the perception of quality in control and operation.

6.2.2 Sequencing the operability tasks

It is apparent that the issue of stability affects the controllability. Likewise, the choice of optimality may influence the flexibility of the plant. Thus, to efficiently use the analysis tools outlined above, one must apply them in a suitable order. We will give a justification below for the order of analysis we have chosen. Basically this involves looking at the relationships between the different issues and finding the sequence that does not render previous work ambiguous. This also involves considering the set of decisions that has to be made on the plant and operating point. Fig. 6.1 summarizes the consequential relations between the analysis tasks.

The following points justify why the sequence *stability - optimality - measurements - manipulated variables - flexibility - controllability* was found to be best.

- *Stability* is a basic inherent feature that alone can decide the fate of a design. This is a very important dynamic feature of the plant, being linked with performance as

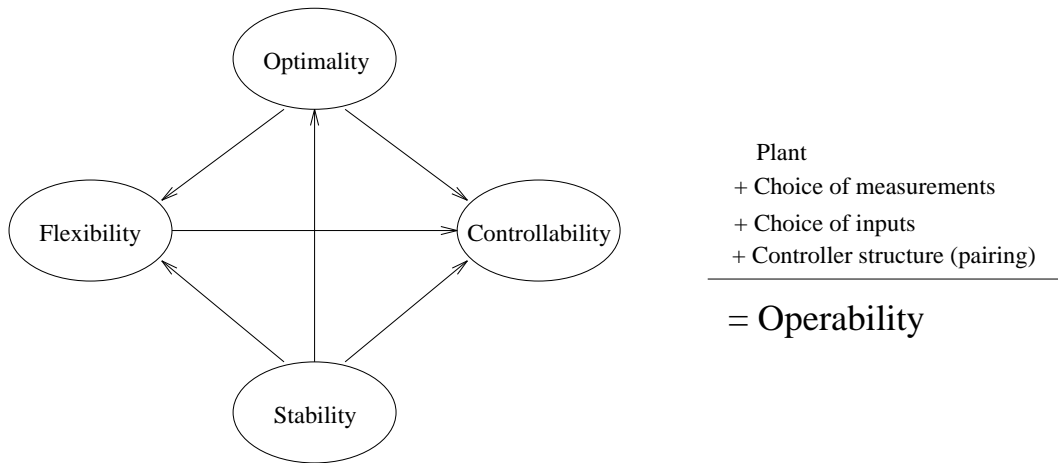


Figure 6.1: Consequential relations between operability conditions.

well as safety, economics, maintenance etc. Hence, stability should be evaluated first. *Instability*, however, may not warrant a design change, depending on the possible solutions to alleviate this (for example control).

- *Optimality* is the measure by which one rates the different designs. Performing this task without considering stability may lead to a design with inherent limitations that no controller may alleviate. It is reasonable to assess optimality next since this stage does not demand information about the controller structure.
- *Measurements* represent the main objectives of the plant, and deciding which to use for control is the first step not only concerned with the plant, but also with the controller. The selection process must be done after the optimality calculations, since changing the operating point through the optimality conditions may also change the number of control objectives to be met (constraint control).
- *Manipulated variables* are chosen based upon the measurements to be controlled and their interacting qualities. Doing this at an earlier stage would mean choosing without even knowing if they would be able to perturb the process at all.
- *Flexibility* is a quality of the chosen design, but also linked with the operating point and the chosen controller structure. This is reasonable since the effect of disturbances or imposed changes varies with the operating conditions. Also, assessing flexibility without the controller structure may hide information pertinent to the true operating mode. A typical flexibility requirement is that the plant can operate at a reduced capacity. A measure of flexibility is then how economically the process can operate under such conditions, which clearly demands knowledge of the use of manipulated variables.
- *Controllability* should conclude the operability assessment. This follows since controllability assesses servo performance and disturbance rejection, which are the final properties upon which the plant and control system are to be judged.

Figure 6.2: HDA plant

Also, controllability is a measure of *quality*, in which subtle changes from other operability considerations may change the judgement.

Of course, it could be argued that all these aspects interact in a more complicated way than implied by a sequential treatment. For example, since stability of a nonlinear system depends on operating point, there is a two-way interaction between these two issues. However, we believe the procedure defined above is the best sequencing of tasks.

6.3 Example

The HDA plant involving the hydrodealkylation of Toluene to Benzene is shown in Fig. 6.2. The chosen structure of the HDA plant includes a reactor, several heat exchangers, a flash drum, a stabilizer and two distillation columns plus mixers and splitters. For a comprehensive description refer to Douglas (1988). The model was implemented in SPEEDUP, an equation oriented simulator. Implementation specific details are given in appendix.

Optimization of the process is done with respect to overall economics, denoting the target as the **Economic Potential**, or EP. This value includes capital and operating costs, also considering fuel value of byproducts as well as use of utilities. Typical shortcut calculations are used for the equipment costs.

1	Cooling water temperature
2	Downstream pressure
3	Fuel value
4	Toluene and H_2 feed temperature

Table 6.1: Plant disturbances

6.4 Operability Study

6.4.1 Stability

It has been established that the process is unstable when energy-integrated (for example by looking at the eigenvalues of the process). Hence, the forthcoming analysis will be performed with one stabilizing controller implemented; between the reactor feed temperature and the furnace fuel flowrate. Controllability analysis can be performed on unstable plants, but the stabilization here is natural, giving a reduced problem to analyze.

6.4.2 Optimization

The optimal operating point of the plant is calculated at steady state without regarding backoff from the constraints. The constraints are either specifications to the process or design restrictions on equipment. 14 variables were optimized to find the most economic operating point. Five of these were against their constraints at the solution. An **Economic Potential** $EP = 3.87M\$$ was realized at the optimum.

At this optimum the production was at its upper bound, the H_2 /Aromatics ratio on its lower bound and the flash inlet temperature also at its lower bound. The flash outlet pressure was at its upper bound. Finally, the purity was at the lower bound.

6.4.3 Measurements

The bounded variables from the optimization are prime candidates for control, insofar as they can be measured. This work does not consider state estimation or related topics. We thus assume that the mentioned plant objective are available as measurements.

Plant control consists of disturbance rejection as well as setpoint tracking. We would thus like to establish if there are feasible measurements for detection of the disturbances. The actual evaluation of performance will be done in the later sections.

There are a number of disturbances, which are either fast or slow. Focusing on disturbances that change faster than every few minutes will put emphasis on control issues that can't be handled in other ways. These are therefore omitted. The disturbances that are most important are given in table 6.1.

Disturbances in the cooling water temperature can be detected since the flash inlet temperature is a candidate measurement. The compressor has been modeled with constant discharge pressure. Downstream pressure disturbances will affect the flash vessel

1	Production rate
2	Flash vessel outlet pressure
3	Reactor inlet H_2 /Aromatics ratio
4	Flash vessel inlet temperature
5	Product purity

Table 6.2: Plant measurements

and thus the reactor exit pressure. Having the flash outlet pressure as measurement will allow detection of this disturbance. The fuel value will only enter through the reactor preheater, which is already controlled for temperature stability. The feed temperature disturbances will also be treated in the same manner and are thus omitted. Feed rate disturbances are not considered since the feeds are usually used for either scheduling or control and flow measurements are usually available upon entry to the plant.

The purity of the benzene product is assumed only affected by the toluene and diphenyl content since the amount of methane and hydrogen is so minute. We thus find that one product composition measurement will suffice for monitoring the product purity.

The current objectives thus seems adequate and we arrive at the set of measurements in table 6.2. There are obviously control needs here that are not addressed, such as surge control of the recycle loop compressor. The control for these purposes are not included as they are considered intrinsic to the units themselves.

6.4.4 Scaling

To be able to interpret the data correctly all measurements, manipulated variables and disturbances have been scaled to within $< -1 : 1 >$. This ensures that results are on a comparable basis. The manipulated variables are scaled to a 20% variation, while the measurements and disturbances have heuristically chosen scalings as shown in table 6.3. This gives the allowable perturbations corresponding to a $< -1 : 1 >$ range.

6.4.5 Choosing manipulated variables

The available manipulated variables are given in table 6.4.

There exist several heuristics for determining which manipulated variables to use in multivariable control. These are usually concerned with the closeness between manipulated variable and measurement to assure sufficiently speedy response. There are other rules considering which inventories to control etc. Attempts have also been made to develop the control system along with the plant, from the initial input-output model and onwards (Ponton and Liang, 1992). These invariably start with feed/product rate control and add controllers (multivariable or loopwise) as elements of the plant are

Measurement	Value	Scaling
Flash inlet temp. [$^{\circ}C$]	37	2.2
Production rate [kmol/hr]	121	2.27
Product purity [%]	99.98	0.01
Reac. H_2 /Aromatics ratio	4.8	0.2
Flash outlet pressure [atm]	31.0	0.34
Disturbance		
Cooling water [$^{\circ}C$]	15	5
Downstream Pressure [atm]	23.8	3.4

Table 6.3: Measurement and disturbance scalings

1	Benzene column reflux ratio
2	Benzene column reboiler vapor flow
3	Compressor power
4	Pre-flash cooler duty
5	Gas feed flow
6	Toluene feed flow
7	Flash liquid outlet valve opening
8	Flash vapor outlet valve opening
9	Flash inlet valve opening
10	Purge outlet valve opening
11	Stabilizer reflux ratio
12	Stabilizer vapor flow
13	Toluene column reflux ratio
14	Toluene column reboiler vapor flow

Table 6.4: Available manipulated variables

added. This approach will invariably limit the available actuators for each successive step, allowing less flexibility in assigning these manipulated variables.

Another possible method (for linear models) is to examine the singular value decomposition (or even simpler, look at the magnitudes of G). Manipulated variables corresponding to very small singular values will in general not have enough power to effectively move the plant. The smallest singular value ($\underline{\sigma}$) can also be used to judge the attainable performance of the plant (Morari, 1983). Selection of manipulated variables (from a larger set) can thus be done by finding the subset that gives the least reduction of $\underline{\sigma}$. Here it is especially important that the variables are scaled to avoid comparing results on an incompatible basis.

Here $\underline{\sigma} = 2.37$ when including all manipulated variables and objectives 1, 2, 4, 5, 6. Reducing the number of manipulated variables to a square controller give the three best alternatives in table 6.5. Note that size of the search space (given a square

Set	Inputs	σ
1	[4 5 6 9 10]	1.55
2	[1 4 5 6 10]	1.34
3	[1 5 6 9 10]	1.00

Table 6.5: Ranked set of manipulated variables.

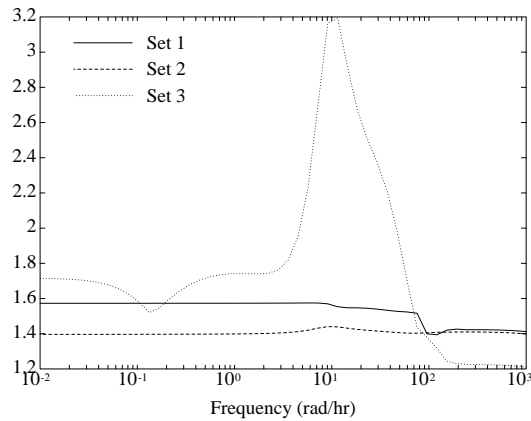


Figure 6.3: Required control action for perfect control (Maximum value).

control strategy) increases with $\frac{\#u!}{\#y!}$, where $\#u$ and $\#y$ are the number of alternative inputs and number of outputs, respectively. However, an incremental search removing successively the least significant input give close to the best answer. A variety of this approach was used here.

Evaluating the three chosen sets give us the following comments:

- Set 1: Controlling the product purity without having access to the benzene columns reflux will undoubtedly slow down the response a great deal.
- Set 3: Using both the purge valve opening and the flash inlet valve within the gas recycle loop might cause unstable behavior through competing inventory controllers.

Based on the comments above we proceed the analysis with actuator set 2.

Another way of looking for manipulated variables is to see which combination of manipulated variables can give low values for $u_{required} = G^{-1}G_d d$ for the chosen measurements. This corresponds to control action needed for perfect control, and will often be of higher magnitude than available. But it is an interesting ground on which to compare a selection of possible manipulated variables. This demands that the disturbances be identified, but an estimate of the most prominent disturbances is usually available. The curves in Fig. 6.3 correspond to the maximum value of $u_{required}$, indicating that set 2 requires the least power for good disturbance rejection.

6.4.6 Flexibility

We have chosen to assign flexibility to steady state changes. There are several approaches which can be used, depending on how conservative one wants the estimate. Possibilities include mutually exclusive or worst-case changes as well as applying “perfect control” or a real control system for the evaluation.

Not only is the operating point of the plant important on the flexibility, also the choice of the manipulated variables and measurements play a part here.

The disturbances involve cooling water temperature and downstream pressure. All enumerations of their extremal values were applied to the controlled plant (we used the multi-loop scheme as found through Λ below). No cases had steady state deviations or breached constraints.

Flexibility is concerned with the different steady state operating points. Thus, the choice of analysis method can have impact on the economics of the plant through the long term use of manipulated variables. At the optimal operating point, all control schemes are equal in terms of cost. When several operating points enter the evaluation, different control schemes will execute the control task by using different actuator efforts. Based on this fact (and looking at either disturbances or setpoints), control schemes can be ranked by how they tax the different utilities.

Another interpretation of flexibility that might be pertinent to mention is *disturbance range*, or how large disturbances can be handled without the process hitting constraints. This is not primarily an economic consideration, but can be a valuable source of information where no amplitude of the disturbances may be identified beforehand. Such an assessment will give rise to an optimization problem and also demand weights on the disturbances to get a useful answer. We do not considered this here.

6.4.7 Controllability

As previously noted controllability is a quality statement subject to individual treatment. One must also remember that intolerable effects in one plant might be permitted or even considered normal or beneficial in others. Thus, the selection of controllability analysis that will be used here may be considered to be a selection of possible methods.

The (scaled) steady state plant and disturbance gain matrices:

$$G(0) = \begin{pmatrix} -1.563 & 2.850 & 0.905 & 1.324 & -1.636 \\ -0.151 & 8.086 & 1.566 & 7.199 & -1.164 \\ -0.527 & 13.594 & 7.868 & -5.957 & -2.283 \\ 0.797 & -2.896 & -3.612 & -7.504 & 1.378 \\ -0.053 & 8.726 & -0.090 & -0.241 & -8.527 \end{pmatrix}$$

$$G_d(0) = \begin{pmatrix} 2.185 & 1.929 \\ 0.210 & 1.372 \\ 0.736 & 2.691 \\ -1.114 & -1.624 \\ 0.074 & 10.051 \end{pmatrix}$$

Several disturbance gain elements are greater than 1.0, indicating that control is indeed necessary.

Condition number: The condition number, $\gamma = \frac{\bar{\sigma}}{\underline{\sigma}}$, giving the ratio between the smallest and largest singular value, is here 9.42. This tells us how power applied to the plant will respond to sensitivities in different plant directions. This value is low and the plant is not considered ill-conditioned.

Looking at the disturbance condition number ($\gamma_d = \frac{\|G^{-1}g_d\|}{\|g_d\|}\bar{\sigma}_G$) in conjunction with the ordinary condition number reveals that the disturbances do not lie in the most difficult direction of the plant, in fact γ_d is close to one at low and intermediate frequencies.

Singular values: Following the discussion above, $\underline{\sigma}$ can be used to judge how versatile the controlled plant will be. With $\underline{\sigma} = 1.34$ there should not be any problems with long term controller saturation.

It is also of interest to find out which plant direction corresponds to $\underline{\sigma}$ through the SVD-decomposition $G = U\Sigma V^T$. Since the matrices U and V are unitary ($\|u_i\| = \|v_j\| = 1.0$), the values of each vector can be interpreted as fractions of the different inputs/outputs affected by the specific singular value. We find here that neither $\bar{\sigma}$ or $\underline{\sigma}$ are linked to single inputs only, which can give difficulties for ill-conditioned plants. The same results are found for the output directions U .

Poles and Zeros: The process is, as mentioned earlier, stabilized with one loop around the reactor heat integration circuit. Thus, there are no unstable poles in the plant. One negative pole at a frequency of $0.098rad/hr$ may contribute towards some oscillatory behavior though. There is a zero in the right half plane at $\omega = 592rad/hr$ ($9.9rad/min$ or a period of 38 s). The RHP-zero will limit the attainable closed-loop bandwidth, but seems to be beyond the desired or achievable bandwidth anyway.

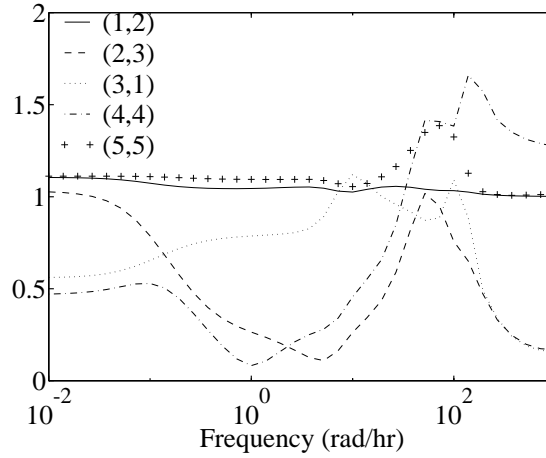
It can be added that input set 1 has RHP zeros at much lower frequencies ($\omega = 3.20rad/hr$), which will decidedly hamper the control. Set 3 on the other hand has no RHP zeros below $1e4$.

Relative gain array: The relative gain array, while telling about interaction and possible pairings, also gives information about sensitivity to modeling error. The steady state values for the mentioned objectives and input set 2 are

$$\Lambda = \begin{pmatrix} -0.11 & \mathbf{1.11} & 0.11 & -0.03 & -0.07 \\ -0.22 & -0.01 & \mathbf{1.03} & 0.35 & -0.15 \\ \mathbf{0.56} & -0.01 & 0.29 & 0.21 & -0.05 \\ 0.77 & -0.08 & -0.32 & \mathbf{0.47} & 0.16 \\ 0.00 & -0.01 & -0.11 & 0.00 & \mathbf{1.11} \end{pmatrix}$$

A possible set of pairings has been emphasized, although *no* choice of controller has to be made at this point.

The low values for the preferred pairings indicate that the plant will not be sensitive to modeling errors and uncertainty. The frequency dependent RGA is also given in Fig. 6.4 to show that the pairing is reasonable in most of the frequency range of interest. In case a multiloop controller is used, the chosen pairings are given in table 6.6. These pairings are also indicated as control loops in Fig. 6.5.

Figure 6.4: Relative gain array, λ_{ii} , for the preferred pairing.

Output	Input
Flash inlet temperature	Pre-flash cooler duty
Production rate	Gas feed flow (H_2)
Product purity	Benzene column reflux ratio
H_2 /Aromatics ratio	Toluene feed flow
Flash outlet pressure	Purge valve opening

Table 6.6: Preferred decentralized pairings for the HDA process.

Performance relative gain array: Devised from the nominal performance bounds on the decentralized closed loop control error, the PRGA, or $\Gamma = G_{diag}G^{-1}$ where $G_{diag}(s)$ is the matrix consisting of only the diagonal elements of $G(s)$, overcomes one of the shortcomings of Λ by indicating if any triangular (one-way) interaction is present in the process. Large offdiagonal PRGA-elements γ_{ij} means that setpoint following in one loop (loop j) results in large interaction in loop i (unless $|g_{ii}c_i| > |\gamma_{ij}|$). For the HDA process with the chosen pairings (Γ must be recalculated for each new set of pairings), we show in Fig. 6.6 how loop 3 suffers from some mild one-way interaction from loops 2 and 4, giving increased loop gain requirements at low frequencies. The frequency where Γ crosses 1 is still much lower than the anticipated bandwidth of the system, indicating no control problems. If a multiloop scheme is used, loop 3 should be fast to accommodate the interactive properties. There is also some high frequency interaction between the control loops, mainly above the bandwidth. The effects are summarized in Table 6.7. When the PRGA increases at high frequency, this means there is a pole excess in $G_{ij}, i \neq j$ compared to G_{ii} . This in return give a zero excess in the off diagonal elements of the PRGA. The PRGA is based on the assumption that $S = (I + GC)^{-1} \approx (GC)^{-1}$, which holds only at frequencies below the bandwidth ($\omega < \omega_B$). This makes the evaluation at high frequency very uncertain, where loop

Figure 6.5: HDA plant with decentralized control loops corresponding to preferred pairing

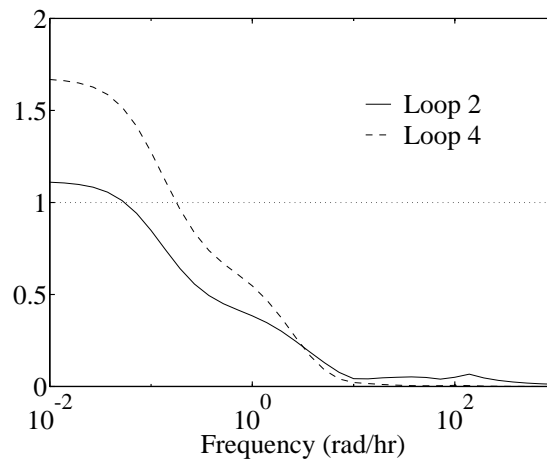


Figure 6.6: Performance relative gain, γ_{ij} showing interaction from loops 2 and 4 on loop 3.

gains will be negligible anyway. The high-frequency interaction indicated by the PRGA is therefore not considered important.

Closed loop disturbance gain: The closed loop disturbance gain, CLDG or $\Delta = G_{diag}G^{-1}G_d$, gives the effect of the disturbances on the control error under multiloop control. The CLDG plot in Fig. 6.7 shows only the $\delta_{i,j}$ elements that are significant. It shows that the downstream pressure gives high bandwidth requirements, while the cooling water has a small direct effect which may or may not cause problems. Note that the disturbances are rejected well in the other control loops.

Note that the purity control loop (y_3) is most sensitive to disturbances (as well to

To loop	Interaction from loop				
	1	2	3	4	5
1	-	H	H		
2		-	H		
3		L	-	L	
4		H	H	-	
5		H	H	H	-

Table 6.7: Interaction between control loops using the PRGA. H: high frequency interaction. L: low frequency interaction.

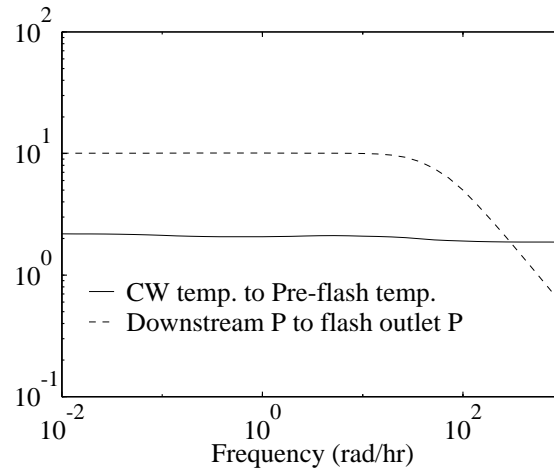


Figure 6.7: Closed loop disturbance gain, Δ_{ij}

interaction as indicated by Γ above), so particular scrutiny should be applied to this measurement. Also, if a sequential controller design procedure is to be applied, this controller should be the fastest to accomplish efficient disturbance rejection.

Relative disturbance gain: The relative disturbance gain β introduced by Stanley (1985) is based on the same principle as the RGA and has the same property of being independent of scaling. $\beta = (\tilde{G}G^{-1}G_d)/G_d = \Delta/G_d$, where $'/'$ denotes element by element division, can be viewed as the ratio of the disturbance effect on a measurement with and without control.

$$G_d = \begin{pmatrix} 2.18 & 1.93 \\ 0.21 & 1.37 \\ 0.73 & 2.69 \\ -1.11 & -1.62 \\ 0.07 & 10.05 \end{pmatrix} \quad \beta = \begin{pmatrix} 1.00 & 0.00 \\ 0.00 & 0.00 \\ 0.00 & 0.00 \\ 0.00 & 0.00 \\ 0.00 & 1.00 \end{pmatrix}$$

Comparing G_d (open loop effect on y) with β , the controller has removed the effect of the three disturbances from most of the measurements. Measurements 2, 3 and 4

Controlled measurement	K	τ_I (hr)
Flash inlet temperature	435	0.94
Production rate	80.0	0.09
Product purity	10.0	1.00
H_2 /Aromatics ratio	33.0	1.00
Flash outlet pressure	0.98	0.0017

Table 6.8: Controller tunings, HDA process.

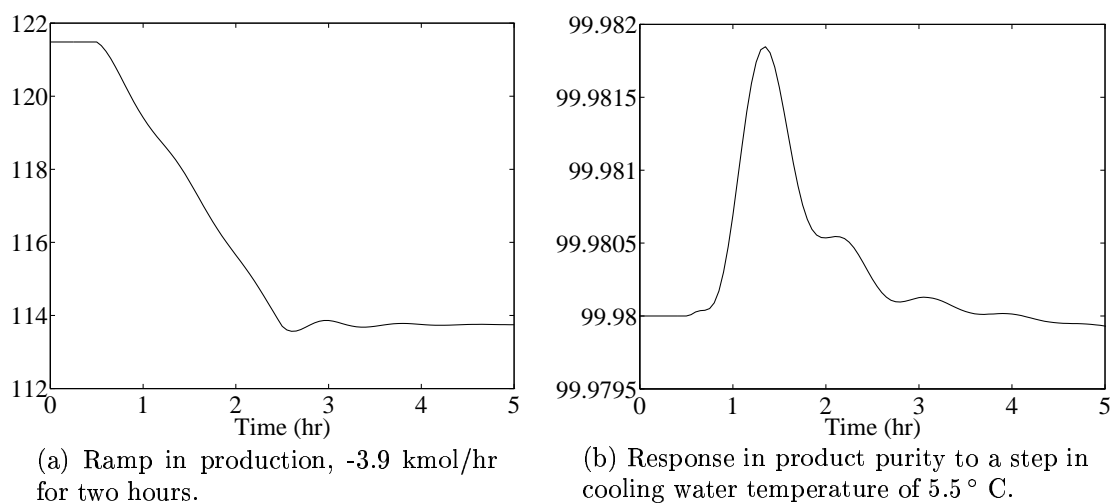


Figure 6.8: Simulation results for HDA plant under decentralized control.

now suffer negligibly from d , while measurements 1 and 5 could favorably been better controlled. This matches closely with the conclusions from the CLDG above.

6.5 Simulations

Simulations were performed to assess the behavior of the controlled system. This included setpoint changes and various types of disturbances.

A set of decentralized PI controllers of were used during the simulations. The PI controller tunings in Table 6.8 were found using the Ziegler-Nichols tuning rules.

Fig. 6.8 shows the response to a production setpoint change and cooling water temperature (CWT) disturbance. CWT was the worst disturbance, i.e. a change in downstream pressure was even better rejected. The control system performs well, giving satisfactory settling and tracking.

6.6 Discussion

Assessing operability is often done without considering how the different issues (properties of the plant and operating point, and decisions made upon it) affect each other. We have in this work shown how a structured approach to operability assessment has advantages in maximizing the information value.

Operability analysis gives much insight into which measurements, manipulated inputs and disturbances that will create limitations during controller design and subsequent operation.

The HDA process is controllable and flexible once the instability of the heat-integrated reactor is resolved. The downstream pressure is the most demanding disturbance, while the third control loop (Benzene purity - Reflux) is most prone to degradation due to interaction.

Controlling the purity through the heavy impurities alone performs well. The HDA plant will have reasonable performance properties with multiloop control.

The following can be regarded as poor properties that one should avoid in plant control design:

1. Excessive controlled variables.
2. Ineffective manipulated variables.
3. Prohibitive interaction.

These properties can all be identified by the proposed procedure. Point 1 is undesirable but not dangerous (unless contributing to interaction), and can be alleviated by removing an unnecessary control (loop). Point 2 & 3 can be treated by localizing other/better manipulated variables for the given measurement set. Point 3 may of course be resolved with multivariable control.

References

- [1] Douglas, J.: "Conceptual Design of Chemical Processes", Mc Graw Hill, 1988.
- [2] Morari, M., 1983, "Design of Resilient Processing Plants - III, A General Framework for the Assessment of Dynamic Resilience", *Chem. Eng. Sci.*, **38**, 11, 1881-1891.
- [3] Ponton, J.W. and D.M. Liang, 1993, "A Hierarchical Approach to the Design of Process and Control Systems", *Chem. Eng. Res. Des.*, **71**, 181-189.
- [4] Stanley, G., Marino-Galarraga, M. and McAvoy, T.J., 1985, "Shortcut Operability Analysis I, The Relative Disturbance Gain", *Ind. Eng. Chem. Proc. Des. Dev.*, **24**, 1181-1188.

Column	Section	Lumps	à Trays
Stabilizer	Rectifying	1	3.40
	Stripping	1	3.55
Product	Rectifying	3	5.02
	Stripping	3	3.85
Toluene	Rectifying	1	3.28
	Stripping	1	3.28

Table 6.9: Column properties.

Appendix 1. Model details for HDA plant.

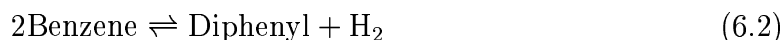
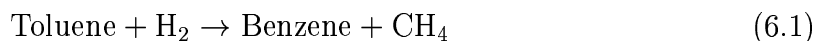
The SpeedUp implementation of the HDA plant was done by Christophe Brognaux, undergraduate student at Imperial College, London. Major modeling details and the objective function for the optimization will be presented here. The detailed models are not included due to the size of the material. More information can also be found in Douglas (1988).

Unit operations with time constants less than 10 seconds were modeled as instantaneous, i.e. did not include dynamics. This was done for the furnace, mixer, purge, compressor and heat exchangers, although the heat exchangers include some dead-time. Dynamic models were made for the reactor, distillation columns and gas/liquid separator.

Thermodynamics The thermodynamic calculations were based upon polynomial or exponential curve fittings. The following dependencies were included in the calculations: density - $\rho(T, P, x)$, enthalpy - $H(T, P, x)$, k-values - $k(T)$, $(C_P/C_V - 1)/(C_P/C_V)$ - $\gamma(T, x)$.

Distillation To reduce the computational load the distillation columns are divided into tray lumps, giving fewer differential equations. The three columns of the HDA plant are made up of a feedtray, total condenser and reboiler in addition to the stripping and rectifying section, which have the properties according to Table 6.9. Constant relative volatilities were used in each respective tray (lump).

Reactor The plug flow reactor was modeled as a series of mixed tank reactors. 19 tanks were found to be suitable. The reaction had an Arrhenius type temperature dependency and the competing reactions are:



The heat of reaction ΔH_R is assumed only from the first (endothermic) reaction as the production of byproduct is low.

Separator A volume of 8.2 m^3 was found to be suitable. The ratio of height to diameter was chosen to be 6.

Feed effluent heat exchanger The exchangers area is 277 m^2 . A heat transfer coefficient of $568 \text{ W/m}^2\text{K}$ was used.

Objective function The main objective is to find the design that maximizes the **Economic Potential**, or EP. Decomposed into cost areas the objective becomes: EP = product value + purge fuel value - raw material cost - utilities cost - capital cost. Here follow some central parameters for cost estimation:

The plant is assumed to have 8150 hours uptime per year. All purge is assumed sold for fuel value.

Item	Cost	Unit
Toluene	14.08	\$/kmol
Benzene	18.89	\$/kmol
Gas (Hydrogen)	2.90	\$/kmol
Steam	2.37	\$/MJ
Cooling water	0.0222	\$/MJ
Fuel	3.79	\$/MJ
Electricity	0.0397	\$/kWh

The cost calculations follow the correlations of Guthrie as summarized in Douglas (1988).

Chapter 7

Operability of Integrated Plants

Erik A. Wolff* and Sigurd Skogestad†
Chemical Engineering
University of Trondheim - NTH
N-7034 Trondheim, Norway

Presented at
PSE-94, Kyongju, Korea, May-June 1994.

Abstract

Various approaches exist for synthesizing plant-wide control, from heuristics to mixed-integer nonlinear programming (MINLP). Few specifically address the problems associated with heat and mass integration in processes. This paper extracts many integration specific aspects and discusses their effect on plant control. The focus is on limitations and tradeoffs within operability. Guidelines are presented for finding good control strategies for integrated plants. We hope this can initiate some work alleviating the engineers problems with this issue.

*Present Address: ABB Environmental, Box 6260 Etterstad, N-0603 Oslo, Norway

†Address correspondence to this author. Fax: 47-73594080, E-mail: skoge@kjemi.unit.no

7.1 Introduction

Design of control systems for complete plants is a difficult and comprehensive task. Often the overall problem is simplified by dividing the process into subsystems, which are considered more or less independently. Typically, this gives rise to multiloop control systems which have the advantage of simplicity in commissioning, startup, shutdown and tuning. Systems of this kind cover more than 90% of the applied control in industry today.

Increased energy and raw material efficiency has been a major force in recent research (for example Linnhoff and Hindmarsh, 1983), giving rise to plants which are more integrated. The integration can be achieved through heat exchange, recycling, combined process units (for example reactive distillation) or aggregated process units (flotation). This integration of process units may occur during initial design or at a later point in the plant lifecycle. The requirements for these two cases are different, since an add-on integration scheme does not usually have the same freedom to change process paths and unit configuration to facilitate better operation. We will in this paper limit our work to initial designs.

The best controlled plant could be viewed as the one found by tailoring the process and control system to each other. However, this usually creates an unmanageable task. The main problem in integrating design and control is the exponential growth in the number of alternatives as the problem size increases. First, steady state process design is itself a combinatorial problem. Second, to evaluate the controllability of a given design, one must consider the best of a number of alternative control structures, which again is a problem that rapidly increases with size. Thus, to integrate design and control one must first be able, for a given process design, to suggest a reasonable control structure and evaluate its control characteristics. In the literature review we have therefore also included references to work on plant wide control system design (structure selection).

Many authors have presented work that has tried to unify the design and control stage of process development. The wish to combine these tasks and the many facets of their implementation (heuristic, mathematical programming, analysis/judgement) have provided the multitude of approaches that exist today. As major directions they can be termed “concurrent”, “sequential” or “iterative”. We will here look at applying control strategy solutions to proposed designs, i.e. a sequential approach.

The control system applied to a plant has to comply with many different operational needs. These requirements can be summarized in that we want the plant to be “operable”. We thus define:

Operability: The ability of the plant (together with the control strategy) to achieve acceptable static and dynamic operation. This includes switchability, flexibility and controllability, safety and fault tolerance.

It is of interest to assess the operability to ensure that proper operation is feasible for the integrated plant as a whole.

The objective of this paper is to isolate and describe the features of integrated plants that affect operability. Operability is here assessed by considering the choice of

measurements and actuators, flexibility and controllability. The difficulties in analyzing the degrees of freedom for integrated plants are illustrated. We look at operability limitations and tradeoffs and present guidelines to help identify operability deficiencies.

7.2 Previous work

This brief review covers the main trends within control of integrated plants and plant-wide control. The references are given chronologically to easier see the developments within the area.

Buckley (1964) proposed to divide plant-wide control into two levels; first material balance (MB) control followed by quality control. The justification relies on the fact that MB and quality control are on different time scales and thus almost independent of each other (MB - slow, Quality - fast). This separation is somewhat arbitrary and proves even less clear for integrated processes. Buckley has a somewhat pessimistic view on operability: "...it is usually necessary to go to a semi-works or pilot plant to demonstrate integrated operation, *process operability*, a final flowsheet and process economics".

Foss (1973) regarded the fundamental problem in process control as not the development of more sophisticated control but rather a framework for selecting manipulated and measured variables for control. The same challenge exists today for plant wide control and control of integrated plants. Foss also claims that "it is the presence of coupling among many variables that is primarily responsible for the near inscrutable complexity of dynamic processes".

Rinard (1975) mentioned operability in his paper and extended the discussion to *integrated* plants, where he anticipated more interaction, less independent manipulated variables and slower response than for un-integrated designs.

Umeda *et al.* (1978) presented a logical structure for control system synthesis. The emphasis is on applying control to all process units individually followed by a coordination phase removing controllers until the system is not overspecified. Structural matrices and heuristics are used during the second phase.

Morari *et al.* (1980) presented an approach to systematic control system design. Here the focus is on decomposition for optimal control.

Morari (1981) subscribed to the need for decomposition in control system synthesis and gave a good discussion on practical results. Structuring of the control tasks, selection of measured and manipulated variables, and interdependencies between design and control are viewed as demanding problems.

Nishida *et al.* (1981) stated that "...the synthesis of control systems for complete chemical plants is a problem within a steady state environment", and held that the most important development to come is identifying the interaction and finding the basic variables that will affect the structure of the plant. The dynamic aspects of both interaction and control have received a rising interest, while the identification problem still holds.

Govind and Powers (1982) proposed synthesizing control systems using structural information (e.g. cause-effect graphs) and simple models.

Stephanopoulos (1982) gave a comprehensive review of problems in process control and stated that identification of manipulated variables, measurements and controller structure is “where novel and imaginative formulations are needed”. Decomposition is emphasized and the article also treats issues such as fault detection and startup/shutdown.

Grossmann *et al.* (1983) defined operability as encompassing flexibility, controllability, reliability and safety although their focus is on using mathematical programming for generating flexible processes.

Calandranis and Stephanopoulos (1986) looked at the interaction between operability and design of heat exchanger networks. Instead of generating a single criteria for operability they checked if the various networks were operable within a predetermined set of operating (including disturbance) parameters. This also allows for identifying what factors limit the realization of the desired operational range. The approach concentrates on detecting *inoperability* at steady-state and is not easily transferred to general process plants. The checking of corner points within the parameter space does not always suffice.

Georgakis (1986) proposed to use extensive variables to reduce interaction to one-way and simplify control design.

Fisher *et al.* (1988) evaluated both controllability and operability when looking at the interface between design and control. Their example contained process integration without this being an issue. The controllability analysis checked for enough manipulated variables and operability is considered as extent of overdesign.

Kravanja and Glavič (1989) have evaluated total heat integrated plants, but only considered control to alleviate a specific problem; a cyclic feed disturbance.

Georgiou and Floudas (1989) used structural modeling to pose the control synthesis problem as a MILP. The framework for generating all feasible control structures is based upon the concepts of connectability, controllability and observability. Selection within structures is not addressed.

Perkins (1989) looked at the interaction between design and control by considering both fast and slow effects, which transforms to the assessment of controllability, switchability and flexibility, or summarized as operability. Linear analysis indices are acknowledged as well as economic indicators.

Price and Georgakis (1992) gave a good discussion on control of large scale systems. The article introduced the terms “self-consistency” and “primary process path” which give additional understanding to Buckley’s material balance control.

Morari (1992) reviewed the effect of design on *controllability* and pointed out:

1. Steady state controllability criteria are unqualified for analyzing dynamic behavior.
2. Ad hoc controller tuning may quantify irrelevant design changes as attractive.
3. Better, simpler controllability criteria are needed before algorithmic synthesis techniques to trade off controllability and economics become meaningful.

Point 3 is valid in general while point 2 can be extended to design of integrated plants; the effect of a design change holds more significance when the flowsheet is reoptimized

to account for this change.

Ponton and Liang (1992) adapted Douglas' (1988) stepwise design theory to control system design by designing the control system in parallel with the plant.

Schmidt *et al.* (1992) investigated the operability of energy integrated distillation columns. The heat-pump between reboiler and condenser reduced the operating space and gave instability. The instability was easily dealt with by control and did not have a major impact on controllability.

Bouwens and Kösters (1992) commented on the trend towards more integrated plants and recognize that operability is also important under non-steady state operating conditions.

Downs and Vogel (1993) presented a challenge problem for studying and evaluating control technology. This example is well suited for studying plant wide and integrated control issues.

To summarize; there have been proposed many techniques for large scale process control, but there is still a great need for future work in this area. Design rules that specifically treat (the more and more common) integration aspects would certainly be helpful. This work addresses several topics concerned with this deficiency.

7.3 Plant-wide control system design

This chapter evaluates the utilization of degrees of freedom (DOF) in design of control systems. Degrees of freedom are usually defined as the number of variables minus the number of equations. We will here adopt the more convenient description of "independent" manipulated variables, often symbolized by an actuator valve. This simplifies the discussion and focus' on our main concern; control system design.

We first consider how the DOF are often identified starting at the highest abstraction level (a single in-out box) and working downwards. Then the design on control systems is addressed before we discuss implications for integrated plants.

7.3.1 "Top-down" selection of controlled and manipulated variables

The first step in designing a complete control system is often a degree of freedom analysis. One generally starts from the top by identifying the overall control objectives (for example production) and then moves towards the bottom of the control hierarchy. To check that there exist degrees of freedom (independent variables, valves, etc.), a "tick-off" procedure is useful, that is one identifies for each objective a degree of freedom.

There must be *at least* as many DOF (variables, valves, etc.) as there are control objectives to be met. For controllability reasons (speed of response) this requirement must also be satisfied locally. This gives another justification for performing the DOF analysis as a "tick-off" procedure identifying possible single-loop control structures (pairings). Some of these variables may be constrained, for example using the feed to a distillation column for control is limited by flooding and weeping conditions in the

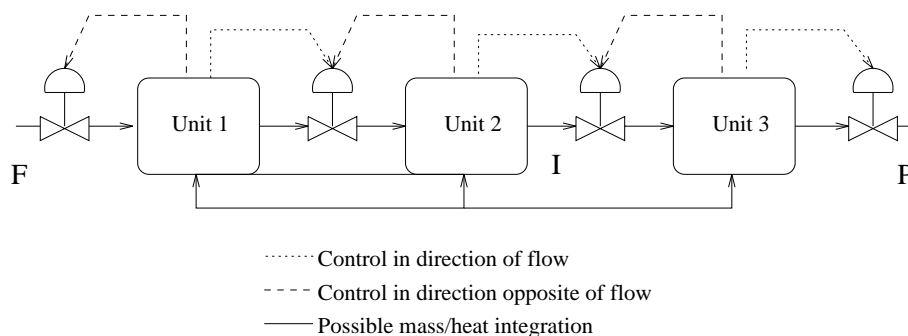


Figure 7.1: Production control schemes

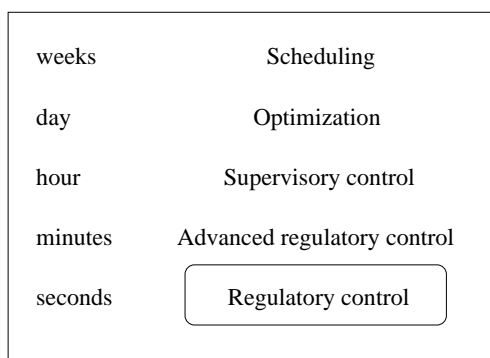


Figure 7.2: Control system hierarchy

column. This may create a need for using more DOF's than objectives for control. For example, one may need several downstream paths to take care of large disturbances.

Note that the selection of overall control objectives will affect the subsequent control system design. Consider the flowsheet in Fig. 7.1 where “Unit i ” can be a single or several aggregated unit operations. Here three alternative objectives determine the production rate: 1) process all available feed F , 2) maximum production due to intermediate variable I reaching constraint or 3) produce given amount P . This decision will decide if inventory control will be in the direction of flow or opposite. The best choice (given available alternatives) will also consider how integration links the process subsystems together. Direction of control should enclose subsystems generating disturbances.

7.3.2 “Bottom-up” design of control systems

The control system is usually designed “bottom-up” and the final control structure may of course be different from the pairings which were more or less arbitrary found in the tick-off DOF analysis.

Control systems are usually designed in a hierarchical fashion to accomplish stabilization, servo-control, optimization, fault detection and more. This gives a control system that is divided by the “time-constant” of the given operation as shown in Fig. 7.2. The regulatory control system will stabilize the plant, remove the effect of disturbances and provide “new” degrees of freedom (setpoints) for the supervisory and

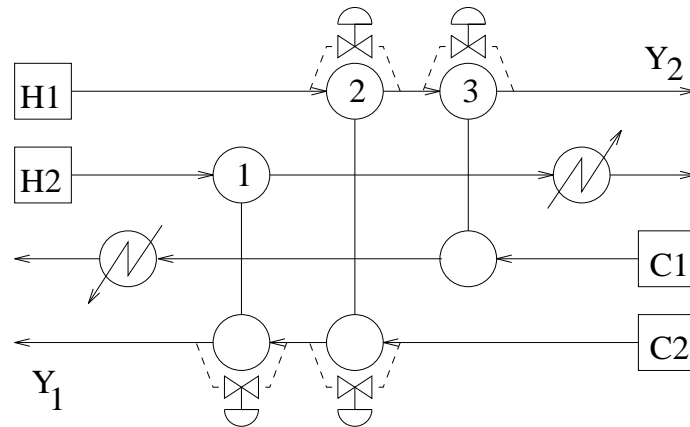


Figure 7.3: Heat exchanger network with alternative control bypass placements.

optimizing control to manipulate the long-term operation of the plant.

A tentative schedule for constructing control loops must first give attention to stabilizing any unstable or very slow modes including variables that may reach constraints (such as variables which are not “self-regulated” or are very sensitive to disturbances). In general one should use manipulated variables (physically) close to an objective for control, and seek to avoid using manipulated variables that may easily reach their constraint or impose performance limitations for higher levels (not easy). Second, one should close other important loops, these are typically quality loops (compositions). Any remaining degrees of freedom can be used for optimizing the plant either statically or dynamically.

Material balance control. It is obvious that one cannot have good flow control as well as good level control in the same process section. This may be resolved by understanding which variables are critical and which can and should be able to fluctuate. For example “sloppy” control of holdups is beneficial to reduce flow variations.

7.3.3 Implications for integrated plants

Degrees of freedom have so far been treated as a commodity of finite size; really the essence of the tick-off procedure. Unfortunately, this does not always hold. The last DOF and the last objective may end up at each end of the process, giving an unrealistic solution. With many actuators there is also the problem of matching the speed of response. Although the controllability analysis may point this out, high frequency disturbances or fast inventory control may render a slow actuator without the ability to comply with the needs.

The use of available DOF must also be weighed against the overall objective of the process; are there conflicts between the regulatory control and the overall objectives? This will be illustrated by an example, the heat exchanger network in Fig. 7.3. The network is shown in the grid representation, with hot streams H_1 and H_2 being cooled by heating up cold streams C_1 and C_2 . The heat exchangers (represented by the vertical connections) are denoted 1, 2 and 3 and there is also a heater and a cooler in the flowsheet. The control objectives are the temperatures Y_1 and Y_2 and possible

bypass locations are indicated. Common rules for regulatory control of heat exchanger networks advise placing the bypasses close to the objectives, which favors using the bypasses on exchangers 1 and 3. However, exchanger 2 is an “inner match” exchanger, that is, both exit streams continue to other process stream exchangers. *Not* using exchanger 2 for control will incur an energy penalty in the heater and cooler. In this case the favored bypasses for regulatory control are a bad choice in terms of energy usage.

7.4 Effects of integration

This section discusses limitations and tradeoffs in control stemming from integration design issues.

7.4.1 Operability limitations

The problems in controlling integrated plants come from the fact that constraints are introduced and the number of DOF change compared to the original process. Many areas in the plant construction give rise to control problems, including:

Heat Exchanger Networks:

- There must exist separate paths for all control loops.
- The gain of the manipulated variables decreases sharply when the effect must pass through several exchangers and may yield problems with constraints.

Recycle systems:

- Effective gain increases.
- Inverse responses may occur for some control configurations using purge flowrate as manipulated variable.
- Using purge/recycle for control depends on the available gain (relative size) in the system and the effects of redirecting disturbances.

Plant-wide:

- Integration (interconnections) may remove DOF (reboiler/condenser integrations) or add DOF (recycle flow). This means that experience gained from controlling single units may not apply.
- Effects of disturbances and control action propagate further, i.e. applying control may disturb other objectives (ex: bypass).

We are mostly concerned with the behavior of the closed-loop system, which is usually much faster than the corresponding open-loop system. An example of this is a distillation column, which may be very sluggish in open-loop, while the problem in closed-loop is the interaction between composition control loops, not sluggishness. In

closed loop the effects of integration may be more or less pronounced than in open loop.

Despite this goal, there are also benefits from investigating the open-loop characteristics of the system, one example being the frequency dependent behavior used in controller design. We also use the notion of “perfect control” in investigating the closed-loop behavior, thus avoiding to actually create a controller for the given system for analysis purposes.

7.4.2 Operability tradeoffs

Introducing integration may consist of many steps for a large process plant (during design or retrofit). Each step should ideally contribute to a single definable improvement to ease evaluation. This is not always the case (as with any process modification), leading to tradeoffs between plant properties. Some of the possible contradictory decisions that arise are:

Comparing integrated design alternatives. A base case design is often performed before integration is evaluated, and during this phase the critical control objectives are usually established. The development of an integrated plant depends on all the elements/units combined, so the number and nature of objectives may change through integration, obscuring the basis for comparison.

Constraints. Applying control to account for perturbations will at the same time require that the process is operated a distance from the important constraints (Perkins, 1989). The amount of slack that separates the operating point from the constraints is a measure of how important these constraints are, a realization of how good the control is and how large the expected perturbations are. Better control will allow larger savings due to operation closer to the constraints. Integration may reduce the available gain of the actuators and demand larger back-off than the unintegrated plant.

Operability breakdown. There exists a tradeoff between the individual operability issues, each giving different limitations on the plant. “Flexibility” may demand certain equipment ratings to cover all operating points. “Controllability”, considering transient behavior, may necessitate larger, smaller or reconfigured equipment. Preferred control strategy may also differ considering different timescales. Both issues will vary within the operating space.

Process pinches and control. Process pinches may appear between process units or within the units themselves. Their effect on control depends on which process perturbations are to be handled and which manipulated variables are used. Heat and composition perturbations will often be damped when approaching/crossing a pinch. This is a beneficial effect if the disturbance and critical measurement are separated by a process pinch. On the other hand, the pinch may make a measurement insensitive to the intended manipulated variable.

Controlling intermediate variables. The critical measurements in a control system may themselves not be the best or only alternatives for control in a plant. Intermediate variables may present a better control solution because they are easier to control, more accessible or create an additional damping in an important process unit.

In HENs for example, pinch design and energy efficiency rules recommend having utilities only at the end of the heating or cooling procedure. This situation may change when there are process streams that are hotter than the hot utility or colder than the cold utility. Utility exchangers may then be unavailable for final temperature control, although these exchangers may dampen perturbations in the interior of the HEN.

Heat integrated networks may suffer from too few possible manipulated variables with sufficient gains for control. Thus the incentive to reduce disturbances where possible arises.

Overdesign. A flowsheet and the embedded unit operations are always developed according to some assumptions about the plant, operating conditions, proposed production and purity specifications. Since these may change over time some overdesign is always included. Additional attention to overdesign may arise from issues such as benefits in control and anticipation of increased demand, i.e. debottlenecking. The latter question is highly plant individual, while the first shows some generality. Several authors have looked into the control benefits from overdesign, for example, Jacobsen and Skogestad (1991) have investigated the effects on distillation columns. The cost/effect tradeoff of overdesign may move significantly under integration. The same overdesign issue may affect different control objectives in different direction, for example disturbance rejection and speed of response.

Variable mismatch. Mismatches may exist between manipulated and controlled variables that enable small disturbances in one stream/channel to adversely affect others. Temperature control can be seen as a mere stabilizing effect at one point of the process, while the same temperature is vital for composition disturbances in following flash tanks. Consider flashing a two-phase stream whose composition spans many components. A relatively small temperature change may shift one component from a product stream to another, thus disrupting later purification stages.

7.5 Illustrative cases

7.5.1 Example 1: HDA plant

Douglas (1988) has proposed several alternative flowsheets for the conversion of Toluene to Benzene (hydrodealkylation of toluene, or HDA-process), including varying degrees of heat integration. The un-integrated alternative is shown in Fig. 7.4. Some alternative heat integrated flowsheets are shown in a condensed representation in Fig. 7.5. Here a dashed thick line means an added heat exchanger between the indicated process units; the heat transferred links the two process units together. In general we therefore denote them heatlinks. Not only will the proposed integrated flowsheets have different structural paths for disturbance propagation between process units, but a parameter optimization will give each plant a different operating point. This and other features complicate the evaluation of operability between the different plant alternatives. We will show that the operability issue for heat integrated plants may depend on the number of, functionality and placements of the heatlinks.

Figure 7.4: HDA-process with no heat-integration, flowsheet F_0

Following the development of a more integrated flowsheet (increase in the number of heat links in the process), the possible additions for the HDA process are:

- F1. Reactor feed-effluent heat exchanger.
- F2. Recycle column condenser to Product column reboiler.
- F3. Reactor effluent to Stabilizer boiler, or
- F4. Reactor effluent to Product column boiler.
- F5. Both additions 3 and 4.
- F6. Reactor effluent to Recycle column reboiler.

F_i with indices 0 to 6 represent the flowsheets mentioned above with 0 being the plant with no heat integration. The same indices are also used in comparing operability. The recycle column operates at elevated pressure in flowsheets $F_2 - F_6$ to accomplish the integration.

Heat exchange between reactor feed and effluent will generally look like Fig. 7.6, which corresponds to the F_1 case. Additional energy recovery ($F_2 - F_6$) is done by splitting this heat exchanger and letting the effluent heat other sinks intermittently.

An operability study has previously been done on the least integrated flowsheet, i.e. F_1 (Wolff *et al.* 1994)[‡], this addition being the most significant for energy savings. Control of the reactor inlet temperature was part of the design for stabilization purposes. The control loops given in Table 7.1 were recommended. The role of these (and other) manipulated variables must be investigated with respect to how they can be transferred to use in the more integrated cases.

[‡]This corresponds to chapter 6 in this thesis

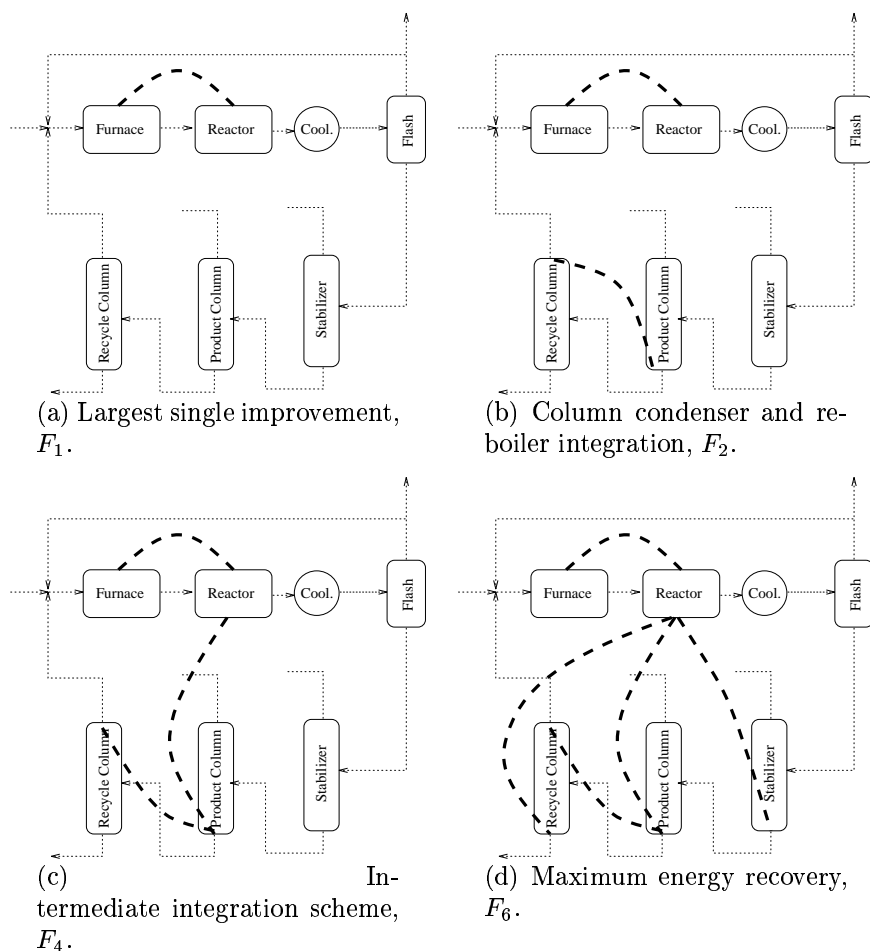


Figure 7.5: Alternative integration schemes for the HDA process

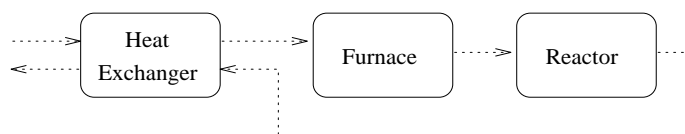


Figure 7.6: Feed effluent heat exchange around reactor.

Limitations and tradeoffs through integration. Earlier studies (e.g. Wolff *et al.* (1994)) have primarily considered two disturbances (downstream pressure and cooling water temperature), but other scenarios are also discussed in the following.

Flowsheet F_1 involves a feed/effluent exchanger that destabilizes the reactor. Two solutions for alleviating this exist, both will also remove other temperature disturbances to the reactor. Using a bypass around the exchanger for stabilization would need a prohibitive large bypass. Stabilization through controlling the furnace exit temperature (and thus the adiabatic reactor outlet) is instead recommended from economic reasons.

F_2 demands higher pressure in the recycle column (507 vs. 101 psi) which might give

Measurement	Manipulated variable
Flash inlet temperature	Pre-flash cooler duty
Production rate	Gas feed flow
Product purity	Product column reflux ratio
H_2 /Aromatics ratio	Toluene feed flow
Flash outlet pressure	Purge valve opening

Table 7.1: Preferred pairings for the HDA process.

added separation costs. The condenser is run utility free, so any control must involve a bypass. Slack control (for example due to constraints) seems admissible, since increased diphenyl content will move the byproduct reaction towards the intended product.

F_3 links the stabilizer reboiler and reactor effluent, limiting the control over the H_2 , CH_4 content in the stabilizer bottoms, and thus the feed to the product column.

F_4 is very similar to F_3 , integrating the product column reboiler with the reactor effluent, but different in that there is no integration upstream of the product column.

F_5 links the stabilizer and product column reboiler through the reactor effluents course. This creates a new path for disturbances to propagate, especially since any control with the stabilizer boilup must be through a bypass, which will generate disturbances for the product column.

F_6 , with the added integration of the reactor effluent and recycle column reboiler, has removed almost all direct control actuators from the distillation train. There seem to be few means to maintain flexibility even if the plant can be run at the optimal operating point.

Evaluation of integration schemes. To summarize; flowsheets F_1 , F_2 , F_3 and F_4 seem to have a good possibility of being both controllable and flexible. F_5 and F_6 create additional problems by introducing new disturbance paths. Flexibility may also be at loss with primarily bypass actuators in the separation system.

The identified disturbances are already taken care of and the recommended actuators are not modified by the integration. The interaction properties of the process, as indicated by the diagonal elements of the relative gain array

$$\Lambda_{F_1}(0) = [1.11 \ 1.03 \ 0.56 \ 1.03 \ 0.47]$$

indicate that interaction is not the most prevalent problem of design F_1 . The integration schemes that are proposed lie mostly downstream of, or far away from the preferred control loop as found for flowsheet F_1 . We therefore assume that interaction is not the primary difficulty for the proposed flowsheets.

From the discussion above, no “negative” conclusions seem possible, although a “threshold” appears to exist between F_4 and F_5 (from the introduction of new disturbance paths), with the former being more feasible.

As long as the development of the process design and the control system are sequential tasks this approach can be rewarding in eyeing integration alternatives that

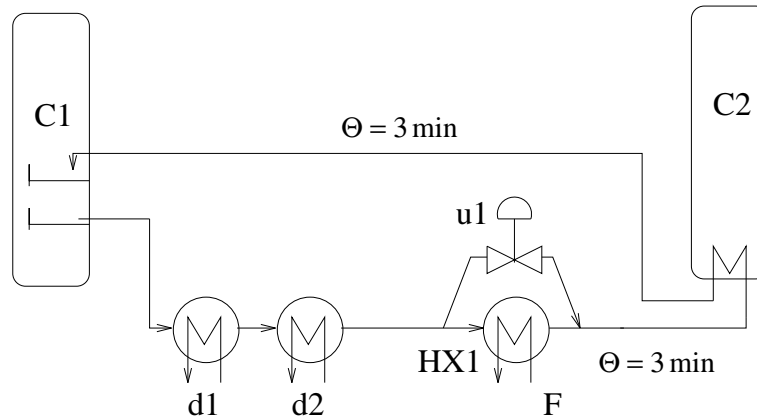


Figure 7.7: Distillation column pumparound

can cause control difficulties. A more concurrent design/control development scheme will necessarily differ. Startup and shutdown issues may also discard design schemes.

7.5.2 Example 2: Distillation column pumparound

This example, a column pumparound, illustrates how integration, despite creating additional degrees of freedom, displays problems due to lacking leverage in the manipulated variables.

Problem description. Refinery distillation often uses pumparounds to manipulate specific cuts from the different column sections. A simplified flowsheet of such a system is given in Fig. 7.7. Pumparounds may be quite large and utilizing the latent heat in these streams is economically significant. In this example the pumparound stream from column C_1 goes through two small heaters before heating stream F of variable size and reboiling column C_2 . The first two heat exchangers may be viewed as disturbances only. HX_1 has a duty in the range 1 – 14MW depending on the feed to the plant. There is a deadtime of approximately three minutes between the major units in the flowsheet. The pumparound should remove a constant duty from column C_1 while providing a stable and reliable energy source for column C_2 .

Limitations and tradeoffs. Problems arise from the the varying duty in the heater HX_1 , since the power of the manipulated variable, the bypass fraction, is nearly diminished at the lower operating point. The desired duty in C_1 , C_2 and HX_1 all put constraints on the operability. Large deadtimes between units are also detrimental. Clearly, excellent control of C_1 will have at least some interests contradictory towards control of C_2 .

Some possible changes to the process and control actuators are shown in Fig. 7.8. Better overall control can be reached by adding an auxiliary cooler or heater or redesigning the piping and control scheme. Adding control to bypass HX_1 and C_2 altogether will give faster control of the duty removed from C_1 , at the cost of disruptions to the cold side of HX_1 . Moving the heat loads from serial to parallel operation is also possible. Using split ratios for control instead of bypasses may give more flexibility (larger driving forces in all exchangers) and better switchability (trade effect in HX_1

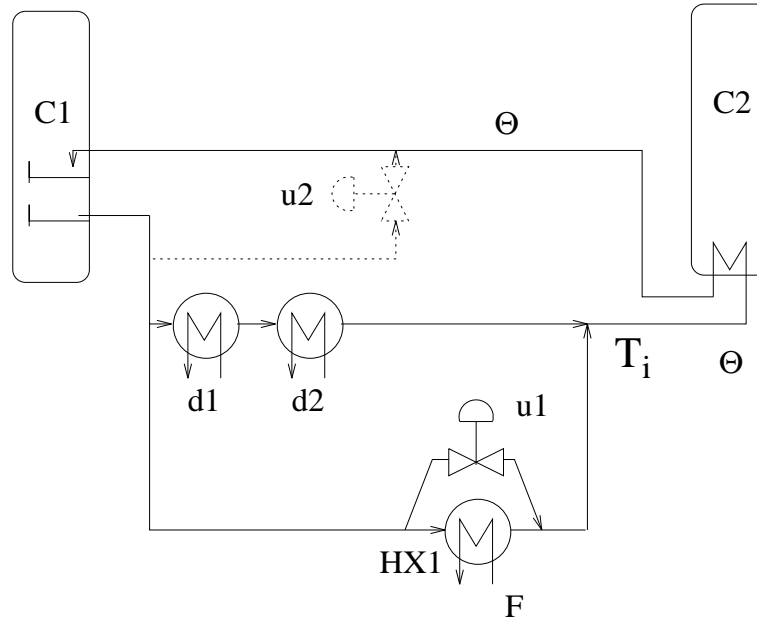


Figure 7.8: Column pumparound: proposed modifications to enhance operability.

with $d1, d2$). Which objective to give priority (C_1 or C_2) will also be more independent with parallel exchangers. Controlling the intermediate temperature T_i (for example with u_1) may help stabilize the duty removed from column C_2 .

7.6 Guidelines

Interaction, constrained manipulated variables and changes in DOF limit control alternatives in integrated plants. We present the following guidelines for control of integrated plants:

- Choose preferably manipulated variables that do not disturb other process equipment.
- Avoid redirection (propagation) of disturbances.
- Look for control solutions with side benefits, for example help stabilize other equipment.
- Integrate preferably column condenser/reboiler that is not an important manipulated variable or is associated with a non-critical measurement.
- If an important condenser/reboiler is integrated, then assure that bypass gain or auxiliary exchanger is large enough for control purposes.
- Consider shifting heat loads in parallel instead of in series for better control.
- Prefer process modifications that are beneficial to several facets of operability (flexibility, controllability, etc.).

- Feed-effluent heat exchangers around exothermic reactors are sources of instability. A stabilizing controller can also dampen or remove other perturbation sources and thus need less control than the non-integrated flowsheet.
- Controlling pressure rather than flowrates gives better disturbance rejection properties in gas-phase inventory control. This should also create more stable operating conditions in pressure sensitive equipment (VL-equilibrium) such as columns and flash tanks. Avoid using manipulated variables that will lead to composition changes in downstream units.

7.7 Conclusion

It is possible to identify areas within process integration that have a large effect on the operability of the plant. The constraints imposed by integration can severely limit the operation space and be detrimental towards disturbance rejection. Feed-effluent heat exchangers remove inherent stability, but this usually induces no loss in operability.

We have proposed guidelines for the development of operable plants in view of several integration topics. Integrated plants exhibit problems extending the scope of plant wide control.

References

- [1] Buckley, P.S., 1964, "Techniques of Process Control", Wiley, New York.
- [2] Bouwens, S.M.A.M. and P.H. Kösters, 1992, "Simultaneous Process and System Control Design: An Actual Industrial Case", *Preprints IFAC workshop on Interactions between process design and process control*, London, Sept. 1992.
- [3] Calandranis, J. and G. Stephanopoulos, 1986, "Structural Operability Analysis of Heat Exchanger Networks", *Chem. Eng. Res. Des.*, **64**, 347-364.
- [4] Douglas, J., 1988, "Conceptual Design of Chemical Processes", Mc Graw Hill.
- [5] Downs, J.J. and E.F. Vogel, 1993, "A Plant-wide Industrial Process Control Problem", *Comp. Chem. Engng.*, **17**, 3, 245-255.
- [6] Fisher, W.R., M.F. Doherty and J.M. Douglas, 1988, "The Interface between Design and Control. Parts 1. & 2.", *Ind. Eng. Chem. Res.*, **27**, 597-605.
- [7] Georgakis, C., 1986, "On the Use of Extensive Variables in Process Dynamics and Control", *Chem. Eng. Sci.*, **41**, 6, 1471-1484.
- [8] Georgiou, A. and C.A. Floudas 1989, "Structural Analysis and Synthesis of Feasible Control Systems - Theory and Applications", *Chem. Eng. Res. Des.*, **69**, 600-618.

- [9] Grossmann, I.E., K.P. Halemane and R.E. Swaney, 1983, "Optimization Strategies for Flexible Chemical Processes", *Comp. and Chem. Eng.*, **7**, 4, 439.
- [10] Jacobsen E.W. and S. Skogestad, 1991, "Design modifications for improved control of distillation columns", *EFChE Symposium COPE-91*, Barcelona, Spain, Oct. 91. Published in: Puigjaner and Espuna (Eds.), *Computer Oriented Process Engineering*, Elsevier, 123-128.
- [11] Kravanja, Z. and P. Glavič, 1989, "Heat Integration of Reactors - II. Total Flow-sheet Integration", *Chem. Eng. Sci.*, **44**, 11, 2667-2682.
- [12] Linnhoff, B. and E. Hindmarsh, 1983, "The Pinch Design Method for Heat Exchanger Networks", *Chem. Eng. Sci.*, **38**, 5, p. 745-763.
- [13] Morari, M., Y. Arkun and G. Stephanopoulos, 1980, "Studies in the Synthesis of Control Structures for Chemical Processes, Part I & II", *AIChE J.*, **26**, 2, 220-246.
- [14] Morari, M., 1981, "Integrated Plant Control: A Solution at Hand or a Research Topic for the Next Decade?", *Proc. CPC-2*, Georgia, 467-495.
- [15] Morari, M., 1992, "Effect of Design on the Controllability of Chemical Process Plants", *Preprints IFAC workshop on Interactions between process design and process control*, London, Sept. 1992.
- [16] Perkins, J.D., 1989, "Interactions Between Process Design and Process Control", *Proceedings DYCORD+89*, 349-357.
- [17] Ponton, J.W. and D.M. Liang, 1993, "A Hierarchical Approach to the Design of Process and Control Systems", *Chem. Eng. Res. Des.*, **71**, 181-189.
- [18] Price, R.M. and C. Georgakis, 1992, "A Plant-wide Regulatory Control Design Procedure using a Tiered framework", Paper 128b, AIChE Annual Mtg. 1992, Miami, Florida.
- [19] Nishida, N., G. Stephanopoulos and A.W. Westerberg, 1981, "A Review of Process Synthesis", *AIChE J.*, **27**, 3, 321-351.
- [20] Rinard, I.H., 1975, "Process Control of Highly Integrated Processes", *Preprints Conference on Innovative Design Techniques for Energy Efficient Processes*, Northwestern University, March 1975.
- [21] Schmidt, T.M., A. Koggersbøl and S. Bay Jørgensen, 1992, "Design and Operability of an Energy Integrated Distillation Column", *Preprints IFAC workshop on Interactions between process design and process control*, London, Sept. 1992.
- [22] Stephanopoulos, G., 1982, "Synthesis of Control Systems for Chemical Plants - A Challenge for Creativity", *Proc. PSE '82*, Kyoto, 131-165.
- [23] Umeda, T., T. Kuriyama and A. Ichikawa, 1978, "A Logical Structure for Process Control Systems Synthesis", *Proc. IFAC Congress*, Helsinki, 271-278.

- [24] Wolff, E.A., J.D. Perkins and S. Skogestad, 1994, "A Procedure for Operability Analysis", Proceedings to ESCAPE-4, Dublin, Published in *Inst Chem. Eng. Symp. Ser.* (UK).

Chapter 8

Postscript

8.1 Discussion

This thesis has primarily investigated the inherent operational characteristics of process units and combinations thereof that display interactive behavior. The need for this investigation rises from the increased integration in today's process design, putting higher demands on the control.

The results in this thesis have focused on a number of specific cases covering a wide specter of plant equipment. Besides stressing the general value of assessing controllability during design, the results can also generalize to other equipment, for example:

- Secondary measurements may be exploited in reactors, dryers, biological processes and more.
- Integrated separation, like the Petlyuk column, may conceptually be a viable solution for extraction, reactive distillation and possibly staged operations such as ore upgrading or waste reclamation.
- The problems encountered in control of heat exchanger networks (such as low gain and large delays) are conceptually similar to those found in plant-wide control, where in some cases no immediate or natural actuator can be found.

Deadtime has not been treated in detail in chapter 2 or 6 and this may be considered a drawback. However, deadtimes often vary and can be substantial for even the smallest loop. Pipe transport and intermediate storage may also largely exceed equipment deadtime in many cases. Additionally, their exact values are more often than not undefined until beyond the P&ID stage. Thus, a unified treatment of actuators preserves the possibility to match design with control through plant layout to give a more controllable plant.

Model detail has varied considerably between the different chapters, from linear to mixed nonlinear and static, with and without energy balances, etc. Modeling issues

have not been the priority as long as the models have sufficed to illustrate important principles. A possible exception is the Petlyuk column, where the work is intended to show the feasibility of the design as well as demonstrate control of units with internal integration.

Controllability and flexibility have been considered in relation to a specific optimal operating point. It can be argued that controllability should be considered at all operating points considered within the flexibility scope. This is correct in principle, but counterarguments beheld here are:

- Nonlinearities are often most prevalent at some parameter limit, as demonstrated in chapter 3, where the recycle flow will eventually skyrocket if the purge rate is reduced too far. Such operating conditions are highly detrimental and are usually avoided in good practice. Controllability analysis is thus at least *representative* for the operating range.
- The information load to be evaluated will increase sharply for even a small operating space (counted in dimensions), making the results less useful instead of more useful.

Benefactors of other methods for optimal control structure selection (e.g. MINLP with monetary objective function) face similar problems; vastly increasing the optimization problem and using a rather arbitrary method for selection (for example the best average objective over some discretized operating range).

The choice of control structure and controller type plays an important role in plant operation. This thesis has focused on decentralized multiloop control due to the high representation of this controller type in process industry. Feedforward, optimal control, adaptive control etc. are of course also important in practice. However, the following points were considered when choosing control algorithm:

- There is a close relationship between frequency domain analysis tools and multiloop control.
- Using advanced control will shift the focus from the inherent plant properties to the control algorithms.
- The simplicity of multiloop control and a uniform treatment throughout the thesis will benefit the reader.

This work has shown the strength of the frequency domain analysis tools. The simplicity and versatility of these methods hold promise for even more developments in the future.

8.2 Conclusions

The main contributions of this thesis are summarized in the points below:

Chapter 2 summarizes the use of analysis tools for controllability assessment and presents a set of new controllability measures. The benefits of combined use of such tools are described and explained through an FCC example.

Chapter 3 treats the dynamic and control implications of recycle streams in a reactor system. The use of purge as an active control variable has been investigated and simplified analytical expressions for the process behavior have been developed. Multivariable analysis of recycle problems (especially with purge) is new.

Chapter 4 treats the use of secondary measurements in control. The use of temperature cascades for composition control in distillation has been quantified in terms of controllability. Analytical expressions have been developed for tuning of the secondary loop. Looking at regulatory level tuning to reduce interaction with other control levels is new.

Chapter 5 is the first major work to investigate control of the Petlyuk design. The multiple steady states noted by Chavez have been treated in light of control specifications and explained better. Serious operational problems have been discovered for four-point control, related to “holes” in the feasible operating region. These correspond to instability from setpoint increases *and* decreases in the side product purity. Other control configurations have also been investigated. Operation is viable, but more work is needed.

Chapter 6 treats operability assessment of entire plants, with focus on the benefit from structuring the analysis tasks and applying controllability analysis. Complete operability analysis on total plants is largely new.

Chapter 7 is one of the first works to specifically look at which aspects of integrated plants may change the inherent operability. Benefits and drawbacks are evaluated for a variety of process equipment. Guidelines are presented.

Appendix A suggests extensions to the relative gain array, Λ , that make selection of control strategy for large scale systems easier. Convergence properties and anomalies are discussed based on computational evidence.

8.3 Directions for future work

The main idea for any design or control study is to make the chemical (or other) processes safe, economical and controllable to mention a few points. There are some significant deficiencies in current plant-wide control and control of integrated plants. The most important is viewed to be the lack of a simple measure on which to judge alternative control structures. Secondly, any control may be inadequate if the underlying design is bad. Usable methods do not exist at present that can exploit a concurrent development of the equipment, flowsheet and control system design.

More specifically, chapter 2 misses a treatment of deadtime and multivariable controllers to be complete. The “range” based measures suffer from their difficult numerical solution. Better algorithms will enhance the frequency dependent (complex) results (as discussed in chapter 3).

The recycle problem in chapter 3 should be extended to other flow patterns and actuator sets, thus allowing more general conclusions to be made. Including the energy

balance will probably yield interesting results and also allow treatment of other MIMO control problems (adiabatic reactors, temperature control).

Chapter 4 would benefit from also considering the DV and LB composition control configurations. Applications considering multicomponent distillation would be interesting.

Chapter 5 lacks an investigation of how the (physical) design affects the dynamic and control properties. A comparison with other component systems and an analytical explanation of the described “holes” would also be helpful. Including pressure and detailed thermodynamics will probably reveal more peculiarities.

Chapter 6 would benefit from a more stringent treatment of the different heat integrated plant alternatives. There was not enough time to treat this in full. The same applies to chapter 7 and its treatment of the different HDA plant flowsheets. Better flexibility measures are needed, preferably considering closed-loop flexibility.

Appendix A contains extensions to the RGA that would benefit from numerical proofs.

Appendix A

A Note on the Pairing of Large Systems Based on the RGA

Erik A. Wolff* and Sigurd Skogestad[†]
Chemical Engineering
University of Trondheim - NTH
N-7034 Trondheim, Norway

Unpublished

Abstract

This paper examines the problem of choosing pairing in a decentralized control system based upon the relative gain array (RGA or Λ). For large systems (dimension $n \geq 4$), choosing pairing based on heuristic rules becomes difficult. The presented method, which involves the iterated calculation of the relative gain array, greatly simplifies this task and gives a single preferred pairing. A pairing on positive RGA is indicated if one exists. Otherwise a pairing on negative RGA is supplied. The method gives good results for the examined problems and is based on diagonal dominance. The results are based on computational evidence only.

*Present Address: ABB Environmental, Box 6260 Etterstad, N-0603 Oslo, Norway

[†]Address correspondence to this author. Fax: +47-7359-4080, E-mail: skoge@kjemi.unit.no

A.1 Introduction

The relative gain array, RGA or Λ for short, was initially presented by Bristol (1966). From the start the RGA was primarily a tool for selecting control pairings. Since then the RGA has been linked with many other plant (model) properties such as sensitivity to model uncertainty. Grosdidier *et al.* (1985) developed many results on the numerical properties of the RGA. Skogestad and Hovd (1990) give a thorough survey of the frequency-dependent RGA and its properties.

For a square plant $G(s)$ the relative gain is defined as the ratio of the “open-loop” and “closed-loop” gains between input u_j and output y_i . It is defined at each frequency as

$$\lambda_{ij}(s) = \frac{(\partial y_i / \partial u_j)_{u_{l \neq j}}}{(\partial y_i / \partial u_j)_{y_{l \neq i}}} = g_{ij}(s)[G^{-1}(s)]_{ji} \quad (\text{A.1})$$

and a RGA-matrix is computed from

$$\Lambda(j\omega) = G(j\omega) \times (G^{-1}(j\omega))^T \quad (\text{A.2})$$

where \times denotes element-by-element multiplication or Hadamard product. The individual entries in Λ (at any frequency) can be found by

$$\lambda_{ij}(G) = \frac{(-1)^{i+j} g_{ij}(\det G_{ij})}{\det G} \quad (\text{A.3})$$

where G_{ij} is G with row i and column j removed.

It is worth noting that the RGA is independent of scaling, and must only be rearranged (*not* recomputed) when considering different control pairings. When using the RGA for selecting a decentralized controller pairing, one should pair on RGA values close to 1 (assuming a stable plant). A pairing corresponding to RGA values close to 1 indicates that there will be little interaction between control loops.

Triangular plants yield $\Lambda = I$, and plants where Λ is different from I are called interactive (G has significant offdiagonal elements). It is established that plants with large RGA-values, in particular at high frequencies, are fundamentally difficult to control.

Choosing pairing for decentralized control based on the RGA is usually an ad hoc task, trying to pair on positive λ_{ij} elements not too far from one. With large systems (i.e. $n > 3$) the choice becomes increasingly difficult as more alternatives arise. This difficulty relates to judging the numerical values, for example; is 2.0 better than 0.4? For plants where many possible pairings are possible, a tradeoff also exists; is 2 and 0.3 better than 5 and 0.6? This paper will try to help resolve this problem. Examples of size 3×3 and 4×4 illustrate the properties of the method, although the benefit becomes more evident for larger plants.

This work is different to other work on large scale systems and RGA (e.g. Manoussiouthakis *et al.* (1989)), which concentrate on finding viable structures of subsystems of size m , $1 \leq m \leq n$, where n is the size of the problem. This decomposition into subproblems faces the same problems as the ordinary RGA of judging values, although it may be efficient for singling out very independent subsystems. Unfortunately, the effort of covering the search space increases by $(n!)^2$.

We first present the theoretical basis of this work. Then we cover some numerical examples showing the basic properties of the method. An extension to the method is then proposed and an algorithmic procedure is described. Some remaining problems are then discussed. To avoid confusion, note that a superscript k to Λ or λ indicates the k 'th iteration in the calculations, whereas a subscript ij denotes a pairing position.

A.2 Method

Johnson and Shapiro (1986) have investigated the mapping

$$A \rightarrow \Lambda(A) \tag{A.4}$$

with respect to elemental numeric properties. Results are also presented regarding the repeated application of this mapping, or iterate of $\Lambda(A)$. Central to this work is their Theorem 1, which is stated here:

Theorem 1 *Let A be a positive definite Hermitian matrix. Then*

$$\lim_{k \rightarrow \infty} \Lambda^k(A) = I \tag{A.5}$$

Proof: See reference.

This work looks at applying Eq. A.5 to process control problems, which are generally not positive definite. Thus, the immediate question is if Eq. A.5 can be extended to allow for this. We first use the elemental property that row and column exchanges in A give an equal rearrangement of rows and columns in $\Lambda(A)$. This, in turn, must also propagate to $\Lambda^2(A)$, etc. By induction, rearranging rows and columns in A will result in the same row and column exchanges in $\lim_{k \rightarrow \infty} \Lambda^k(A)$. The iterate will thus converge to a permutation of the identity matrix I , called P . The essence of this lies in the first row and column exchange performed on A , since this will in general *not* preserve positive definiteness.

We have thus shown that Eq. A.5 can at least be relaxed to every matrix A that can be *rearranged* into a positive definite matrix. Unfortunately, determining if any general matrix A can be rearranged to a positive definite matrix is not trivial (search increases by the square of matrix dimension).

When A is positive definite, the maximum eigenvalue of each subsequent iterate $\Lambda^k(A)$ is strictly decreasing and bounded below by 1. This result is used in the proof of Theorem 1. The *lack* of positive definiteness will make such a proposition untrue. However, it will not profess anything about the global convergence properties or how useful the end result is.

So, despite this shortfall in proving an extension of Eq. A.5 for all matrices A , we define for any (process gain) matrix G

$$\Lambda^\infty(G) = \lim_{k \rightarrow \infty} \Lambda^k(G) = P \tag{A.6}$$

where P is a permuted identity matrix. In general this result holds, although special cases exist in which convergence is not guaranteed (these are mentioned later). We therefore look at the properties and significance of Λ^∞ .

We begin by considering a stable plant, i.e. such that pairing on positive RGA is preferred. Assume then a gain matrix G with RGA such that a pairing on positive λ_{ij} values is possible. Take the RGA of the RGA and a pairing will eventually become more apparent. Repeat the procedure until convergence and the result is a matrix P with 1 at the positions to pair upon and 0 otherwise.

Johnson and Shapiro claim that the mapping $\Lambda(A)$ is “more” diagonally dominant than A , such that Λ^∞ is the “filtering” of the prevailing diagonal dominance in A . It has been tried to link the pairing found by Λ^∞ with those resulting from diagonal dominance criteria, such as $\|\Lambda - I\|$ and $\|E\|$ where $E = (G - G_{diag})G_{diag}^{-1}$ describes the “amount” of off-diagonal elements in G . Neither of these criteria coincide with the presented method for all cases.

A.3 Examples

A.3.1 Example 1: Select one of several pairings.

The following randomly generated matrix will serve as example on how the presented method selects a pairing:

$$G = \begin{pmatrix} 0.99 & 0.95 & 0.28 & 0.94 \\ 0.49 & 0.07 & 0.91 & 0.05 \\ 0.27 & 0.50 & 0.53 & 0.76 \\ 0.09 & 0.38 & 0.46 & 0.77 \end{pmatrix} \quad (\text{A.7})$$

The RGA of G is

$$\Lambda(G) = \begin{pmatrix} 2.16 & -2.39 & -0.30 & 1.53 \\ 0.72 & -0.17 & 0.41 & 0.04 \\ -2.44 & 9.33 & 2.12 & -8.01 \\ 0.55 & -5.77 & -1.23 & 7.45 \end{pmatrix} \quad (\text{A.8})$$

Using inspection only there are several possible pairing strategies, all pairing on g_{32} , but with several other combinations of u and y appearing rather equal. Applying the iterate we get

$$\Lambda^2(G) = \begin{pmatrix} 2.24 & -2.36 & 0.44 & 0.68 \\ -0.43 & 0.19 & 1.25 & -0.01 \\ -0.91 & 6.07 & -0.91 & -3.25 \\ 0.11 & -2.90 & 0.22 & 3.58 \end{pmatrix} \quad (\text{A.9})$$

and

$$\Lambda^3(G) = \begin{pmatrix} 1.24 & -0.39 & 0.07 & 0.07 \\ 0.00 & 0.03 & 0.97 & -0.00 \\ -0.27 & 2.25 & -0.04 & -0.94 \\ 0.02 & -0.89 & 0.00 & 1.87 \end{pmatrix} \quad (\text{A.10})$$

Since $\Lambda^i(G), i > 1$ is neither a gain matrix or a RGA thereof, the notion of pairing should be used with caution. Thus, when we say that $\Lambda^i(G), i > 1$ indicates a pairing,

we refer to the original gain matrix G . With this in mind Eq. A.10 seems to indicate a set of pairings quite clearly. Several additional iterations give us

$$\Lambda^6(G) = \begin{pmatrix} \mathbf{1.00} & 0.00 & 0.00 & 0.00 \\ 0.00 & 0.00 & \mathbf{1.00} & 0.00 \\ 0.00 & \mathbf{1.00} & 0.00 & 0.00 \\ 0.00 & 0.00 & 0.00 & \mathbf{1.00} \end{pmatrix} \quad (\text{A.11})$$

and a single pairing is indicated.

A.3.2 Example 2: Counterexample to conventional pairing rule.

Hovd and Skogestad (1992) presented an example where the conventional rule of pairing on RGA elements close to 1.0 doesn't apply:

$$G(s) = t(s) \begin{pmatrix} 1 & -4.19 & -25.96 \\ 6.19 & 1 & -25.96 \\ 1 & 1 & 1 \end{pmatrix} \quad (\text{A.12})$$

where $t(s)$ is a common transfer function for the whole plant. The RGA of $G(s)$ at all frequencies is

$$\Lambda(G) = \begin{pmatrix} 1 & 5 & -5 \\ -5 & 1 & 5 \\ 5 & -5 & 1 \end{pmatrix} \quad (\text{A.13})$$

The obvious solution is to pair on the diagonal elements of $\Lambda(G)$. Unfortunately this will (with three decentralized controllers) give an overall unstable system for Zeigler-Nichols tuned controllers. Using Λ^∞ as described above yields the following solution:

$$\Lambda^\infty(G) = \begin{pmatrix} 0 & \mathbf{1} & 0 \\ 0 & 0 & \mathbf{1} \\ \mathbf{1} & 0 & 0 \end{pmatrix} \quad (\text{A.14})$$

which corresponds to pairing on RGA values of 5. Hovd and Skogestad have shown that this pairing is superior to the one found through $\Lambda(G) = I$.

A.3.3 Example 3: Convergence properties

The following matrix is studied

$$G = \begin{pmatrix} 100 & 100 & -199 \\ 100 & -199 & 100 \\ -199 & 100 & 100 \end{pmatrix} \quad (\text{A.15})$$

Calculations show that the elements in $\Lambda(G)$ initially reduce towards P by (approximately) a factor n per iteration, where n is the dimension of the system. The values of the iterates of G , $\Lambda^k(G)$ are given in Table A.1 for the (1,1) element. The other values

k	1	2	3	...	10	11	12	13	...	42
$\lambda_{11}^k(G)$	33.44	11.26	3.87	...	0.46	0.56	0.46	0.56	...	1.00

Table A.1: Convergence of Λ^k for example 3.

develop similarly.

The symmetry of G leads the calculations into a 'limit cycle' like behavior with element values between -1 and 1. This is also shown in Table A.1. Although the final answer may be attributed to numerical error, it is visible by Λ^{11} , where minor digits already point out the preferred pairing ($\lambda_{11} = 0.562\dots25$ vs. $\lambda_{21} = 0.562\dots23$). Inspection of $\Lambda(G)$ shows us that there are only two possible pairings on positive λ values and that these two pairings are otherwise *equal in term of λ_{ij}* . This explanation fits very nicely; deciding between two equal pairings is difficult.

All 'ordinary' engineering cases that have been investigated have converged to P (with elements $(0, 1) \pm 10^{-2}$) in 5-8 iterations.

A.3.4 Example 4: Indefinite pairing subject to uncertainty

For cases where G is such that $G \pm dG$ gives two different pairings, some Λ^k display large values due to Λ^{k-1} almost losing rank. Experience gives us that although G is not ill-conditioned, then $\Lambda^k(G)$, $k \in [1, n]$ may be ill-conditioned. Consider for example the matrix G which converges to a pairing given by $\Lambda^{11} = I_3$:

$$G = \begin{pmatrix} 1.50 & -0.79 & 0.33 \\ 1.89 & -0.10 & -0.79 \\ -2.39 & 1.89 & 1.50 \end{pmatrix} \quad \Lambda(G) = \begin{pmatrix} 0.52 & 0.19 & 0.28 \\ 0.89 & -0.08 & 0.19 \\ -0.41 & 0.89 & 0.52 \end{pmatrix} \quad (\text{A.16})$$

Here the condition number $\gamma(G) = 4.43$, indicating no special numeric deficiencies. Assuming $dG = dg_{13} = +0.01$, a different pairing is then recommended. By following the successive iterates we find that $\gamma(\Lambda^1(G)) = 950$, i.e. $\Lambda^1(G)$ nearly loses rank. Comparing the two pairings show that the first case corresponds to pairing on a negative RGA value. The implications of this are not clear, but might pose difficulties for some cases of problems.

$\Lambda^i(G)$ will not always become ill-conditioned when the pairing is close to undetermined. Consider for example the matrix G which converges to a pairing in 6 iterations:

$$G = \begin{pmatrix} 0.84 & 0.71 & 0.08 \\ 0.21 & 0.83 & 0.76 \\ 0.84 & 0.09 & 0.63 \end{pmatrix} \quad \Lambda^6(G) = \begin{pmatrix} 0.00 & \mathbf{1.00} & 0.00 \\ 0.00 & 0.00 & \mathbf{1.00} \\ \mathbf{1.00} & 0.00 & 0.00 \end{pmatrix} \quad (\text{A.17})$$

The condition number of G is $\gamma(G) = 2.88$ and the element values of all the iterates Λ^i , $i \in [1, 6]$ are within ± 1 . One would guess that the results are indicative of a preferred pairing for plants $G \pm dG$, where dG is for example some uncertainty. However, increasing g_{11} by 0.05 to 0.89 (calling this gain matrix G') causes a different pairing to be preferred, namely $\Lambda^6(G') = I_3$. Both these matrices have comparable RGA values,

such that their difference would otherwise not lead to a different conclusion in terms of pairing:

$$\Lambda(G) = \begin{pmatrix} 0.56 & \mathbf{0.52} & -0.08 \\ -0.13 & 0.56 & \mathbf{0.58} \\ \mathbf{0.58} & -0.08 & 0.50 \end{pmatrix} \quad \Lambda(G') = \begin{pmatrix} \mathbf{0.57} & 0.51 & -0.08 \\ -0.13 & \mathbf{0.58} & 0.55 \\ 0.56 & -0.08 & \mathbf{0.52} \end{pmatrix} \quad (\text{A.18})$$

The pairings found by applying Λ^∞ are emphasized for the two cases. Closer examination reveals that the preferred pairing of G changes at $g_{11} = 0.8668\dots$. The RGA of G and G' both show pairings on $\lambda_{ij} \approx 0.5$. Thus, in this case it seems two (positive) pairings are nearly equal.

Two distinct cases of undefined pairing (subject to uncertainty) have been described: 1) one stable and one unstable pairing with some ill-conditioned Λ^k and 2) two stable pairings. It would be of interest to describe the matrix properties that determine which prevail for a given case.

A.3.5 Example 5: Pairing on negative RGA

Consider a $n \times n$ plant G with P unstable poles in *all* elements. Rules given in Hovd and Skogestad (1994) hold that pairing should be on positive RGA elements (i.e. $\lambda_{ij}(0) > 0$) if P is even and on negative RGA elements if P is odd. For example pair on negative RGA-values if there is a single common unstable pole.

The procedure of calculating Λ^∞ recognizes the (assumed) best set of RGA values, corresponding often to a set close to 1.0. Changing the sign of G or $\Lambda(G)$ corresponds to scaling of the input and output channels. Thus, since RGA is independent of scaling, it is not possible to focus Λ^∞ to another pairing criteria by simply changing sign of G or $\Lambda(G)$.

Despite the mentioned problems, pairing on negative RGA values may be the only solution, and what happens then? The following example from Grosdidier *et al.* (1985) is used:

$$G = \begin{pmatrix} 1.0 & 1.0 & -0.1 \\ 0.1 & 2.0 & -1.0 \\ -2.0 & -3.0 & 1.0 \end{pmatrix} \quad (\text{A.19})$$

The RGA of this plant is

$$\Lambda(G) = \begin{pmatrix} -1.89 & 3.58 & -0.70 \\ -0.13 & 3.02 & -1.89 \\ 3.02 & -5.60 & 3.58 \end{pmatrix} \quad (\text{A.20})$$

showing that pairing on only positive λ_{ij} is not possible. The question then becomes which negative RGA element to pair upon? The iterate gives

$$\Lambda^\infty(G) = \begin{pmatrix} 0 & 0 & \mathbf{1} \\ 0 & \mathbf{1} & 0 \\ \mathbf{1} & 0 & 0 \end{pmatrix} \quad (\text{A.21})$$

which corresponds to pairing on the negative RGA value with absolute value closest to 1.0.

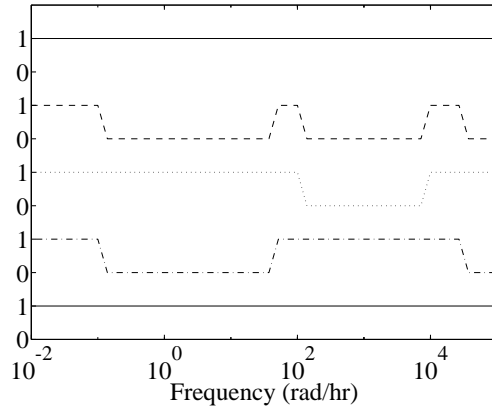


Figure A.1: Frequency dependent Λ^∞ for the HDA process. λ^∞ is listed top down for the recommended control loops.

A.4 Frequency dependent Λ^∞

This calculation is easily done frequency-by-frequency, to resolve if different pairings are preferred in different bandwidth regions. An example is shown in Fig. A.1, which depicts Λ^∞ for the HDA process from Chapter 6. The curves are Λ^∞ augmented so that the control loops corresponding to the preferred pairing are listed top-down.

Following recommendations for the RGA itself, different pairings at steady state and around the bandwidth region should be avoided. Due to the discrete nature of Λ^∞ , results may be more difficult to interpret for intermediate frequencies, since information is suppressed through the iterations.

We see that the results indicate loop 1 and 5 are preferred at all frequencies, whereas loop 2-4 are not. This is in line with the variation over frequency of Λ itself. All control loops are preferred at low frequency and within the bandwidth area, although not at very high frequency.

A.5 Susceptibility to pair on negative λ_{ij}

The method of calculating Λ^∞ will sometimes choose a pairing corresponding to pairing on negative $\lambda_{ij}(G)$, even if a positive pairing exists. This happens primarily when the choice is between a small positive λ_{ij} and a “large” negative λ_{ij} , i.e. closer to 1.0. An example;

$$G = \begin{pmatrix} 0.32 & 0.48 & 0.50 \\ 0.10 & 0.67 & 0.65 \\ 0.51 & 0.85 & 0.41 \end{pmatrix} \quad \Lambda(G) = \begin{pmatrix} 1.14 & -1.79 & 1.65 \\ -0.29 & 1.07 & 0.23 \\ 0.15 & 1.73 & -0.88 \end{pmatrix} \quad (\text{A.22})$$

The relative gain of G shows that there are two possible pairings on positive λ_{ij} , albeit including pairing on the values 0.23 or 0.15. Applying the iterate gives $\Lambda^\infty = I_3$, i.e. pair on the negative λ_{ij} closest to 1.0.

Statistical evidence shows that a pairing on only positive λ_{ij} (where a such exists) is preferred in approximately 97% of the cases for random matrices G of size $n = 3$. This

factor drops to below 90% for systems of larger dimension, which in any case removes the justification for the use of Λ^∞ indiscriminately.

A solution is to stop after the first iteration and extract only the positive elements of $\Lambda(G)$, here called $\Lambda'(G)$. Since the RGA will not favor zero gain elements, we can use this in “filtering” out the pairings that are not desired. A pairing is then isolated by computing $\Lambda^\infty(\Lambda'(G))$. Despite being rather “ad-hoc”, this procedure will nearly always converge to a positive pairing if a positive pairing exists. In case a positive pairing does not exist, $\Lambda'(G)$ does not have full rank and a pairing on negative RGA is mandatory. In this case $\Lambda^\infty(G)$ can provide a pairing. The knowledge of no pairing on positive RGA being possible is the nice by-product of such a development. The procedure is formalized in the next section.

A.6 Algorithmic pairing procedure

One can assure that a pairing corresponding to positive RGA, if a such exists, is found by the following procedure:

1. Find $\Lambda(G)$
2. Set $\Lambda' = \lambda'_{ij}$ equal $\lambda_{ij}(G)$ for positive elements of $\lambda_{ij}(G)$ and 0 otherwise.
3. If Λ' does not have full rank then no pairing on positive λ_{ij} is possible. In that case using $\Lambda^\infty(G)$ will give a feasible system, albeit a pairing on negative λ_{ij} . However, the closed loop plant will not have integrity to loop failure.
4. If Λ' has full rank, then a pairing can be found by $\Lambda^\infty(\Lambda')$. Exceptions exist (Johnson & Shapiro):
 - If $G = \frac{1}{2}(P + Q)$, where P and Q are permutation matrices, is non-singular, then $\Lambda(G) = G$ and no single pairing is indicated by $\Lambda^\infty(G)$. G is then called a fixed point.
 - For G of dimension $n \leq 4$ there are a finite number of fixed points. For G of dimension $n > 4$ there are infinite many possible fixed points including $G \neq \frac{1}{2}(P + Q)$ with parameterized entries.

A.7 Discussion

A mathematical result has been put to use in an engineering context for solving the pairing problem of large scale systems. A procedure for algorithmic application has been proposed. The method seems robust in terms of convergence. The method has been introduced to frequency dependent systems, although the interpretation is still uncertain.

Ordinary engineering problems converge to a pairing P within 5-8 iterations. The method is thus not calculation intensive. The number of iterations is not dependent on system size. An easy test for convergence is $\|\Lambda\|_2 < 1 + e$ with for example $e = 10^{-2}$.

The mapping $G \rightarrow \Lambda(G)$ does not always preserve rank. An example is the matrix

$$G = \begin{pmatrix} 1.0 & -1.0 \\ 1.0 & 1.0 \end{pmatrix} \quad (\text{A.23})$$

which gives $\lambda_{ij} = 0.5, \forall i, j$, i.e. $\Lambda(G)$ has rank 1. Calculation of $\Lambda^2(G)$ is thus not possible despite $\Lambda(G)$ showing that two (equal) pairings on positive RGA exist. A better understanding of how the calculation of the RGA may lose rank is necessary to fully understand the behavior that leads to $\Lambda^\infty(G \pm dG)$ giving different pairings.

References

- [1] Bristol, E.H., 1966, "On a new measure of interactions for multivariable process control", *IEEE Trans. Automat. Control*, **AC-11**, 133-134.
- [2] Grosdidier, P., M. Morari and B.R. Holt, 1985. "Closed-Loop Properties from Steady-State Gain Information", *Ind. Eng. Chem. Fundam.*, **24**, 221-235.
- [3] Hovd, M. and S. Skogestad, 1994. "Pairing Criteria for Decentralized Control of Unstable Plants", *Ind. Eng. Chem. Res.* In Press.
- [4] Hovd, M. and S. Skogestad, 1992. "Simple Frequency-Dependent Tools for Control System Analysis, Structure Selection and Design", *Automatica*, **28**, 5, 989-996.
- [5] Johnson, C.R. and H.M. Shapiro, 1986. "Mathematical Aspects of the Relative Gain Array ($A \circ A^{-T}$)", *Siam J. Alg. Disc. Meth.*, **7**, 4, 627-644.
- [6] Manousiouthakis, V., R. Savage and Y. Arkun, 1986. "Synthesis of decentralized Control Structures using the Concept of Block Relative Gain", *AIChE J.*, **32**, 6, 991-1003.